Ioanna Gkoutzamani

Ion Exchange as Pretreatment of Municipal Wastewater Effluent for Reverse Osmosis Desalination

Assessment of treatment performance and prediction of fouling potential on downstream reverse osmosis

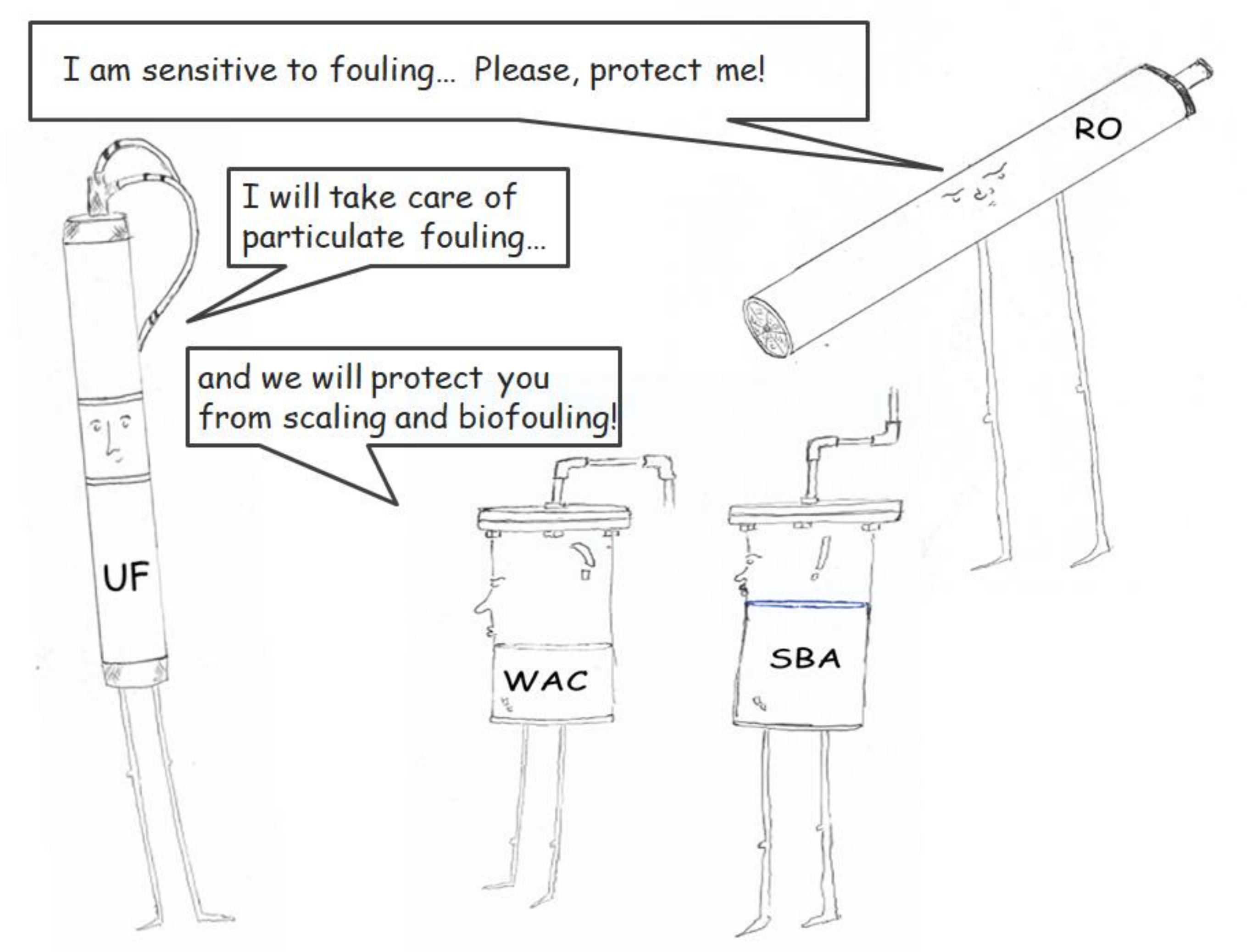

Ion Exchange as Pretreatment of Municipal Wastewater Effluent for Reverse Osmosis Desalination

Assessment of treatment performance and prediction of fouling potential on downstream reverse osmosis

By

Ioanna Gkoutzamani

in partial fulfilment of the requirements for the degree of

Master of Science

in Civil Engineering

at the Delft University of Technology,

to be defended publicly on 04 June 2020.

Thesis committee:		
	Dr. ir. H. Spanjers (chair)	TU Delft
	Prof. dr. ir. J. P. van der Hoek	TU Delft
	Ass. prof. dr. ir. D. Weissbrodt	TU Delft
	Ir. I. Pinel	TU Delft
External Supervisors:		
	Ir. O. Schepers	Evides IW
	Ing. P. van Hartingsveldt	Evides IW

Front cover: Special thanks to Rogelio Peschard Navarrete for the caricature.

Acknowledgments

This report presents my graduation thesis research in partial fulfilment of the Water Management Master of Science from the Faculty of Civil Engineering and Geosciences of TU Delft. The research was carried out in collaboration with Evides Industry Water during the period May 2019 - May 2020. This past year was filled with multiple challenges and hard work. Nevertheless, it was truly an incredible learning experience that helped me evolve professionally and personally.

I would like to thank the members of my graduation committee Henri Spanjers, Jan Peter van der Hoek and David Weissbrodt for their guidance throughout this research. You always provided me with constructive comments and valuable recommendations during our meetings.

Moreover, Ingrid Pinel, I cannot thank you enough for devoting a great amount of time and effort to guide me through an important part of this research.

I am grateful to Evides Industry Water for giving me the opportunity to get involved in Demin 2030 project. A big thank you goes to my colleagues in Evides, Nick Roodlbol, Lisa Wyseure and Ruben Kok. Your technical and practical support was very much needed to conduct my pilot experiments.

Peter van Hartingsveldt, my daily supervisor in Evides, thank you for our endless discussion and for sharing your deep knowledge and passion on the subject. I would also like to sincerely thank my Evides supervisor, Otto Schepers for always finding the time for questions and discussion and for making me feel part of the team from the first moment.

Finally, I would not have made it without the support of my family and friends. Thank you all for being besides me throughout this very special part of my life!

Ioanna Gkoutzamani
Delft, May 2020

Summary

Biofouling and scaling are ongoing challenges for reverse osmosis (RO) membranes application in wastewater reclamation. Adequate RO feed pretreatment is necessary for biofouling and scaling control. The objective of this thesis was evaluated the effectiveness of ion exchange treatment with weak acid cation (WAC) and strong base anion (SBA) resins columns, in series, after ultrafiltration (UF) treatment for the pretreatment of municipal wastewater treatment plant (WWTP) effluent in order to be used for RO desalination. Specifically, the performance of two SBA resins, the Amberlite SCAV4 Cl (SCAV4) and the Amberlite IRA458 Cl (IRA458) for the removal of sulfate, phosphate, nitrate and total organic carbon (TOC) from the RO feed and the subsequent effect on RO biofouling and scaling potential were investigated.

The performance of SCAV4 and IRA458 was assessed at three regeneration levels (120, 100 and 80 g NaCl/L_r) in order to evaluate the effect of the different regeneration levels on anions removal, TOC removal and the operational exchange capacity. The production was monitored and terminated based on a chosen nitrate breakthrough concentration (approximately 50% of feed concentration). Phosphate and sulfate removal was above 97% for both resins at all regeneration levels. TOC removal of about 70% was achieved in all cases. It was also observed that sulfate, phosphate and TOC removal remained the same up to the point where product nitrate concentration reached its feed concentration. The removal of nitrate was influenced by the regeneration levels. For both SBA resins, a lower regeneration level caused a higher nitrate baseline leakage in product water, hence to a lower removal. The macroporous SCAV4 found to have higher selectivity towards nitrate compared to the gel IRA458. Nevertheless, the anion selectivity order for both SCAV4 and IRA458 was $HCO_3^- < NO_3^- < HPO_4^{2-} < SO_4^{2-}$. A minor increase in the operational exchange capacity for both SBA resins was observed at higher regeneration levels. Overall, the influence of the different regeneration levels was found to be limited towards the product water quality and the operational exchange capacity. Also, both SBA resins resulted to similar product water quality. The operational exchange capacity of IRA458 at each regeneration level was higher than that of SCAV4, due to the former's greater total exchange capacity.

The effect on the biofouling and scaling potential of the product water quality of the two SBA resins was investigated with bio-growth potential tests and software tests (WAVE design, PHREEQC 3 and Avista Ci), respectively. The three studied RO feed qualities were (i) municipal wastewater effluent pretreated with UF (SFD-2880XP), (ii) municipal wastewater effluent pretreated with UF (SFD-2880XP) and ion exchange consisting of a WAC (Amberlite HPR8300 H) and the SCAV4 SBA resin columns in series and (iii) municipal wastewater effluent pretreated with UF (SFD-2880XP) and ion exchange consisting of a WAC (Amberlite HPR8300 H) and the IRA458 SBA resin columns in series.

The RO feed quality produced without ion exchange pretreatment supported bacterial growth up to $54 \pm 1.5 \times 10^6$ cells/mL. The RO feed qualities produced with ion exchange pretreatment in the cases of SCAV4 and IRA458 supported bacterial growth up to $3.4 \pm 0.3 \times 10^6$ cells/mL and to $1.25 \pm 0.2 \times 10^6$ cells/mL, respectively. The resulted reduction in the bacterial growth potential was above 90% after ion exchange treatment with either one of the tested SBA resins. The growth-limiting nutrient for the RO feed qualities produced by either SBA resin was phosphorus. The bacterial growth supported by the two RO feed qualities produced with ion exchange pretreatment after extra phosphorus addition was 80% lower than that supported by the RO feed quality produced without ion exchange. This difference suggests that both SBA resins removed a considerable fraction of assimilable organic carbon (AOC). It was concluded that ion exchange pretreatment with either one of the tested SBA resins resulted in nutrients removal (P and C) in the RO feed that lowers the biofouling potential compared to RO feed pretreatment with only UF.

The software results suggest lower scaling potential for several scalant types in the RO feed after ion exchange treatment with the WAC resin and either one of the tested SBA resins. However, the scaling potential of some silica and iron based minerals was high in all RO feed qualities studied, thus anti-scalant dosing might be required. Calcium phosphate scaling potential was found to be high in the RO feed quality produced without ion exchange pretreatment with and without anti-scalant dosing. In contrast, calcium phosphate scaling potential in the two RO feed qualities produced with ion exchange pretreatment was low either with or without anti-scalant dosing.

Abbreviations

A	All nutrients - nitrogen, phosphorus, carbon and trace elements
AOC	Assimilable organic carbon
ATP	Adenosine triphosphate
BDOC	Biodegradable dissolved organic carbon
BFR	Biofilm formation rate
BVs	Bed volumes
C	Carbon
DVB	Divinylbenzene
EC	Electrical conductivity
EPS	Extracellular polymeric substances
F	Feed (IX Feed)
FCM	Flow cytometry
IX	Ion exchange pilot
MBR	Membrane bioreactor
MF	Microfiltration
MFS	Membrane fouling simulator
N	Nitrogen
NF	Nanofiltration
P	Phosphorus
P_1	Product 1
P_2	Product 2
RL	Regeneration level
RO	Reverse osmosis
SAC	Strong acid cation
SBA	Strong base anion
SD	Standard deviation
SI	Saturation index
T	Trace elements
TCC	Total bacterial cell concentration
TH	Total hardness
TOC	Total organic carbon
UF	Ultrafiltration
VW	Volume weighted
VWA	Volume weighted average
WAC	Weak acid cation
WBA	Weak base anion
WWTP	Wastewater treatment plant

Table of Contents

List of Figures

List of Tables

1. Introduction

1.1 Wastewater Reclamation

The growing global industrialization is leading to excessive water consumption and pollution [1]. The increasing industrial water demand can be fulfilled with wastewater reclamation. Further treatment of municipal or industrial wastewater effluent is an attractive approach to produce high quality process water and at the same time reduce effluent discharges in the aquatic environment [2]. Membrane technology is widely applied for wastewater reclamation. Specifically, over the last decades the application of reverse osmosis (RO) membranes for desalination shows a worldwide exponential increase [3]. Their high removal efficiency, stable permeate water quality and simple operation constitutes them an ideal option for the purification of alternative water sources such as wastewater effluent and sea water [4].

The deposition of particles (particulate fouling) as well as salts (scaling), or growth of microorganisms (biofouling) can lead to substantial loss of the overall RO membranes performance, thus being of major concern for stable membrane operation [5]. Fouling of membranes leads to increased pressure drop, decreased membrane flux and reduction in salt rejection. The need for control and prevention measurements is clear and crucial [6].

Several studies have been carried out that focus on particulate fouling, scaling and biofouling related issues and possible prevention methods. Conventional pretreatment options for particulate fouling prevention are coagulation/flocculation, media filtration, cartridge filtration, microfiltration (MF) and ultrafiltration (UF) [5, 7, 8, 9, 10]. Biofouling, prevention or remediation can be accomplished with membrane chemical cleaning, membrane modification and feed water pretreatment. Pretreatment methods for biofouling control are disinfection with biocides (e.g. chlorine, ozone) or UV irradiation, coagulation, media filtration, MF, UF and nanofiltration (NF) [6, 8, 11]. To mitigate scaling three approaches can be considered. These are anti-scalant dosing, optimization of system's operation and feed water pretreatment. Pretreatment methods that can limit scaling are coagulation/flocculation, acidification, carbon dioxide (CO_2) purging, thermal water softening, ion exchange softening, MF and NF [5, 8, 12].

Ion exchange as pretreatment step of a RO unit can reduce scaling and biofouling by removing ions that cause scaling (e.g. calcium, magnesium, sulfate) and nutrients (e.g. phosphate, nitrate, total organic carbon). Cation exchange has been used as a pretreatment step of RO membranes for softening [13]. In several studies, the removal of sulfate, phosphate and nitrate by anion resins has been discussed [14, 15]. However, there are no studies focusing on ions removal by an ion exchange unit with cationic and anionic resin columns as RO feed pretreatment in process water production from municipal wastewater effluent. Anion resins have higher selectivity towards sulfate and phosphate than nitrate [16, 17]. Conflicting results have been reported about anion resins selectivity towards phosphate compared to sulfate [18, 15, 19, 14]. In cases where wastewater containing sulfate, phosphate and nitrate in fluctuating concentrations is treated with ion exchange resins, the anion preference sequence still needs to be investigated. Moreover, the impact of the pretreatment on the RO performance (scaling and biofouling) due to anion removal from the RO feed needs to be researched.

1.2 Evides Industry Water Project Demin 2030

This thesis research is part of an Evides Industry Water project called “Demin 2030”. The latter focuses on demineralized water production by researching the most promising techniques that can be applied in the coming 5 to 10 years in existing and future water purification processes.

Currently, water from the national park Biesbosch is used as a source for demineralized water production to fulfill the needs for process water for DOW production plant in Terneuzen. Part of the “Demin 2030” research aims to eliminate the use of the national park Biesbosch water and extend the reuse of wastewater effluent. DOW Terneuzen aims to reduce its environmental impact by limiting the consumption of water that can be used for drinking water production and by reusing the wastewater effluent from the same factory and the neighboring city.

To fulfill the research needs of the project “Demin 2030”, a pilot plant located in Terneuzen has been built. The treatment line of the pilot plant consists of an UF, an ion exchange and RO modules. The pilot plant’s influent water sources are the effluent of a MBR (membrane bioreactor) from Terneuzen wastewater treatment plant WWTP (municipal effluent) and the effluent from BIOX WWTP of DOW Terneuzen (industrial effluent). The first part of the “Demin 2030” project is to identify the optimal operational conditions for each process unit and investigate the performance of the units in these conditions. Future parts of the project will be to use constructed wetlands as UF pretreatment and to examine the possibility of recycling the RO concentrate for UF backwash and ion exchange regeneration [20]. This thesis belongs in the first part of “Demin 2030” and focuses especially on the ion exchange efficiency and the impact of the produced water quality on the RO modules.

1.3 Objective and Research Questions

The objective of this thesis was to investigate the effectiveness of ion exchange treatment with both cationic and anionic resin columns in series for the pretreatment of municipal WWTP effluent (after UF treatment) in order to be used as RO feed water.

The main research questions were (i) what is the performance of two strong base anion (SBA) resins for the removal of sulfate (SO_4^{2-}), phosphate ($H_2PO_4^-$, HPO_4^{2-}, PO_4^{3-}), nitrate (NO_3^-) and total organic carbon (TOC) and (ii) what is the subsequent effect on the biofouling and scaling potential in a downstream RO membrane unit?

Sub-questions that need to be answered during the research are listed below:

1. What is the removal efficiency of sulfate (SO_4^{2-}), phosphate ($H_2PO_4^-$, HPO_4^{2-}, PO_4^{3-}), nitrate (NO_3^-) and total organic carbon (TOC) by the two SBA resins at different regeneration levels?
2. How does the operational exchange capacity of the two SBA resins change at different regeneration levels?
3. What phosphate ($H_2PO_4^-$, HPO_4^{2-}, PO_4^{3-}), sulfate (SO_4^{2-}) and total organic carbon (TOC) concentrations can be achieved in the product water (RO feed) by running ion exchange unit up to the breakthrough point of nitrate (NO_3^-)?
4. What is the selectivity order between sulfate (SO_4^{2-}), phosphate ($H_2PO_4^-$, HPO_4^{2-}, PO_4^{3-}) and nitrate (NO_3^-) for the two SBA resins?
5. To what extent can the proposed ion exchange unit as a pretreatment step limit the RO biofouling potential?
6. To what extent can the proposed ion exchange unit as a pretreatment step limit the RO scaling potential?

In Table A.1 of Appendix A, the knowledge gap and the main research questions of this study are summarized.

1.4 Research Approach

In this research, the ion exchange pilot unit with both cationic and anionic resin columns in series was placed after the UF pilot unit using municipal WWTP effluent as influent. The performed experiments are listed in Table 1.1. The performance of two SBA resins was evaluated at three regeneration levels, resulting in experiments 1.1, 1.2 and 1.3 for SBA resin 1 and 2.1, 2.2 and 2.3 for SBA resin 2. The results of the experiments with the different regeneration levels for each SBA resin were compared. The best performing regeneration level for each SBA resin was selected based on the obtained operational exchange capacity and the quality of the product water. An "Overrun" of the SBA resins at their best performing regeneration level took place in order to determine the anion selectivity order (experiments 1.4 and 2.4).

An extra experiment was performed for each SBA resins at their best regeneration level to evaluate the effect on the RO performance (Experiment 1.5 and 2.5). The RO performance when RO feed was pretreated with only UF and with both UF and ion exchange with each SBA resin were compared. Subsequently, three RO feed qualities were studied. The RO performance for each water quality was assessed based on biofouling and scaling. The biofouling potential was assessed with bio-growth potential tests in water samples of the three RO feed qualities. The scaling potential was assessed with WAVE design software (DuPont), PHREEQC version 3 software (USGS) and the Advisor Ci software (Avista).

Table 1.1: Organization of experimental work

Name	Experiments details		Date
1.1	SBA resin 1	Regeneration level 1	20/01/20 - 26/01/20
1.2		Regeneration level 2	03/02/20 - 09/02/20
1.3		Regeneration level 3	10/02/20 - 16/02/20
1.4		SBA resin overrun	25/02/20
1.5		Bio-growth potential & software tests	24/02/20 - 12/03/20
2.1	SBA resin 2	Regeneration level 1	20/01/20 - 26/01/20
2.2		Regeneration level 2	03/02/20 - 09/02/20
2.3		Regeneration level 3	10/02/20 - 16/02/20
2.4		SBA resin Overrun	25/02/20
2.5		Bio-growth potential & software tests	24/02/20 - 12/03/20

2. Theory and Literature Review

2.1 Ion Exchange

Ion exchange is the reversible exchange of ions between solid and liquid phases. The chemical expression of an anion exchange reaction is given in Equation 2.1. The M^+A^{nA-} is the ion exchanger and it is in a solid form. The cation M^+ is called the fixed ion. The anions A^{nA-} and B^{nB-} are the counter-ions, while ions in the solution with the same charge as the fixed ion are called co-ions.

$$n_B M^+ A^{n_A-}\ (s) + B^{n_B-}(aq)\ \leftrightarrow n_A M^+_{n_B} B^{n_B-}(s) + n_B A^{n_A-}(aq) \tag{2.1}$$

An important characteristic of ion exchange is that electro-neutrality is preserved both in the exchanger and in the solution. Subsequently, the counter-anions are exchanged in equivalent amounts [21, 22].

Ion exchange finds applications in chemical, pharmaceutical and food industry, but its use for water treatment purposes is proved to be the most widely spread application. Ion exchange can be used for softening, demineralization, organic removal, nitrate removal, oxygen removal and other ions removal [22]. Ion exchange can be applied as a water treatment process with the use of ion exchange resins. The latter are porous plastic beads that contain permanently attached ions (fixed) that can be either positively or negatively charged. Thus, they can be cationic or anionic resins [16].

2.1.1 Ion Exchange Resins Categorization

Ion exchange resins production occurs by the polymerization of either styrene or acrylic monomers. In both cases, the addition of a crosslinking agent usually divinylbenzene-DVB is needed to give the resin physical strength. Depending on the amount of added DVB, the created pores in the resins structure can be larger or smaller [22]. During polymerization, a third component called porogen can optionally be added in the reaction mixture. The porogen does not react with the monomers and it is washed out after polymerization. It is added in order to create larger porous in the resins structure even though more DVB is used (higher crosslinking). When porogen is used during production the resulting resin's structure is macroporous, otherwise it is gelular (gel) [23, 22]. The syntheses of a resin that can be styrene or acrylic and gel or macroporous is called matrix. Specifically, the acrylic or stryrene characterization of the resin matrix can be referred as the backbone of the resin [16].

The second part of ion exchange resins production is called functionalization and it provides the resin with the ion exchange ability by attaching an ionized group to the resin bead. Based on the functional group of the fixed ion, resins can be classified into the following categories [22]:

1. Weak Acid Cation (WAC) – carboxylate ($-COO^-$)
2. Strong Acid Cation (SAC) – sulfonate ($-SO_3^-$)
3. Weak Base Anion (WBA) – dimethylamine ($-CH_2-N(CH_3)_2$)
4. Strong Base Anion (SBA)
    a. Type I – benzyltrimethylammonium ($-CH_2-N(CH_3)_3^+$)
    b. Type II – benzyldimethylethanolamine ($-CH_2-N(CH_3)_2(CH_2CH_2OH)^+$)

WAC resins backbones are acrylic, while SAC resins backbones are styrenic. WBA and SBA resins can have either acrylic or styrenic backbone [22]. WBA resins are considered to be in a free base form, since they do not have exchangeable ions. SBA resins can be Type I or Type II. Differences between Type I and II are listed below [16]:

1. Type II resins are slightly less basic and thus have a slightly lower affinity for hydroxide ions.
2. Type I resins are slightly more chemically stable.
3. Type II resins have slightly greater regeneration efficiency and capacity.

2.1.2 Ion Exchange Resins Properties

The properties of ion exchange resins can be divided in two groups, chemical and physical. The matrix, the crosslinking (%DVB) and the functional group described above are chemical properties of resins. Other chemical properties are the ionic form, the water content, the swelling (reversible and irreversible), the pH range, the salt splitting capacity, the chemical stability and the thermal stability. Physical properties are the physical form, the particle size, the uniformity coefficient, the grading, the density, the shipping weight and the sphericity [22]. Furthermore, an ion exchange resin is characterized by its ion exchange capacity and its selectivity. These two can be considered as the engineering properties and they are generally used in order to determine the performance of a resin under specific operating conditions [16]. Some of these properties are explained below.

Ionic Form

The ionic form refers to the form of the counter-ion that is contained to an ion exchange resin before it is used. An ion exchange resin can be converted to any counter-ion from. The most common commercially available ionic forms for the different functional group can be seen in Table 2.1 [22].

Table 2.1: Most common ionic forms for the different functional groups [22].

Functional group	SAC	WAC	SBA (both types)	WBA
Ionic form	Hydrogen form, sodium form	Hydrogen form	Chloride form	Free base form

pH Range

Ion exchange resins are active in a specific pH range depending on their functional groups. In most cases, SAC and SBA are active in any pH, while WAC and WBA resins are active at a pH above 4 and below 6, respectively [22, 16].

Ion Exchange Capacity

The most important property of an ion exchanger is the total ion exchange capacity (total capacity), which is a measurement of its total content of exchangeable ions. It is expressed as the total number of equivalents of exchangeable ions in a stated form per unit mass (eq/kg or meq/g) or per unit volume (meq/L_r) of the resin. When the capacity is expressed in mass terms, it is called dry weight capacity. Greater operational application has the wet volume capacity where it is expressed in volume terms [22]. It must be mention that apart from the total capacity also the operational exchange capacity of a resin is of high importance. Further information about the operational exchange capacity is available in sub-chapter 2.1.4.

Selectivity

Selectivity is the affinity or preference of ion exchange resins for certain ions. It can be expresses with the selectivity coefficient. For the reaction given in Equation 2.1 the selectivity coefficient of ion B over A for a given temperature is given in Equation 2.2 [16].

$$K_A^B = \frac{\left\{M_{n_B}^{+} B^{n_B -}\right\}^{n_A} \times \left[A^{n_A -}\right]^{n_B}}{\left\{M_{n_A}^{+} A^{n_A -}\right\}^{n_B} \times \left[B^{n_B -}\right]} \tag{2.2}$$

where

K_A^B: selectivity coefficient of ion B over A

{ $M_{nA}{}^{+}A^{nA-}$}, {$M_{nB}{}^{+}B^{nB-}$}: activities of resin-phase for counter-ions A and B, respectively;

[A^{nA-}], [B^{nB-}]: aqueous-phase concentration of counter-ions A and B [mmol/L], respectively.

In diluted solutions that are relevant to water treatment applications, the ions behave independently and the solutions are considered ideal. Therefore, the activity coefficient is assumed to be equal to unity and the activities of the resin-phase for the two counter-ions can be expressed as concentrations [16].

Moreover, the preference for one ion over another can be expressed with the separation factor. For the previous given case the separation factor is given in Equation 2.3.

$$a_A^B = \frac{Y_B \times X_A}{X_B \times Y_A} \tag{2.3}$$

X_i and Y_i are the equivalent fractions of a counter-ion i in the aqueous phase and in the resin-phase, respectively. They are expressed as follows in Equations 2.4 and 2.5 [16].

$$X_i = \frac{C_i}{C_T} \tag{2.4}$$

$$Y_i = \frac{q_i}{q_T} \tag{2.5}$$

where

C_i: aqueous phase concentration of counter-ion i [eq/L]

C_T: total aqueous ion concentration [eq/L]

q_i: resin phase concentration of counter-ion i [eq/L_r]

q_T: total exchange capacity of resin [eq/L_r]

Selectivity depends on chemical and physical properties of the ion exchange resins and the counter-ions. The chemical properties that affect selectivity are the valance and the atomic number of the counter-ions. The greater the valence of an ion the higher the affinity of a resin towards it is. Also, selectivity is increased with an increasing atomic number. However, there are exceptions such as the divalent CrO_4^{2-} that has a lower affinity than some monovalent ions or ions with lower atomic number. The physical properties of an ion exchange resin that have impact on selectivity are its pore size distribution and its functional groups. Moreover, the swelling and the pressure in the resin bead influence the selectivity. Ions with smaller hydrated radius reduce the swelling pressure of ion exchange resins, thus they have higher affinity [24].

Based on the above rules, anionic resins and cationic resins are expected to exhibit the following selectivity orders, respectively [22]:

$OH^- < Cl^- < HCO_3^- < NO_3^- < SO_4^{2-}$

$H^+ < Na^+ < Mg^{2+} < Ca^{2+} < Fe^{3+}$

The place of the divalent HPO_4^{2-} in the above given selectivity order for the anions is expected to be similar to SO_4^{2-} and prior to the monovalent NO_3^-. However, this is not certain because conflicting results have been published over the years. The separation factors of SO_4^{2-} and NO_3^- over Cl^-, provided by Crittenden et al. (2012) are shown in Table 2.2. The higher the separation factor is, the higher the preferenece for the anion by the resin is [16]. The separation factors of SO_4^{2-} and NO_3^- indicate that the latter anion is less prefered than the former, but the separation factor of HPO_4^{2-} is not available. Boari et al. (1976) showed that HPO_4^{2-} is less prefered than SO_4^{2-} and Cl^- by SBA resins, but more prefered than Cl^- by WBA resins [18]. Liberti et al. (1977) showed that the selectivity sequence $HPO_4^{2-} > SO_4^{2-} > Cl^-$ can be achieved in treatment of sythesised sewage waters [14]. Later studies have evidenced poor selectivity of HPO_4^{2-} in presence of competitive ions [25, 15, 19, 17]. Awual et al. (2011) compared the limitation of phostate removal by other ions for a WBA and a SBA [15]. Based on batch experiments the conclusion of the study was that the tested WBA resin prefers phosphate to SO_4^{2-}, NO_3^- and Cl^- while the opossite was noted for the tested SBA. Williams (2013) tested in batch expirements three phosphate selective resins and one non phoshpate selective WBA resin [19]. The outcome of the research was that in the two out of three phosphate selective resins the presence of other ions slightly limits the removal of phosphate, while for the non-phosphate selective resin the limitation is much more significant. The batch study of Zarrabi et al. (2014) showed that even though phosphate removal by a SBA resin is higher than those of NO_3^- and Cl^-, the co-existence of the latter ions in the solution results in decreased removal of phosphate compared to the case where only phosphate is present and the presence of NO_3^- has a more significant effect compared to the presence of Cl^-.

Table 2.2: Separation factors for some anions over Cl^- [16].

Anion	α_{Cl}^{i}
SO_4^{2-}	9.1
NO_3^-	3.2
Cl^-	1.00

In most of the studies discussed above, synthetic solutions were used that were produced either to resemblance wastewater effluent or to contain specific concentrations of competitive ions. But the question of the anion preference sequence remains in the case of ion exchange treatment of real wastewater that contains HPO_4^{2-}, SO_4^{2-} and NO_3^- in fluctuating concentrations. Pilot scale experiments can test the simultaneous removal of the three mentioned anions when municipal wastewater is the pilot's influent stream.

2.1.3 Ion Exchange Operation and Regeneration

In most applications of ion exchange process, influent water passes through beds of resins that are contained in a cylindrical vessel (column). While water passes through the ion exchange resin column, the counter-ions in the solution replace the counter-ions of the resins. Gradually the resins are exhausted up to a point where there are no more spots for counter-ions of the solution to be loaded. The exhaustion of a resin is not uniform. Thus, breakthrough of unwanted ions is noted before the resin is fully exhausted [22]. In Figure 2.1, the gradual exhaustion of a resin bed in relation to the breakthrough curve is depicted. The breakthrough curve represents the relationship between the concentration of a specific ion in product water on the y-axis and the produced water volume (throughput) expressed either in m^3 or in bed volumes (BVs) on the x-axis. A specific concentration based on the required product water quality is decided as the breakthrough concentration that results in a breakthrough point. When the product water quality reaches this breakthrough concentration, the production is terminated and the resin needs to be regenerated.

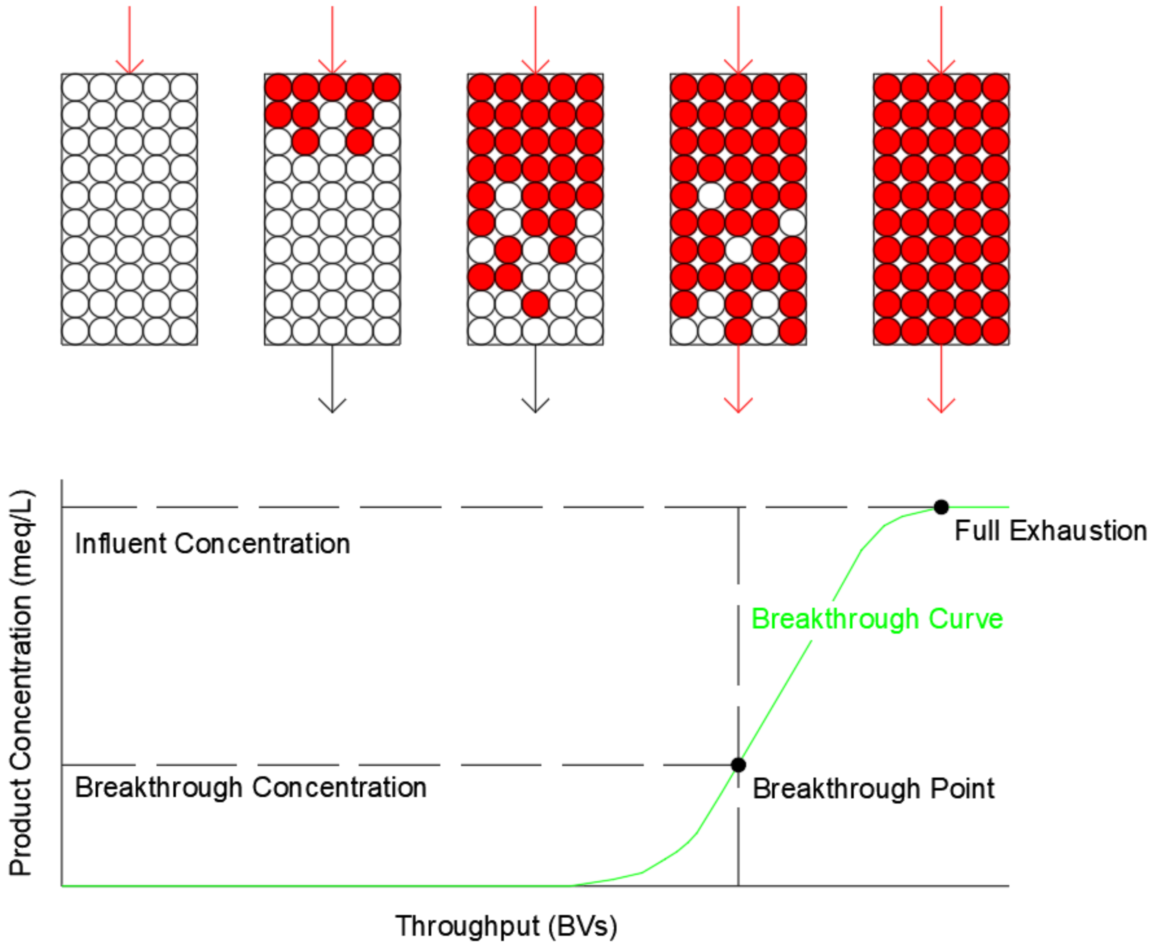

Figure 2.1: Gradual exhaustion of an ion exchange resin bed in relation to the breakthrough curve (created based on [26])

Regeneration is the process where resins return to their original state by replacing the retained ions in the resins during operation with functional group ions [16]. Regeneration is realized by dosing higher amounts of the equivalent ions than required based on stoichiometry. In this way, the selectivity barrier can be overcome. The regeneration ratio is expressed with Equation 2.6 and it is always higher than 100%. The regeneration level is the total amount of regenerant passed (meq) over the resin's column volume (L_r). The regeneration level will affect the performance of next operation batch.

$$Regeneration\ Ratio\ (\%) = 100\ \times \frac{Total\ Regenerant\ Passed\ (meq)}{Stoichiometrically\ Required\ (meq)} \tag{2.6}$$

As it can be concluded, ion exchange is a batch process that consists of an operation and a regeneration part and it can be either co-flow or counter-flow. Moreover, an ion exchange process of mixed beds has been developed for demineralized water production [16].

Co-flow Ion Exchange

In co-flow ion exchange, regeneration's flows direction is similar to the operation's flow direction. The main disadvantage of co-flow regeneration is that SBA and SAC resins columns are not fully regenerated and at the end of the regeneration, a part of the bottom layer remains contaminated. This leads to an early breakthrough of the following operation run. To minimize this problem large amounts of chemical regenerants are needed to be used [16].

Counter-flow Ion Exchange

In counter-flow ion exchange, the regeneration flow direction is opposite of the flow direction during operation. This can happen either when operation flow is downward and regeneration is upward or when operation flow is upward and regeneration is downward. The main advantage of counter-flow compared to the co-flow is that smaller amount of regenerants are needed to be dosed and the resulted product water has a higher quality [27].

Mixed Beds Ion Exchange

Mixed beds ion exchange is used for the production of demineralized water. It is based on water treatment through a resin column containing mixed SAC and SBA resins. This method has been proven to produce better quality water compared to that produced if the SAC and SBA resins were placed in series. The regeneration of mixed beds ion exchange takes place after the two resin types are separated in two layers. Thus, the resins selection is based on their densities and particle sizes. Backwashing places the SBA resin above the SAC resin, because the latter normally is heavier than the former. Regenerant for SBA regeneration is dosed in the top of the columns and simultaneously regenerant for SAC regeneration is dosed in the bottom of the column. Both regenerant solutions are withdrawn at the interface. After regeneration, the resins are well mixed with air scouring [16].

2.1.4 Operational Exchange Capacity

The operational exchange capacity or operational capacity is defined as the total number of exchange sites where ions were exchange during production [28]. The operational capacity is basically the part of the total capacity that can be used in a column operation. Usually, it ranges from 40 to 70% of the total resin capacity and it can be affected by the production flow rate, the regeneration level and the regeneration flow rate [29, 16]. The operational capacity of a resin can be calculated based on the influent concentration and a selected breakthrough concentration. For example, in Figure 2.2 the “yellow highlighted” area restricted by the breakthrough curve of an ion, the horizontal line representing the ion’s concentration of the influent water and the two vertical lines that result from the selected breakthrough concentration equal to the equivalents that have been exchanged during production. This value divided with the resin’s bed volume (L_r) of the column gives the operational capacity as expressed by Equation 2.7 [30]. To obtain the operational capacity of a specific system (treated water, tested resin, production flow rate, regeneration flow rate etc.) a number of batches usually 3 to 5 are need so as the system to get stable. The operational capacity is expected to decrease in every batch up to a point of stability [16]. The amount of regenerant passed over the resin’s column volume, which is the regeneration level (meq/L_r), affects the operational capacity of the following production [22].

$$Operational\ Capacity\ (\frac{meq}{L_r}) = \frac{Area\ (meq)}{Resin's\ Bed\ Volume\ (L_r)} \tag{2.7}$$

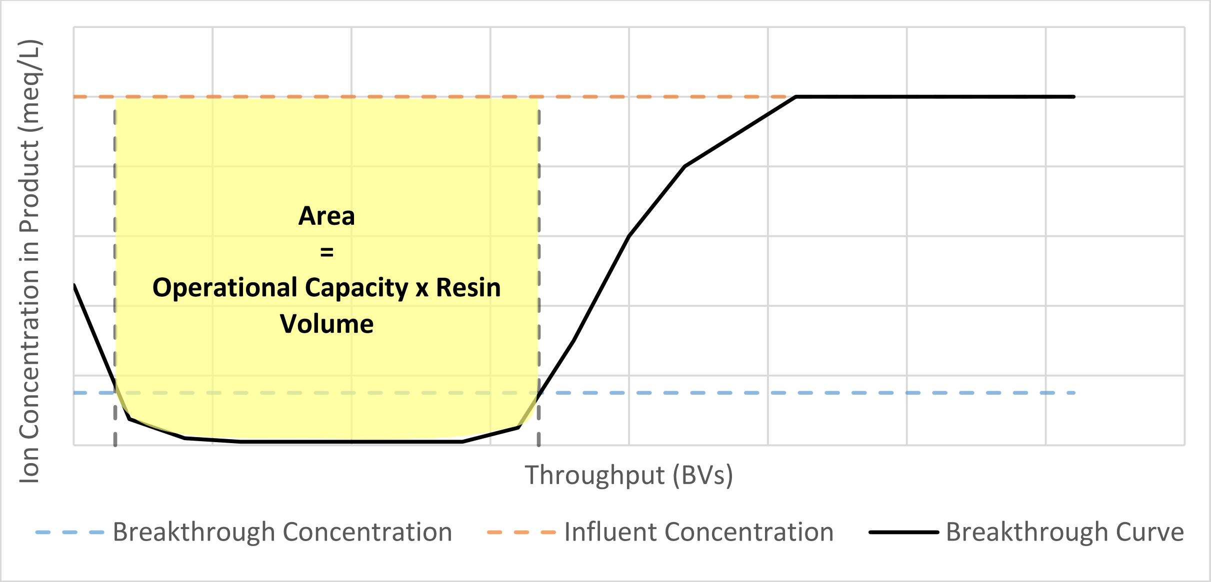

Figure 2.2: Operational capacity estimation from the breakthrough curve, the influent concentration and the selected breakthrough concentration of a certain ion (created based on [30])

2.1.5 Recommended Operating and Regeneration Conditions

An ion exchange cycle (batch) consists of an operation and a regeneration part. Moreover, the regeneration is divided in a series of steps, the backwash or compaction, the chemical dosing (injection of regenerants), the displacement (wash out of regenerants with demineralized water) and the prewash or dump (rinse with demineralized water or feed water) [22]. In this sub-chapter, the typically recommended conditions for all steps included in an ion exchange cycle are presented. It should be mentioned that operation outside the recommended ranges is possible and in some cases even required [31].

Production

In column operation of an ion exchange unit, water passes through the resin bed with a specific production flow rate. It can be expressed as the volumetric flow rate in BVs/h or as the surface area flow rate in m/h (superficial flow velocity through the resin bed). Typical volumetric flow rates and surface area flow rates (velocities) range from 8 to 40 BVs/h and from 10 to 36 m/h, respectively [16]. Based on DuPont Tech Fact 177-03729 [31] the recommended range for the production flow rate is somewhat wider from 6 to 60 BVs/h.

Regeneration 1: Backwash and Compaction

Backwash and compaction are upward flows through the resin bed. Compaction intends to lift the resin bed as a block (fixed bed), while backwash enables the physical cleaning of the resin bed [32].

Regeneration 2: Chemical dosing

SAC resins can be regenerated with acids such as H_2SO_4, HCl, or with NaOH base or with NaCl salt. SBA resins can be regenerated with the NaCl and NaOH. WAC resin regeneration can take place with H_2SO_4, or HCl, or NaOH. WBA resin regeneration can take place with solutions of NaOH or NH_3 or Na_2CO_3. Concentrations in range of 2 to 6 % are suitable for the regenerant solutions of H_2SO_4 and HCl for cation resins, while solutions of NaOH or NaCl have concentrations of 4 to 5 % for anion resins. Flowrates of 2 to 4 m/h allow chemical diffusion into the resin [32].

In DuPont Tech Fact 177-03729 more detailed information about the regenerant quantity and concentration and the regeneration flow and contact time can be found. The flow of the regeneration can be calculated based on the desired contact time and the required regenerant volume, and it should be more than 2 BVs/h. Contact time of at least 20 minutes is required for the cases of SBA, SAC and WAC resins and more than 30 min for WBA resins. Also, an upper limit of 60 minutes contact time for regeneration with H_2SO_4 is applied. The volume of regenerant solution should preferably amount to 1 BV or more [31].

In Table 2.3, the recommended ranges by DuPont Tech Fact 177-03729 for the quantity and the concentration of the regenerant in the case of SBA and SAC regeneration are available. Similarly, relevant information for the regeneration of WAC and WBA is given in Tables 2.4 and 2.5, respectively. In Table 2.4, recommended ranges for WAC regeneration flowrate are also included.

Table 2.3: Recommended ranges of regenerant quantity and concentration for SBA and SAC regeneration [31]

Chemical	Chemical quantity (g/L_r)		Chemical concentration (%)	
	Co-flow	Counter-flow	Co-flow	Counter-flow
NaCl	90 - 240	70 - 120	10	2 - 10
HCl	75 - 15	40 - 80	5	5
H_2SO_4	90 - 240	60 - 100	0.8 - 6	
NaOH	75 - 160	40 - 80	4	2 - 4

Table 2.4: Recommended ranges of regenerant quantity, concentration and flowrate for WAC regeneration [31]

Chemical	Chemical quantity (% total capacity)		Chemical concentration (%)		Flowrate (BVs/h)	
	Dealkalization	Softening	Dealkalization	Softening	Dealkalization	Softening
HCl	105 - 110	110 - 160	2 - 5	2 - 5	2 - 4	2 - 4
H_2SO_4	105 - 110	110 - 160	0.5 – 0.7	0.5 – 0.7	6 - 40	6 - 40
NaOH	-	110 - 160	-	2 - 4	-	2 - 4

Table 2.5: Recommended ranges of regenerant quantity and concentration for WBA regeneration [31]

Chemical	Chemical quantity (% ionic load)	Chemical concentration (%)
NaOH	115	2 - 4
NH_3	150	2 - 6
Na_2CO_3	200	5 - 8

Regeneration 3: Displacement

During displacement, demineralized water is used to wash out the excess regenerant with a flowrate equal to the flowrate of the chemical dosing. Typically, replacement of 2 BVs is enough [32]. In Table 2.6, specific BVs for each resin type proposed by the DuPont Tech Fact 177-03729 can be found.

Table 2.6: Recommended BVs for displacement [31]

Resin	Volume (BVs)	
	Co-flow	Counter-flow
SAC	2	1.5
SBA	3	3
WAC	2	2
WBA	2	2

Regeneration 4: Prewash or Dump

A final fast rinse of 10 to 30 minutes prior to production at a higher flowrate than the flowrate of the regeneration flushes out any traces of the regenerant left [16, 32]. It can take place either with demineralized water known as prewash or with influent water, which is "dumped". DuPont Tech Fact 177-03729 proposes a flowrate of 10 to 30 BVs/h or even equal to the production flow rate. Moreover, the final rinse volume for the different resins based on DuPont Tech Fact 177-03729 can be seen in Table 2.7.

Table 2.7: Recommended BVs for prewash or dump [31]

Resin	Volume (BVs)
SAC	2 - 4
SBA	3 - 8
WAC	4 - 8
WBA	4 - 8

2.2 Reverse Osmosis Membranes Fouling

Reverse osmosis (RO) membranes are spiral wound membranes modules with the highest performance among MF, UF and NF membrane, since they can remove monovalent ions with high rejection efficiency. RO membranes are operated in a cross-flow mode with permeate and concentrate streams production [21]. Since the 1970's, their application for water desalination purposes shows an exponential increase [3]. RO membranes offer the option for desalination of sources such as seawater, brackish water and wastewater effluent and produce a permeate quality which makes them suitable for drinking water and process water production.

Fouling of RO membranes constitutes, however, a limitation to their efficiency and overall performance. Fouling causes higher hydraulic resistance (higher head loss over the membrane module), higher differential pressure and feed pressure, lower flux (lower membrane permeability), reduced salt rejection (reduce product water quality) and gradual membrane biodegradation. These leads to RO membranes' performance deterioration and eventually to higher operational costs due to the need of more frequent cleaning, increased energy demand and membrane replacement [6, 11, 12].

Four different types of fouling can be identified in RO membrane systems. These are particulate fouling, inorganic fouling, organic fouling and biofouling [4, 8]. Particulate fouling is caused by the deposition of clay, silt and silica matter. Inorganic fouling or scaling is the precipitation and scale of inorganic substances such as metal hydroxides, carbonates, sulfates and phosphates. Organic fouling is the deposition of organic substances such as oil, proteins, humic acids and lipids in the membrane surface. Biofouling is the attachment and growth of microorganism in the membrane surface resulting in the formation of biofilms through production of extracellular polymeric substances (EPS) [6, 11, 16]. Microorganism growth depends on organic carbon, phosphorus and nitrogen content in water. The elimination of specifically phosphorus content in the RO feed has been proposed as a solution to biofouling [33]. Pretreatment that targets the limitation of all three above mentioned nutrients in the feed water can potentially inhibit biofouling [6, 11, 34, 35]. Phosphate, nitrate and total organic carbon (TOC) removal can be achieved with anion exchange. To what extent these nutrients can be removed and the subsequent effect on biofouling still needs to be investigated.

2.2.1 Scaling Potential

The scaling potential can be evaluated based on the feed water quality with computations of mineral's saturation state or saturation index. For the general dissolution reaction in equation 2.8, the saturation state and the saturation index are given in Equations 2.9 and 2.10, respectively [5].

$$A_aB_b(s) = aA\,(aq) + bB(aq) \tag{2.8}$$

$$\Omega = \frac{IAP}{K} \tag{2.9}$$

$$SI = \log(\Omega) = \log(\frac{IAP}{K}) \tag{2.10}$$

where

Ω: saturation state or scaling tendency

IAP: ion activity product (Equation 2.11)

K: solubility product equilibrium constant (Equation 2.12)

SI: saturation index

$$IAP = \{A\}_{actual}^{a} \times \{b\}_{actual}^{b} \tag{2.11}$$

$$K = \{A\}_{eq}^{a} \times \{b\}_{eq}^{b} \tag{2.12}$$

where

$\{A\}_{eq}^{a}, \{b\}_{eq}^{b}$: activities in equilibrium

$\{A\}_{actual}^{a}, \{b\}_{actual}^{b}$: actual activities in solution

The saturation state or the saturation index (SI) can be used to determine whether the water is saturated, sub-saturated, or supersaturated with respect to a given mineral, based on the following rules [5, 36]:

1. $\Omega < 1$ or $SI < 0$: sub-saturation, the solid A_aB_b (s) is not expected to be formed
2. $\Omega = 1$ or $SI = 0$: saturation, equilibrium between the solid and the liquid phase of the mineral
3. $\Omega > 1$ or $SI > 0$: supersaturation, the solid A_aB_b (s) is expected to be formed

Moreover, the Langelier Saturation Index is used to specifically predict calcium carbonate scale [5, 16]. The potential for scaling formation can be accurately predicted with PHREEQC 3 software (USGS) that computes the saturation index of minerals in a given water quality. More software have been developed to predict scaling and the required anti-scaling dosing. An example is Advisor Ci (Avista) which provides information about the requirements in anti-scalant dosing and the subsequent mineral's saturation state also known as scaling tendency (%) based on the RO feed water quality [37].

2.2.2 Biofouling Potential

The biofouling potential can be assessed from water samples with measurements of assimilable organic carbon (AOC), biodegradable dissolved organic carbon (BDOC) and adenosine triphosphate (ATP) content of the RO feed water [35]. AOC and BDOC are bacterial growth potential measurements that focus on organic carbon as the main growth-limiting substrate in water. Organic carbon is the limiting nutrient for bacterial growth in most environmental water. However, treated water can become limiting in inorganic nutrients such as phosphorus, nitrogen and trace elements when these are being removed. AOC and BDOC methods do not enable the identification of the limiting nutrient for the bacterial growth [38]. Prest et al. (2015) developed a rapid, easy and sensitive method to evaluate the bacterial growth potential and identify the limiting nutrient in water samples that is based on samples incubation and flow cytometry (FCM) measurements of the total bacterial cell concentrations (TCC). Water samples are incubated with no extra additives and the growth is monitored over time until it reaches a stable cell numbers. A derived test with addition of one or multiple nutrient sources allows the identification of the limiting nutrient in the water. Hence, the bacterial growth that water can support can be assessed and the growth-limiting nutrient(s) can be identified [38].

The biofilm formation rate (BFR) demonstrates the ability of water to promote the growth of bacteria into a biofilm, but the duration of the experiment is several weeks [39]. The need for early warning to prevent biofouling formation in operating RO systems led Vrouwenvelder et al. (2006) to develop a practical tool to predict fouling formation, the membrane fouling simulator (MFS). It can be placed prior to an RO system and it is fed with RO feed water. In low concentrated streams, contact time of seven or more days is required in order to retrieve reliable fouling observations. The fouling potential is monitored in three ways, which are pressure drop over the MFS unit, visual/ microscopic observations using the sight glass existing in the MFS unit and ATP analysis of the coupons sampled from the membrane sheet [40].

3. Materials and Methods

3.1 Pilot Configuration

The ion exchange pilot (IX pilot) used in this study consists of two identical lines in parallel. Each line consists of two columns in series. The first column for both lines was filled with a WAC resin, while the second column was filled with a different SBA resin for each line. The process and instrumentation diagram of the ion exchange pilot is available in Appendix B.

The IX pilot configuration for one line during production is depicted in Figures 3.1. The production flow is highlighted with blue. Online automatic measuring devices of flow, electrical conductivity (EC), pressure and temperature are placed in the influent stream. Also, online automatic measuring devices of pressure, EC and pH exist in the stream between the WAC and the SBA columns and in the product stream (after SBA). Sampling points can be found in the influent, the stream between the WAC and SBA columns and the product streams. The stream between the WAC and SBA columns is send via an automatic sampling point to an online total hardness (TH) analyzer, the Testomat EVO TH (Testomat ECO, DE). The product stream is sent via an automatic sampling point to an online NO_3^- analyzer, the UV400 (TETHYS Instruments, FR). A demineralized water tank and three tanks with the required for the regeneration chemicals are located close to the system (more information is available in sub-chapter 3.4.3). More information about all equipment installed on the pilot and the used chemicals is available in Appendix B.

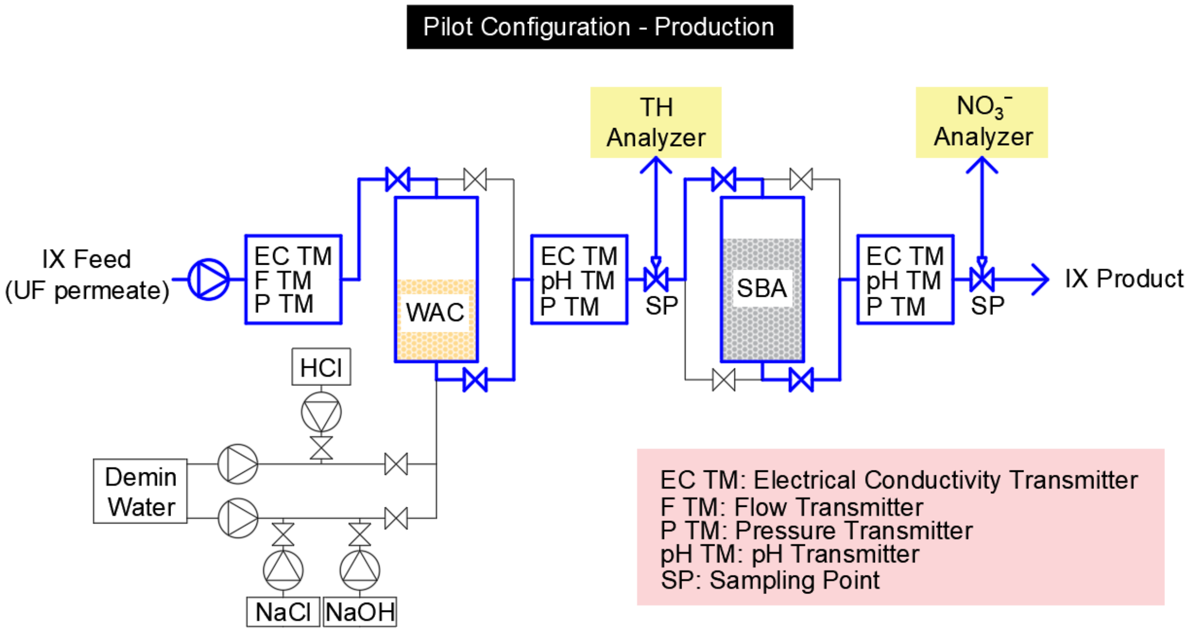

Figure 3.1: IX pilot configuration for one line during production (production flow with blue)

3.2 Feed Water Quality

Municipal wastewater effluent after treatment with an UF membrane (SFD-2880XP, outside-in flow direction) was the influent of the IX pilot. Since the IX pilot consist of two identical lines, two experiments were performed in parallel and one influent sample was collected for every two experiments. The results of the measurements for each sample are available in Appendix C. The measured parameters were electrical conductivity (EC), pH, adenosine triphosphate (ATP), total organic carbon (TOC), bicarbonate (HCO_3^-), chloride (Cl^-), sulfate (SO_4^{2-}), nitrate (NO_3^-), phosphate ($H_2PO_4^-$, HPO_4^{2-}, PO_4^{3-}), silicon dioxide (SiO_2), fluoride (F^-), sodium (Na^+), potassium (K^+), calcium (Ca^{2+}), magnesium (Mg^{2+}), iron (Fe^{3+}), manganese (Mn^{2+}), ammonium (NH_4^+), aluminum (Al^{3+}), barium (Ba^{2+}) and strontium (Sr^{2+}). All measurements were conducted by the independent water laboratory Aqualab Zuid B.V[1]. In Table 3.1 the average and the standard deviation (SD) for all measured parameters of the influent samples are given. It must be noted that TOC measurements are expressed in mg C/L and silicon dioxide (SiO_2) in mg Si/L. Phosphate ($H_2PO_4^-$, HPO_4^{2-}, PO_4^{3-}) measurements are expressed in mg P/L and in this report will be referred as HPO_4^{2-}-P, since HPO_4^{2-} was the dominant species based on the pH of the samples.

Table 3.1: Water quality IX influent

Parameter	Unit	Average	SD
EC	µS/cm	1442.32	290.39
pH	-	7.62	0.08
ATP	ng/L	740.28	499.07
TOC	mg C/L	8.57	1.14
HCO_3^-	mg/L	234.17	76.60
Cl^-	mg/L	275.48	77.83
SO_4^{2-}	mg/L	96.41	8.69
NO_3^-	mg/L	51.50	8.49
HPO_4^{2-}-P	mg P/L	2.79	2.19
SiO_2	mg Si/L	5.22	0.76
F^-	mg/L	0.19	0
Na^+	mg/L	172.06	46.94
K^+	mg/L	29.74	7.53
Ca^{2+}	mg/L	67.07	9.16
Mg^{2+}	mg/L	19.77	5.01
Fe^{3+}	mg/L	0.05	0.01
Mn^{2+}	mg/L	0.10	0.01
NH_4^+	mg/L	4.06	0.17
Al^{3+}	mg/L	0.009	0
Ba^{2+}	mg/L	0.003	0
Sr^{2+}	mg/L	0.29	0.04

3.3 Tested Resins

The WAC resin used in all experiments is the Amberlite HPR8300 H. Resin's properties can be found in Table 3.2. Two different SBA resins were tested. Information about their backbone, matrix, functional group, total exchange capacity and swelling is available in Table 3.3. Both SBA resins have acrylic backbone and a Type I functional group. The SBA Resin 1 is the Amberlite SCAV4 Cl (SCAV4) and it has a macroporous matrix. The SBA Resin 2 is the Amberlite IRA458 Cl (IRA458) and it has a gel matrix.

---

[1] Aqualab Zuid B.V. is recognized by ministerial authority and is accredited by the RvA under registration number L387.

Table 3.2: WAC resin properties

Resin name	Amberlite HPR8300 H
Backbone	Acrylic
Matrix	Macroporous
Functional group	Carboxylic acid
Total exchange capacity	4.70 eq/L_r (H form)
Swelling ($H^+ \rightarrow Na^+$)	60%
Product data sheet	[41]

Table 3.3: SBA resins properties

Resin	SBA Resin 1	SBA Resin 2
Resin name	Amberlite SCAV4 Cl	Amberlite IRA458 Cl
Backbone	Acrylic	Acrylic
Matrix	Macroporous	Gel
Functional group	Type I	Type I
Total exchange capacity	≥ 0.80 eq/L_r (Cl form)	≥ 1.25 eq/L_r (Cl form)
Product data sheet	[42]	[43]

3.4 Operating Conditions

3.4.1 Resins Operating Conditions

Information about the operating conditions for the WAC resin such as height, diameter and resin's bed volume is given in Table 3.4. The total number of equivalents exchangeable ions, referred as total load (T. Load), can be calculated with Equation 3.1 based on the total exchange capacity of the Amberlite HPR8300 H resin (Table 3.2) and the used bed volume in H^+ form. The swelling of Amberlite HPR8300 H resin when it is converted from an H^+ form to a Na^+ form is 60% (Table 3.2). The resin's bed volume in Na^+ form can be calculated with Equation 3.2 based on the 1.6 swelling factor. Finally, the exchange capacity of the resin bed in Na^+ form can be calculated with Equation 3.1. In Table 3.5, information about the operating conditions for the two SBA resins can be found. The total number of equivalents exchangeable ions (T. Load) can be calculated in the same way with Equation 3.1.

Table 3.4: WAC resin operating conditions

WAC in column	K11 & K41
Column inner diameter (m)	0.153
Area (m^2)	0.0184
Resin bed height (H^+ form, m)	0.60
Resin bed volume (H^+ form, L_r)	11.03
Total exchange capacity (H^+ form, eq/L_r)	4.70 (Table 3.3)
T. Load (eq)	51.85
Swelling factor	1.60
Resin bed volume (Na^+ form, L_r)	17.65
Total exchange capacity (Na^+ form, eq/L_r)	2.94

$$T.Load\ (eq) = Total\ Exchange\ Capacity\ X\ Form\ (\frac{eq}{L_r}) \times Resin\ Bed\ Volume\ in\ X\ Form(L_r) \tag{3.1}$$

$$Bed\ Volume\ Y\ Form\ (L_r) = Bed\ Volume\ X\ Form\ (L_r)\ \times Swelling\ Factor \tag{3.2}$$

where

X, Y: two ionic forms of a resin

Table 3.5: SBA resins operating conditions

Resin name	Amberlite SCAV4 Cl	Amberlite IRA458 Cl
SBA in column	K21	K51
Column inner diameter (m)	0.153	0.153
Area (m^2)	0.0184	0.0184
Resin bed height (m)	1.06	1.06
Resin bed volume (L_r)	19.50	19.50
Total exchange capacity (eq/L_r)	0.80 (Table 3.4)	1.25 (Table 3.4)
T. Load (eq)	15.60	24.35

3.4.2 Production Operating Conditions

A down-flow production and up-flow regeneration were used in non-packed resin beds (counter-flow system). The same operating conditions were used in all experiments in order to derive comparable results and conclusions.

The production flow rate was kept stable at approximately 20 BVs/h for all experiments. The velocity through the cross-section of the column can be calculated with Equation 3.3. In Table 3.6 the used production flow rate and the cross-section velocity for the WAC resin and the SBA resins are given.

$$Cross - section\ Velocity\ \left(\frac{m}{h}\right) = \frac{Flow\ Rate\ \left(\frac{m^3}{h}\right)}{Area\ (m^2)} \tag{3.3}$$

Table 3.6: Production operating conditions

Resin name	Amberlite HPR8300 H	Amberlite SCAV4 Cl	Amberlite IRA458 Cl
Flow rate (L/h)	400	400	400
Flow rate (BVs/h)	22.65	20.50	20.50
Velocity (m/h)	21.75	21.75	21.75

3.4.3 Regeneration Operating Conditions

The regeneration consisted of six up-flow steps and one down-flow step, seven steps in total. The first step was backwash of the WAC column. Then, a solution with 2.5% HCl was injected only to the WAC column (red line in Figure 3.2) in order to replace the removed ions with H^+ ions. The acid was displaced from WAC column with demineralized water (displacement 1). A second chemical solution containing 4% NaOH was injected into both the WAC and SBA columns in series[2] (red line in Figure 3.3). The purpose of this step was to replace H$^+$ ions of the WAC resin with Na$^+$ ions, but not to replace the removed ions of the SBA resins with OH$^-$ ions. A third solution containing 8% NaCl was injected to both WAC and SBA columns in series[3] (red line in Figure 3.4). The purpose of this step was to replace the removed ions of SBA resin with Cl$^-$ ions. Then, the excess chemicals from both columns were displaced with demineralized water (displacement 2). The final regeneration step prior to a following production was a down-flow prewash of both columns in series with demineralized water. Information about the used chemicals in purchased form is available in Table 3.7.

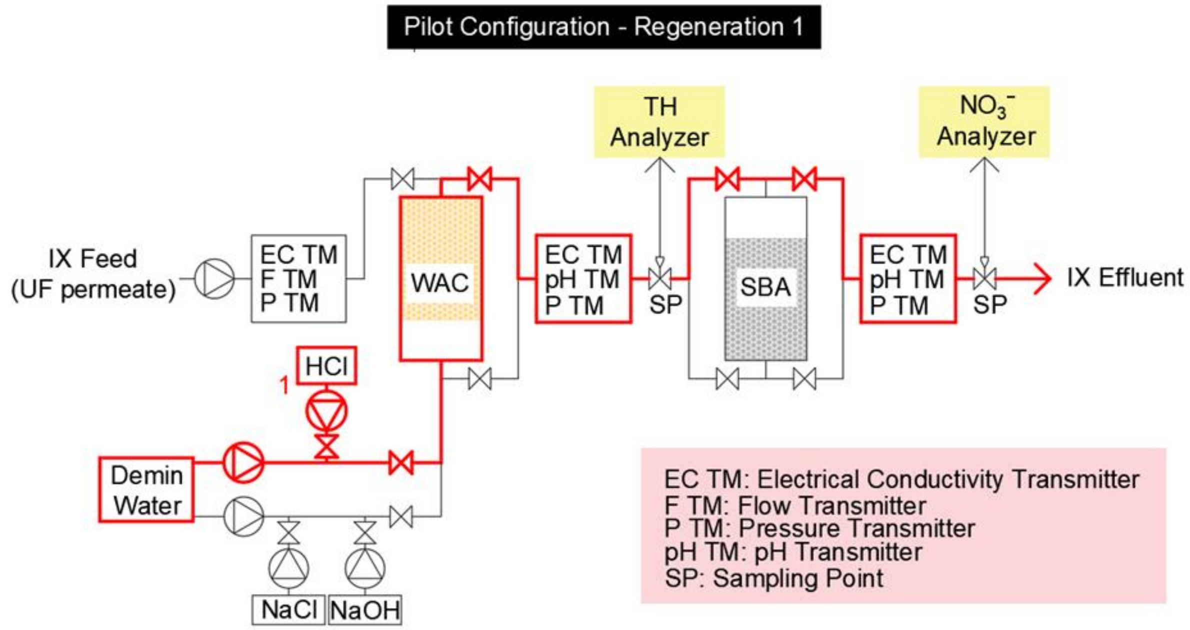

Figure 3.2: IX pilot configuration for one line during regeneration of WAC resin with HCl (regeneration flow with red)

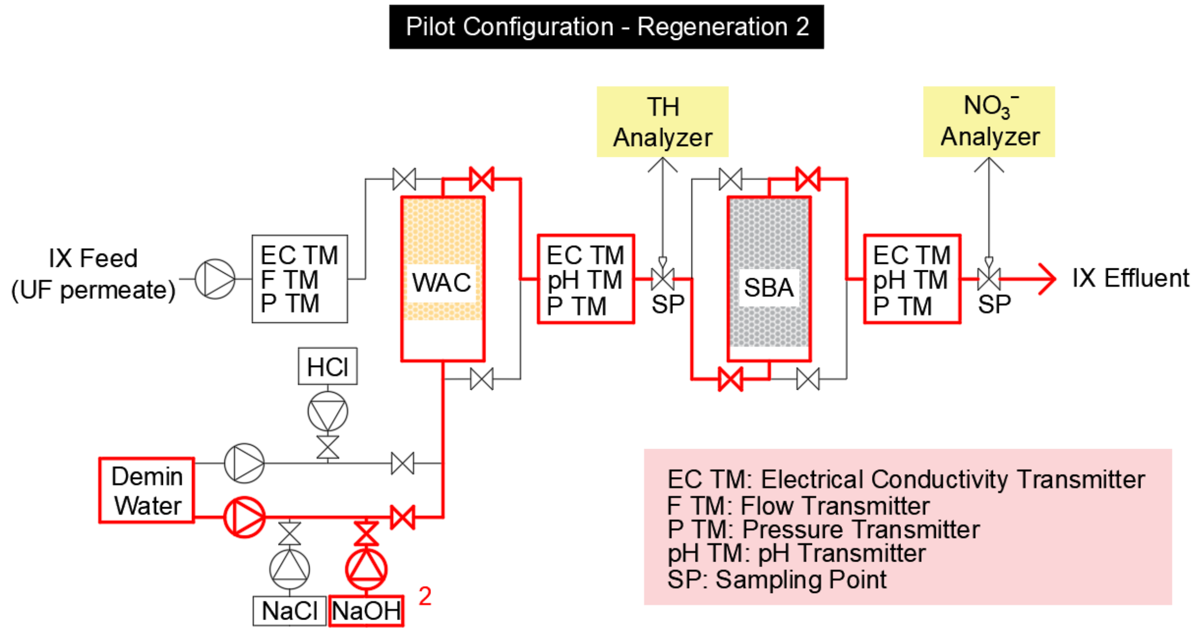

Figure 3.3: IX pilot configuration for one line during regeneration of WAC resin with NaOH (regeneration flow with red)

---

[2] The NaOH solution for WAC resin regeneration was also injected in the SBA column due to pilot's limitations.

[3] The NaCl solution for SBA resin regeneration was also injected in the WAC column due to pilot's limitations.

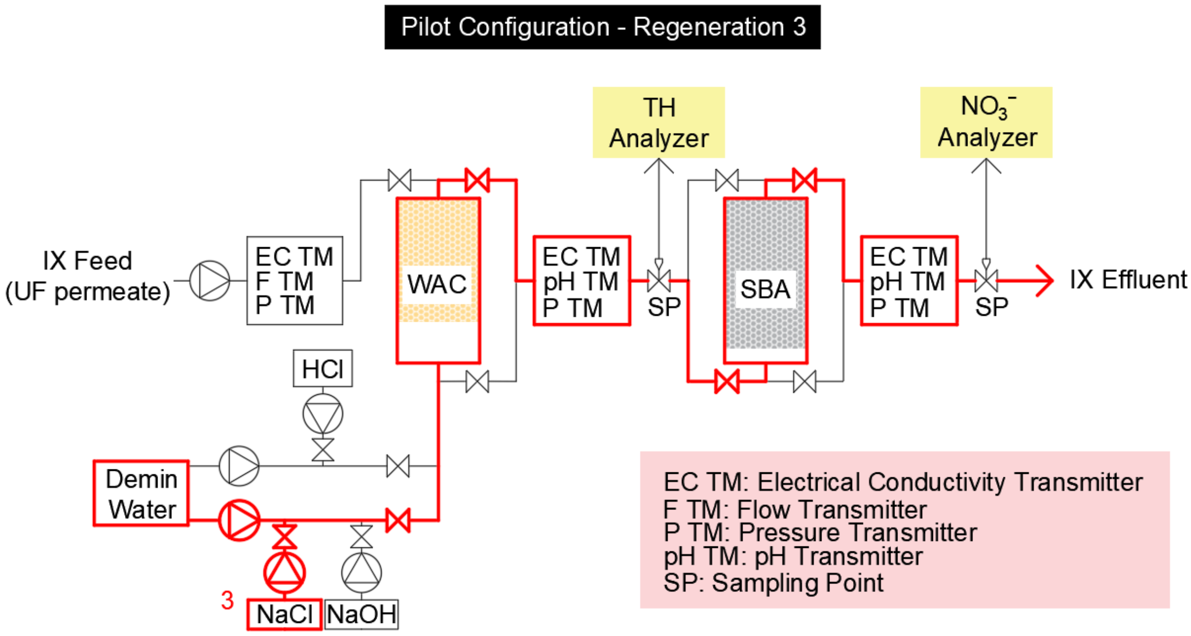

Figure 3.4: IX pilot configuration for one line during regeneration of SBA resin with NaCl (regeneration flow with red)

Table 3.7: Regeneration chemical

Chemical	30 % HCl	50 % NaOH	20 % NaCl
Density (g /L)	1149	1529	1156
Molar weight (g/mol)	36.458	39.998	58.44

Backwash

The backwash through only the WAC column had a flow rate of 180 L/h, which equals to 16.4 BVs/h (H^+ form). The resulted flow per m^2 resin bed is 9.8 $m^3/h/m^2$ and it is in the suggested range of 7 to 15 m/h. The backwash time was 5 min.

WAC Regeneration with HCl and NaOH

The optimal regeneration level of the WAC resin was obtained from two preliminary tests. These tests do not belong to the main research of this master thesis. They were conducted for operational purposes in order to make sure that regeneration with NaOH sufficiently regenerates the WAC resin but does not regenerates the SBA resins with OH^- ions. The optimal regeneration ratio for WAC resin regeneration was found to be 105%. The same WAC regeneration parameters were applied along this study. More information about the two preliminary experiments is available in Appendix D.

In Equation 2.5 of “Regeneration Ratio”, the component “Stoichiometrically Required” is the prior mentioned “T. Load”. The total regenerant passed (required chemical) can be calculated by reforming Equation 2.5 to Equation 3.4. The regeneration levels can be calculated with Equation 3.5. The required amounts of HCl and NaOH used for regeneration based on the 105% regeneration ratio are available in Table 3.8.

$$Total\ Regenerant\ Passed\ (eq) = Regeneration\ Ratio\ \times T.Load\ (eq) \tag{3.4}$$

$$Regeneration\ Level\ (eq/L_r) = \frac{Total\ Regenerant\ Passed\ (eq)}{Resin's\ Volume\ (L_r)} \tag{3.5}$$

The recommended concentration range for the regeneration of WAC resins with HCl is 2 to 5 % and with NaOH is 2 to 4 %. The minimum contact time for WAC resins regeneration is 20 minutes. The flow rate of the regenerant for diluted HCl was 110 L/h. The flow rate for diluted NaOH was 44 L/h. The concentration of HCl and NaOH used were 2.5 % and 4 %, respectively. The resulting flow rate of the dosed chemical can be calculated with Equation 3.6. Equation 3.7 gives the required demineralized water flow rate. The contact time can be calculated with Equation 3.8. In Table 3.9 the used flow rates and the resulting contact times for the HCl and NaOH dosing are given. It can be seen that both contact times were above the minimum of 20 min.

Table 3.8: WAC resin regeneration level

Regeneration ratio (%)	105
Load (eq)	51.85 (Table 3.5)
Total regenerant passed (eq)	54.45
Total regenerant passed (g HCl)	1984.74
Total regenerant passed (g NaOH)	2177.46
WAC resin bed volume (H^+ form, L_r)	11.03 (Table 3.5)
Regeneration level (H^+ form, g HCl/L_r)	179.92
Regeneration level (H^+ form, g NaOH/L_r)	197.39
Regeneration level (H^+ form, eq/L_r)	4.94

$$Chemical\ Flow\ (L/h) = \frac{Flow\ Rate\ (L/h) \times Concentration\ (g\ ch./L)}{Ch.Density\ (g\ pr./L) \times Ch.Content\ (g\ ch./g\ pr.)} \tag{3.6}$$

$$Demineralized\ Water\ Flow\ (L/h) = Flow\ Rate\ (L/h) - Chemical\ Flow\ (L/h) \tag{3.7}$$

$$Contact\ Time\ (h) = \frac{Total\ Regenerant\ Passed\ (g\ ch)}{Ch.Flow\ (L/h) \times Ch.Density\ (g\ pr./L) \times Ch.Content\ (g\ ch./g\ pr.)} \tag{3.8}$$

Table 3.9: WAC resin regeneration flow rates and contact time

Chemical	HCl	NaOH
Flow rate (L/h)	110	44
Flow rate (H^+ form, BVs/h)	10	4
Concentration (%)	2.50	4
Chemical flow rate (L/h)	8	2.30
Demineralized water flow rate (L/h)	102.30	41.80
Contact time (min)	43	74

SBA Regeneration with NaCl

The first three experiments for each tested SBA resin in this research were based on three regeneration levels of NaCl dosing. The recommended regeneration level of NaCl dosing for SBA resins regeneration of a non-packed resin bed in a counter-flow system is 70 to 120 g/L_r [31]. The selected regeneration levels were 80, 100 and 120 g/L_r.

The total regenerant passed and the regeneration ratio for each regeneration level can be calculated with Equations 3.5 and 3.4, respectively. The outcome of these calculations for the two tested SBA resins is given in Table 3.10.

Table 3.10: SBA resins regeneration levels

Regeneration level	RL1	RL2	RL3
Regeneration level (eq/L_r)	2.05	1.71	1.37
Regeneration level (g NaCl/L_r)	120	100	80
SBA resin bed volume (L_r)	19.50		
Total regenerant passed (eq)	40.02	33.35	26.68
Total regenerant passed (g NaCl)	2338.62	1948.85	1559.08
Amberlite SCAV4 Cl load (eq)	15.60		
Amberlite SCAV4 Cl regeneration ratio (%)	257	214	171
Amberlite IRA458 Cl load (eq)	24.35		
Amberlite IRA458 Cl regeneration ratio (%)	164	137	110

The recommended concentration for SBA resins regeneration with NaCl is 10 %. The minimum contact time for SBA resins regeneration is 20 minutes [31]. The flow rate of the regenerant for NaCl dosing was chosen to be equal to that flow rate of the regeneration with NaOH (44 L/h). The used concentration of NaCl was 8 %[4]. The chemical flow rates, the demineralized water flow rate and the contact time can be calculated with Equations 3.6, 3.7 and 3.8, respectively. The flow rates for the NaCl dosing used in all experiments are given in Table 3.11. The resulting contact times for the three regeneration levels are given in Table 3.12. It can be seen that all contact times were above the minimum of 20 min.

Table 3.11: SBA resins regeneration flow rates

Chemical	NaCl
Flow rate (L/h)	44
Flow rate (BVs/h)	2.25
Concentration (%)	8
NaCl flow rate (L/h)	15.25
Demineralized water flow Rate (L/h)	28.75

Table 3.12: SBA resins regeneration contact time

Regeneration level	1	2	3
Contact time (min)	40	33	26

---

[4] The selected NaCl concentration is lower than the recommended by DuPont Tech Fact 177-03729 [31]. This choice was the result of hydraulic limitations of the IX pilot. Operation out of the recommended ranges is possible.

Displacement

The flow rate for HCl displacement was the same as with the flow rate of HCl dosing and the flow rate for NaOH/NaCl displacement was the same with the flow rate of NaOH/NaCl dosing. Typically, 2 BVs are enough to wash out the excess of chemicals [31]. The operating conditions for the two displacement steps are given in Tables 3.13 and 3.14.

Table 3.13: Displacement of HCl

Flow rate (H^+ form, BVs of WAC/h)	10
Flow rate (L/h)	110
Throughput (H^+ form, BVs of WAC)	7
Contact time (min)	42

Table 3.14: Displacement of NaOH and NaCl

Flow rate (WAC-Na^+ form and SBA, BVs/h)	1.18
Flow rate (L/h)	44
BVs of WAC in Na^+ form and SBA (L)	37
Throughput (WAC-Na^+ form and SBA, BVs)	3
Contact time (min)	152

Prewash

The final step prior to production was prewash. The selected flow rate was 180 L/h. The resulting BVs/h for each column is within the suggested range by DuPont Tech Fact 177-03729. The throughput and the contact time are given in Table 3.15.

Table 3.15: Prewash

Flow rate (L/h)	180
Flow rate (BVs WAC/h)	10.20
Flow rate (BVs SBA/h)	9.24
BVs of WAC in Na^+ form and SBA (L)	37
Throughput (WAC-Na^+ form and SBA, BVs)	4.85
Contact time (min)	60

3.5 Determination of Resin Performance

3.5.1 Batches Operation, Breakthrough Point and Sampling

The performance of the two SBA resins at the tree regeneration levels given in sub-chapter 3.4.3 was based on their operational capacity and products water quality. For a specific system (tested resin, regeneration level etc.) a number of batches usually 3 to 5 are required so as the system to get stable. Each resin at each regeneration level (system) ran according to the operating conditions given in sub-chapter 3.4 for four or more batches (Appendix E). The NO_3^- concentration of the product water was measured with the online NO_3^- analyzer UV400 (TETHYS Instruments, FR) every 5 min. Also, the online TH analyzer Testomat EVO TH (Testomat ECO, DE) was measuring the TH concentration of the water streams after the WAC resin and before the SBA resins every 15 min. The production was stopped at a chosen breakthrough point based on the measured NO_3^- concentration and not at the full exhaustion of the resins. The chosen breakthrough concentration of NO_3^- was 30 mg/L (Table 3.16). For every batch, a NO_3^- breakthrough curve was made and a simplified operational capacity was calculated (see sub-chapter 3.5.2).

Table 3.16: NO_3^- breakthrough concentration

Average feed NO_3^- (mg NO_3^-/L)	51.50
Average feed NO_3^- (mg NO_3^--N/L)	11.63
Average feed NO_3^- (mmol/L or meq/L)	0.83
Breakthrough NO_3^- (mg NO_3^-/L)	30
Breakthrough NO_3^- (mg NO_3^--N/L)	6.77
Breakthrough NO_3^- (mmol/L or meq/L)	0.48
Breakthrough/Average (%)	58

In the final batch, samples of feed water and of product water were collected (Table 3.17). The feed samples were collected at the beginning of the production. The product water samples were collected along the production with higher frequency over the end of the production. The collection time of each sample during all experiments can be found in Appendix F.

Table 3.17: Number of samples for each sampling point per experiment

Number of samples	Experiment Resin. Regeneration Level					
Sampling point	1.1	1.2	1.3	2.1	2.2	2.3
Feed	1	1	1	1	1	1
Product	8	8	7	8	8	7

The measured parameters were electrical conductivity (EC), pH, adenosine triphosphate (ATP), total organic carbon (TOC), bicarbonate (HCO_3^-), chloride (Cl^-), sulfate (SO_4^{2-}), nitrate (NO_3^-), phosphate (HPO_4^{2-}-P), silicon dioxide (SiO_2), fluoride (F^-), sodium (Na^+), potassium (K^+), calcium (Ca^{2+}), magnesium (Mg^{2+}), iron (Fe^{3+}), manganese (Mn^{2+}), ammonium (NH_4^+), aluminum (Al^{3+}), barium (Ba^{2+}) and strontium (Sr^{2+}). All measurements were conducted by the independent water laboratory Aqualab Zuid B.V.

Based on the water quality of the collected samples breakthrough curves of the removed anions and TOC were drawn. Moreover, the operational capacity, the (volume) weighted average product water quality and the ion removal were calculated (see sub-chapters 3.5.2 and 3.5.3). Curves that give the relation between the regeneration level and the subsequent operational capacity for both resins were produced. Based on these curves, the assessment of resins performance as far as the operational capacity is concerned could be made. The best performing regeneration level for each SBA resin was selected based on the removal of NO_3^-, SO_4^{2-}, HPO_4^{2-}-P and TOC, the operational capacity and the used amount of chemical for regeneration.

3.5.2 Methodology of Calculations: Operational Capacity

The formula for the calculation of the operational capacity was given in Equation 2.7 of the theory chapter. The "Area" component of this equation refers to the equivalents of ions removed over a production run. This component was computed based on different inputs (i) for all batches resulting in the simplified operational capacity and (ii) for the last batch resulting in the operational capacity of the experiment.

For the simplified calculation of the operational capacity, it was assumed that all equivalents of HPO_4^{2-}-P, SO_4^{2-} and NO_3^- in the feed water were removed up to the breakthrough point. The IX feed water quality was not measured in each batch. The concentrations of HPO_4^{2-}-P, SO_4^{2-} and NO_3^- in the municipal wastewater effluent of Terneuzen (UF feed, thus IX feed) are measured twice per week. The closest measurement to every batch was used for the calculation of the simplified operational capacity. The volume of water produced up to the breakthrough point, known as throughput was calculated with Equation 3.9. The "Area" component for the simplified operational capacity was calculated with Equation 3.10. Thus, the simplified operation capacity is given by Equation 3.11.

$$Throughput\ (L) = Run\ Time\ (h) \times Flow\ Rate\ (\frac{L}{h}) \tag{3.9}$$

$$Simplified\ Area = \sum_{i=1}^{3} C_{Feed,i}\ (\frac{meq}{L})\ \times V(L) \tag{3.10}$$

where

i=1: HPO_4^{2-}-P

i=2: SO_4^{2-}

i=3: NO_3^-

$C_{Feed,\,i}$: feed concentrations of removed anions [meq/L]

V: throughput (volume of water produced) up to breakthrough [L]

$$Simplified\ Operational\ Capacity\ (\frac{meq}{L_r}) = \frac{Simplified\ Area\ (meq)}{Resin's\ Bed\ Volume\ (L_r)} \tag{3.11}$$

The operational capacity calculated based on the water quality of the collected feed and product samples was computed with Equation 3.12. The equivalents of ions removed ($Area_i$) in the interval between two product samples were calculated with Equation 3.13.

$$Operational\ Capacity\ (\frac{meq}{L_r}) = \frac{\sum_{i=1}^{n} Area_i\ \ (meq)}{Resin's\ Bed\ Volume\ (L_r)} \tag{3.12}$$

where

i: sample number

n: total samples number

$$Area_i = \left(\sum_{k=1}^{n} C_{Feed,k} - \sum_{k=1}^{n} C_{i,k}\right)(\frac{meq}{L})\ \times (V_i - V_{i-1})(L) \tag{3.13}$$

where

i: sample number

k: removed anion

n: total number of removed anions

$C_{Feed,k}$: concentrations of removed anions k in feed sample [meq/L]

$C_{i,k}$: concentration of removed anion k in sample i [meq/L]

V_i: throughput (volume of water produced) up to sample i [L]

V_{i-1}: throughput (volume of water produced) up to sample i-1 [L]

3.5.3 Methodology of Calculations: Weighted Average and Removal

The volume weighted average quality of the product water was calculated based on the product samples water quality for all ions, TOC and ATP with Equation 3.14. The removal achieved for all ions, TOC and ATP was calculated with Equation 3.15.

$$C_{VWA} = \frac{\sum_{i=1}^{n} C_i V_i}{V_n} \tag{3.14}$$

where

i: sample number

n: total samples number

C_{VWA}: volume weighted average concentration of a water quality parameter [mg/L]

C_i: concentration of a water quality parameter at sample i [mg/L]

V_i: throughput (volume of water produced) up to sample i [L]

V_n: throughput (volume of water produced) up to breakthrough [L]

$$Removal\ (\%) = \frac{C_{Feed} - C_{VWA}}{C_{Feed}} \times 100\% \tag{3.15}$$

where

C_{Feed}: feed concentration of a water quality parameter [mg/L]

C_{VWA}: volume weighted average concentration of a water quality parameter [mg/L]

3.6 Selectivity Order Experiments – SBA Resin Overrun

The best performing regeneration level for each SBA resins were used in the selectivity order experiments. The goal of these experiments was to determine the order in which the anions breakthrough. In this way, the place of HPO_4^{2-} in the anion selectivity order was found for the case of ion exchange treatment of municipal wastewater that contain HPO_4^{2-}, SO_4^{2-} and NO_3^- in fluctuating concentrations.

For these experiments, the water production did not stop at the 30 mg NO_3^-/L breakthrough concentration but it was continued, over the feed NO_3^- concentration, until a second anion in the product water reached its feed concentration. The continuation of the production while NO_3^- concentration in product water was higher than the NO_3^- feed concentration is referred in this research as "Overrun" of the SBA resins. During the experiment, the NO_3^- concentration of the product water was monitored with the online analyzer. Moreover, several grab samples of the product water were collected spread during production. The first samples were taken after the point where NO_3^- concentration was higher than 30 mg NO_3^-/L (previous breakthrough point). The HPO_4^{2-}-P concertation was measured in all samples with Hach Lange LCK 349 cuvette tests. Three of the grabbed product samples for each resin were selected based on the measured HPO_4^{2-}-P to be send to Aqualab for detailed analyses similar to the previous experiments.

3.7 RO Performance Estimation Experiments

3.7.1 Sample Collection and Transportation

The best regeneration level for each SBA resin was used in the RO performance estimation experiment. For each SBA resin, samples of the product water were collected in 10 L jerrycans at specific interval during production. A representative product water sample (composite) of 4 L for each SBA resin was then obtained by mixing the content of the jerrycans in appropriate percentages. Detailed information about the mixing ratios used for the representative product samples can be found in Appendix H. Also, one sample of 4 L from the feed water was collected.

2 L of each composite sample was used for the bio-growth potential test. The other 2 L was used for water quality analyses performed by Aqualab Zuid. The measured parameters were electrical conductivity (EC), pH, adenosine triphosphate (ATP), total organic carbon (TOC), bicarbonate (HCO_3^-), chloride (Cl^-), sulfate (SO_4^{2-}), nitrate (NO_3^-), phosphate (HPO_4^{2-}-P), silicon dioxide (SiO_2), fluoride (F^-), sodium (Na^+), potassium (K^+), calcium (Ca^{2+}), magnesium (Mg^{2+}), iron (Fe^{3+}), manganese (Mn^{2+}), ammonium (NH_4^+), aluminum (Al^{3+}), barium (Ba^{2+}) and strontium (Sr^{2+}).

3.7.2 RO Feed Qualities Organization

The three water samples used in the experiments correspond to three RO feed qualities as presented in Table 3.18. The samples names were based on the samples relevance to the IX pilot. These names were (i) “IX Feed” for the IX pilot feed (UF permeate), (ii) “Product 1” for the representative product water sample from SBA resin 1 (SCAV4) and (iii) “Product 2” for the representative product water sample from SBA resin 2 (IRA458).

Table 3.18: RO performance estimation – RO feed qualities

RO feed quality	Description	Relevance to IX pilot
1	RO feed pretreated with UF	IX Feed
2	RO feed pretreated with UF and IX - WAC & SBA resin 1	Product 1
3	RO feed pretreated with UF and IX - WAC & SBA resin 2	Product 2

3.7.3 Bio-growth Potential Test and Limiting Nutrient Determination

A methodology derived from Prest et al. (2015) [38] was applied to evaluate the bacterial growth potential of the sampled RO feed qualities and to identify the limiting nutrient. The method is based on incubation of water aliquots without nutrient addition (blank) and water aliquots after addition of different nutrient sources. The nutrient causing higher microbial growth compared to the blank and to the other conditions is identified as limiting nutrient in the tested water. Growth monitoring is performed with flow cytometry (FCM) measurements of the total bacterial cell concentrations (TCC) in water samples.

Samples Preparation and Handling

The IX Feed, the Product 1 and the Product 2 samples were stored in 2L glass vials and were transported on melting ice in a cooling box until analyses. The samples were filtered with a 0.45 µm pore size filter before the experiment in order to avoid predation. Each sample was divided in fifteen aliquots of 30 mL in 45 mL-volume Greiner tube to test five nutrient conditions in triplicates. The five types of aliquots that were produced from each one of the three sampled RO feed qualities are described in Table 3.19. Type 1 was an aliquot without any extra additives, denoted as blank. The concentration of N in the three samples was in excess compared to P and C. For this reason, N limitation was not expected and its assessment was combined with trace elements limitation. Therefore, type 2 was an aliquot with extra addition of N and trace elements (T). Type 3 was an aliquot with extra addition of P. Type 4 was an aliquot with extra addition of organic C. Finally, type 5 was an aliquot with extra addition of all previously mentioned nutrients (A). The N, P and C sources used for the limiting nutrient identification and their concentration in the final aliquots are available in Table 3.20. For the trace element additions, a Vishniac solution was used at a dilution of 1:50000 in the final aliquots (Table 3.21). All aliquots were incubated in the dark at 30 ^{o}C for 13 or more days, with constant mixing. The caps of the samples were opened and closed every day to ensure oxygen availability for the bacterial growth.

Table 3.19: Aliquots of the three RO feed qualities

Aliquot type	RO feed quality	1	2	3
		IX Feed	Product 1	Product 2
1	Blank	FB	P_1B	P_2B
2	Sample + N + T	FNT	P_1NT	P_2NT
3	Sample + P	FP	P_1P	P_2P
4	sample + C	FC	P_1C	P_2C
5	Sample + all (+ N + T + P + C)	FA	P_1A	P_2A

Table 3.20: Organic and inorganic nutrients additives

Nutrient	Compound	Compound concentration	Element concentration
N	Sodium nitrate ($NaNO_3$)	60 mg/L	10 mg N/L
P	Sodium phosphate monobasic dihydrate ($NaH_2PO_4\ 2H_2O$)	25 mg/L	5 mg P/L
C	Sodium acetate trihydrate ($CH_3COONa\ 3H_2O$)	283 mg/L	50 mg C/L

Table 3.21: Vishniac's trace elements solution in 1:50000 dilution

Compound	Stock solution concentration (kg/L)
$EDTA.H_2Na_2\ 2H_2O$	1
$FeSO_4\ 7H_2O$	0.0998
$ZnSO_4\ 7H_2O$	0.044
$CaCl_2\ 2H_2O$	0.1636
$MnCl_2\ 4H_2O$/ $MnSO_4\ H_2O$	0.1012/ 0.0864
$Na_2MoO_4\ 2H_2O$	0.0436
$CuSO_4\ 5H_2O$	0.0314
$CoSO_4\ 7H_2O$/ $CoCl_2\ 6H_2O$	0.0322 / 0.0279

Flow Cytometry (FCM) Measurements

TCC measurements were performed by flow cytometry along the incubation period of the aliquots until the stationary growth phase was reached. A BD Accuri™ C6 instrument (BD Accuri cytometers, BE) was used for the flow cytometry (FCM) measurements. Water samples of 500 µL were stained with 10 µL/mL SYBR® Green I (1:100 dilution in Milli-Q water) and incubated in the dark at 37 °C for 10 min before measurement. When required, the samples were diluted with Milli-Q water to obtain a bacterial cell concentration adapted to the flow cytometer, i.e. less than 2000 cells/µL. The flow cytometer used is equipped with a volumetric counting hardware, calibrated to measure the number of particles in 50 µL of a 500 µL sample. A pre-set flow rate of 50 µL/min was used. A threshold value of 700 was applied on the green fluorescence channel (FL1). All measurements were performed in duplicates. The data of all measurements were processed with the BD Accuri™ C6 software. Density plots of green fluorescence (FL1; 533 nm) against red fluorescence (FL3; >670 nm) were used to visually distinguish the stained bacterial cells and instrument noise or sample background. An electronic gate was used to select the signals of bacteria (e.g. in Figure 3.5). The exact same gate was used for all measurements in the form of a fixed template.

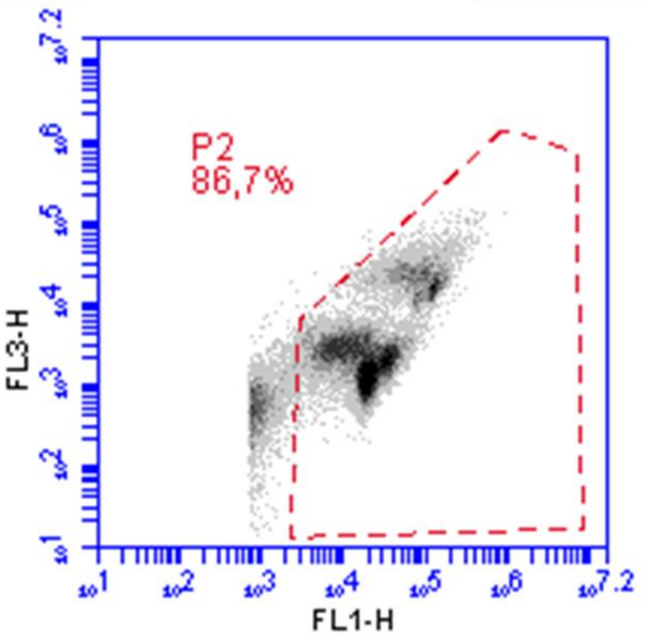

Figure 3.5: Density plot and gate (Red polygon)

Bacterial Growth Potential and Limiting Nutrient Identification

Bacterial growth curves were obtained after plotting the TCC in time for each aliquot type. Net bacterial cell growth was calculated from the increase of TCC between the start and the end of sample's incubation. Standard deviations were calculated from the triplicate aliquots. The bacterial growth potential of the three RO feed qualities was assessed by comparing the net bacterial cell growth of samples FB, P_1B and P_2B (aliquot type 1 of Table 3.19). The limiting nutrient for bacterial growth of each RO feed quality was assessed based on the comparison of the net bacterial cell growth of the first four aliquot types. For example, for Product 1 P_1B, P_1NT, P_1P and P_1C where compared. Finally, the aliquot type 5 was used as a positive control.

3.7.4 RO Scaling Experiments – Software Run

The water quality measurement of samples IX Feed, Product 1 and Product 2 were used as inputs for the RO feed in WAVE design software (DuPont). The RO design used for the software run is based on the design of the future full-scale RO unit for DECO factory of Evides Industry Water (Demin 2030 project). The outline of the design is given in Table 3.22. WAVE design software based on the feed water quality and the selected recovery provides information about the RO permeate and RO concentrate water quality.

Table 3.22: RO design in WAVE design software

Recovery		85 %	
Feed flow		281 m^3/L	
Stage	Pressure vessels (PVs)	Elements/ PV	Elements type
1	31	6	ECO PRO 400i
2	15	6	ECO PRO 400i
3	6	6	ECO PRO 400i

WAVE design software provides also solubility warnings about potential scaling issues and signal of anti-scalant dosing requirements. However, in order to obtain more accurate scaling potential information PHREEQC 3 (USGS) and Advisor Ci (Avista) software were used.

Both the RO feed water quality and RO concentrate water quality (obtained by WAVE design) of the three RO feed qualities were simulated with PHREEQC 3 in order to evaluate the scaling potential in the first RO stage as well as in the last RO stage. In this way, if any scalant type becomes saturated during RO operation could be identified. The saturation indices of a range of minerals were predicted. The following rules were followed to assess results:

1. A positive saturation index (SI) indicates precipitation of minerals (scaling may occur)
2. A negative saturation index (SI) indicates dissolution of minerals (no scaling)
3. A saturation index (SI) within the range of [-0.2,0.2] indicates equilibrium between the solid and the liquid phase of minerals (no scaling)

The scaling potential after anti-scalant dosing was evaluated with the use of Advisor Ci. The feed water quality for the three RO feed qualities, the aiming recovery (85%) and the same amount of recommended anti-scalant was used (2.0 mg/L of Vitec 3000) in Advisor Ci. The minerals saturation state also referred as scaling tendency (%) was computed by the software. A saturation state above 100% indicates high scaling potential [37].

4. Results and Discussion

4.1 Results Resins Performance at Different Regeneration Levels Experiments

4.1.1 Breakthrough Curves Profile

The breakthrough curves of the removed anions for Amberlite SCAV4 Cl (SCAV4) and Amberlite IRA458 Cl (IRA458) at regeneration level 2 (100 g NaCl/L_r) are depicted in Figure 4.1. The breakthrough curves for both resins at all three regeneration levels follow a similar pattern. For this reason, the breakthrough curves of the removed anions for both resins in the other two regeneration levels are given in Appendix F. Also, more details for all experimental results can be found in the same appendix.

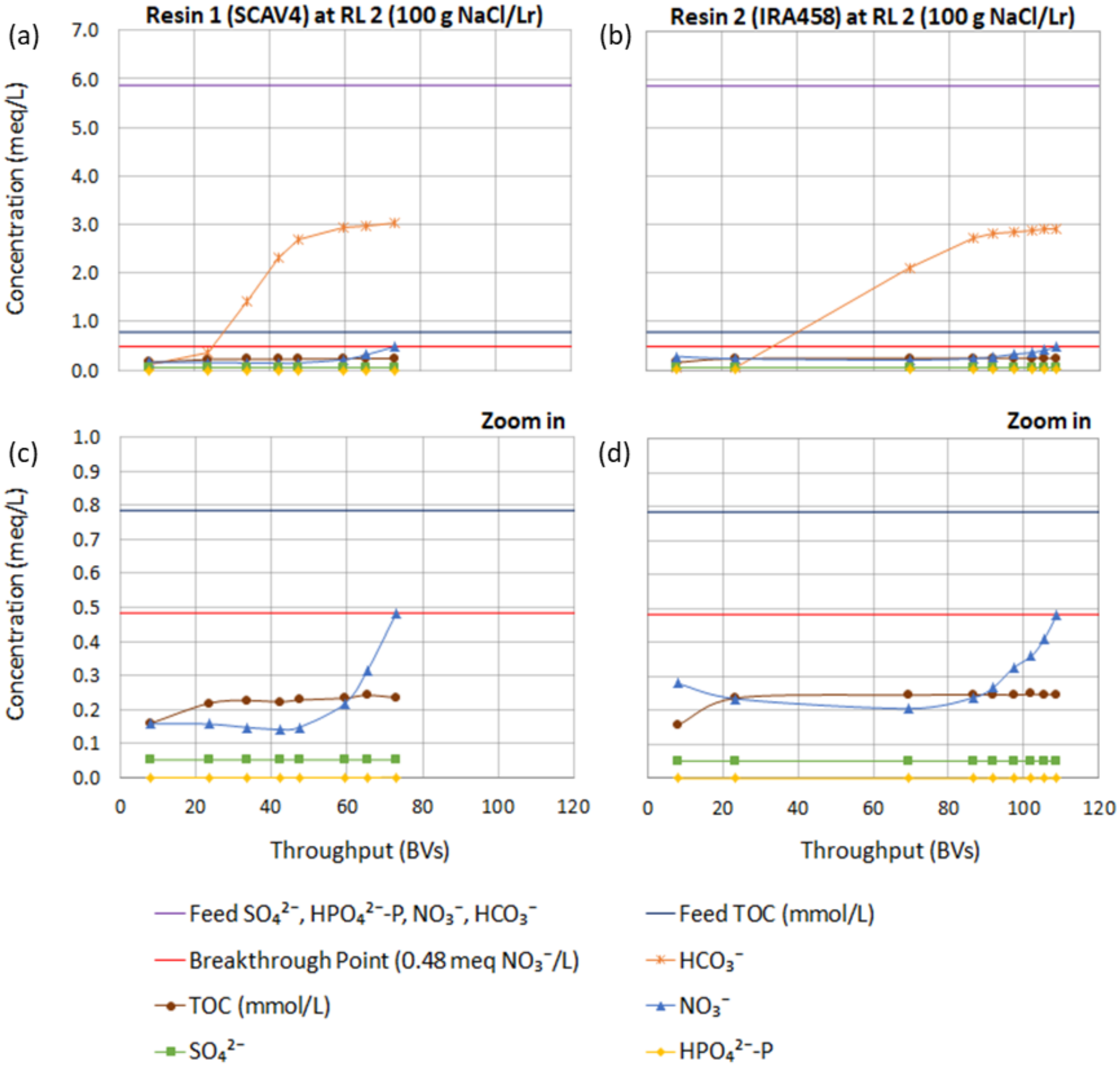

Figure 4.1: Breakthrough curves of removed anions and TOC (a) Resin 1 (SCAV4) at regeneration level 2 (100 g NaCl/L_r), (b) Resin 2 (IRA458) at regeneration level 2 (100 g NaCl/L_r), (c) *Resin 1 (SCAV4) at regeneration level 2 (100 g NaCl/L_r)* – Zoom in, (d) *Resin 1 (IRA458) at regeneration level 2 (100 g NaCl/L_r)* – Zoom in.

Both SCAV4 and IRA458 resins removed HCO_3^-, NO_3^-, SO_4^{2-} and HPO_4^{2-}-P anions[5]. Specifically, the removed anions were exchanged for Cl^-. HCO_3^- was the first anion to break through during production as it can be seen in Figures 4.1a and 4.1b. The second anion that broke through was NO_3^-. In Figures 4.1c and 4.1d, y-axis adjusted graphs (up to 1 meq/L) of the breakthrough curves of NO_3^- and the concentrations of HPO_4^{2-}-P, and SO_4^{2-} in product water samples for SCAV4 and IRA458 at regeneration level 2 (100 mg NaCl/Lr) are given. SO_4^{2-} concentration in all product water samples of all experiments was below detection limit (0.1 meq/L). HPO_4^{2-}-P concentration in most product water samples of all experiments was below the detection limit (0.0012 meq/L) and in all of them below 0.01 meq/L. The production was stopped at a chosen breakthrough concentration of NO_3^- (0.48 meq/L). Hence, SO_4^{2-} and HPO_4^{2-}-P concentrations remain in low levels up to NO_3^- breakthrough concentration. TOC was also removed by SCAV4 and IRA458 and its concentration in the product water remained stable throughout production.

The anion selectivity order based on the results is the following:

$HCO_3^- < NO_3^- < SO_4^{2-}, HPO_4^{2-}$

SCAV4 and IRA458 resins have lower affinity towards HCO_3^- than NO_3^-. Also, NO_3^- is less preferred than SO_4^{2-} and HPO_4^{2-}. The order of SO_4^{2-} and HPO_4^{2-} in the selectivity order cannot be determined from the results of these experiments.

Moreover, SCAV4 was found to have slightly higher selectivity towards NO_3^- compared to IRA458. This can be explained by the fact that SCAV4 is macroporous resin while IRA458 is gel. Macroporous resins usually have greater affinity for a given ion than gel resins because of the combination of larger porous and higher crosslinking that provides a heterogeneous distribution of structurally dense and tortuous regions of high charge density [22].

From Figures 4.1c and 4.1d, a leakage of NO_3^- in the product water can be noticed from an early point in the production. NO_3^- was detected even in the first product water sample of every experiment. This NO_3^- leakage that remained stable through production up to a point that the breakthrough of NO_3^- started (usually 4th or 5th sample) would be referred in this report as "baseline leakage". In ion exchange column operation, the resin bed is loaded resulting in the formation of ion layers throughout the resin bed [22]. Both SBA resins (SCAV4 and IRA458) before first use were in Cl^- form as depicted in Figure 4.2a. During first production the resins bed was loaded with ions of HCO_3^-, NO_3^-, SO_4^{2-} and HPO_4^{2-}-P, which were exchanged creating layers in the resin bed as shown in Figure 4.2b. The order of the layer derives from the selectivity order discussed above. At the end of the first production, the NO_3^- layer reaches the bottom of the column as it can be seen in Figure 4.2c. Ion exchange resins cannot be fully regenerated and a part of the resin bed remains exhausted [16]. In the experiments, the regeneration was upward (counter-flow system) and the resin beds were non-packed. As a result, during regeneration the resin beds were not compacted causing a high mixing of the resin bed. Subsequently, the resins that remained exhausted after regeneration were spread throughout the resin bed and hence near the outlet (Figure 4.2d). In the following production, SO_4^{2-} and HPO_4^{2-}-P ions that have higher affinity compared to NO_3^- pushed the remained NO_3^- towards the bottom of the column leading to the NO_3^- baseline leakage that was observed in all experiments.

---

[5] Based on the pH of the samples the dominant phosphate species was the divalent HPO_4^{2-}.

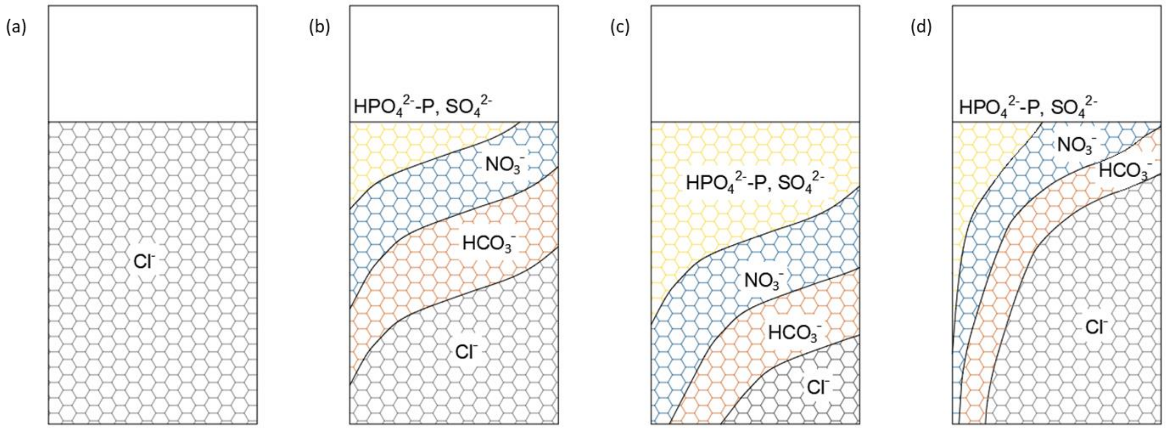

Figure 4.2: Anion layers in the resin bed (a) before first production, (b) during first production, (c) in the end of the first production, (d) after regeneration/ before following production

In Table 4.1, the volume weighted average baseline leakage of NO_3^- for the two resins at the three regeneration levels is given. It was noted that a lower regeneration level resulted in a higher concentration of NO_3^- baseline leakage for both resins. When lower amount of NaCl is dosed during regeneration, less Cl^- ions are available to regenerate the SBA resins and a bigger part of the resin bed remains exhausted. Thus, a higher concentration of NO_3^- is contained in the resin bed in the following production that leads to higher concentration of NO_3^- to be pushed out of the resin bed by the competitive ions.

Table 4.1: NO_3^- baseline leakage at the different regeneration levels

NO_3^- baseline leakage (mg/L)			
Regeneration level (g NaCl/L_r)	120	100	80
Resin 1: SCAV4	4.60	9.40	17.20
Resin 2: IRA458	7.90	14.05	22.20

4.1.2 Operational Capacity

The operational capacities that were calculated based on HCO_3^-, NO_3^-, HPO_4^{2-}-P, SO_4^{2-} and TOC removal for the two SBA resins at the three regeneration levels are given in Table 4.2 and in Figure 4.3. The operational capacity calculated at the different regeneration levels for SCAV4 was 36 to 46% of its total capacity. The operational capacity of IRA458 was 35 to 42 % of its total capacity. The total capacity of IRA458 is higher than that of SCAV4. Consequently, the operational capacities achieved at each regeneration levels for IRA458 were higher than that for SCAV4. The operational capacity usually ranges between 40 and 70% of the total resin capacity [29]. The ratios of the operational capacity over the total resin capacity achieved in the experiments are closer to the lower limit of the above mention range. In a column process, in order to maintain an acceptable product water quality, the production is terminated at a chosen breakthrough concentration of a certain ion (breakthrough point); as a result, a part of the resin bed is not exhausted. The chosen breakthrough concentration has an effect on the achieved operational capacity [16]. In the experiments of this research, the chosen breakthrough concentration was 30 mg NO_3^-/L (50% of the feed NO_3^- concentration). If a breakthrough concentration above 30 mg NO_3^-/L was chosen, the calculated operational capacity would have been higher and thus the ratio over the total capacity would have been greater, because a bigger number of the available exchange sites (Cl^- form) would have been used.

Table 4.2: Operational capacity at the different regeneration levels – Resins 1 (SCAV4) and resin 2 (IRA458)

Regeneration level (g NaCl/L_r)		120	100	80
Resin 1: SCAV4	Operational capacity (eq/L_r)	0.328	0.367	0.287
	Operational capacity/ Total capacity (%)	41	46	36
Resin 2: IRA458	Operational capacity (eq/L_r)	0.530	0.451	0.431
	Operational capacity/ Total capacity (%)	42	36	35

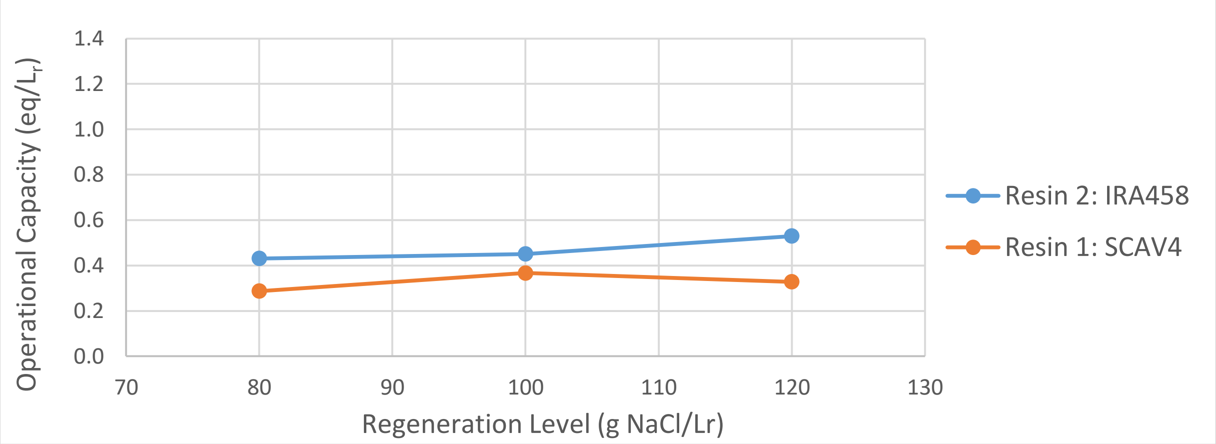

Figure 4.3: Operational capacity at the different regeneration levels – Resins 1 (SCAV4) and resin 2 (IRA458)

The operational capacity depends on the regeneration level [22]. It was observed that a higher regeneration level resulted in an increase of the operational capacity. As it was mentioned before in column operation, resins are not totally regenerated and part of the resin bed remains exhausted [16]. When higher amount of NaCl is dosed during regeneration, more Cl^- ions are available to regenerate the SBA resins and a smaller part of the resin bed remains exhausted. Therefore, a greater number of exchange sites is available for ion exchange to take place in the following production. All calculated operational capacities follow this rule with only exception that of SCAV4 at regeneration level 1. On the day of the experiment for the regeneration level 1 (120 g NaCl/L_r), the anion feed concentration was higher compared to the other two experimental days (Table 4.3). Specifically, the concentration of HPO_4^{2-}-P was triple, of SO_4^{2-} was approximately 15 % higher and HCO_3^- was approximately 50% higher. The presence of competitive ion has been reported to affect the removal of a certain ion [17, 19]. Thus, the increased concentrations of the competitive anions might have resulted in NO_3^- product water concentration to reach the breakthrough concentration faster. Subsequently, the computed operation capacity of SCAV4 for regeneration level 1 is lower than expected.

Table 4.3: Feed anion concentrations in the experiments of the three regeneration levels

Regeneration level (g NaCl/L_r)	120	100	80
HCO_3^- (meq/L)	4.26	3.11	2.62
SO_4^{2-} (meq/L)	2.29	1.92	2.08
NO_3^- (meq/L)	0.94	0.79	0.98
HPO_4^{2-}-P (meq/L)	0.49	0.14	0.13
Sum (meq/L)	7.98	5.96	5.82

4.1.3 Volume Weighted Average Product Water Quality and Removal

The product water quality obtained by the volume weighted average concentrations of the anions and TOC at the three regeneration levels for SCAV4 and IRA458 are given in Tables 4.4 and 4.5, respectively. The subsequent removal percentage based on the feed concentrations for SCAV4 and IRA458 is shown in Figure 4.4.

The resins were regenerated into Cl^- form, thus the removed anions were exchanged for Cl^- ions. Cl^- has higher affinity towards SBA resins compared to HCO_3^- [22]. However, HCO_3^- was partially removed (below 50%) by both SBA resins. A possible explanation is that the selectivity barrier was overcome due to high content of HCO_3^- equivalents in the feed water. SO_4^{2-} concentration at all regeneration levels was below the detection limit of 5 mg/L and its removal was 97% to 98%. HPO_4^{2-}-P concentration was in most cases below or equal to the detection limit of 0.02 mg/L with a removal of 99% to 100%. The only exception was experiment 1.1 (SCAV4 – RL1), where the volume weighted average HPO_4^{2-}-P concentration was 0.10 mg/L, but the removal was 99% since on that experimental day the feed concertation of HPO_4^{2-}-P was much higher than on the other two.

TOC is negatively charged and during ion exchange treatment is partially removed by exchange and partially by adsorption. Typically, TOC removal by SBA resins is about 50 to 70% [22]. The removal of TOC by both SCAV4 and IRA458 at all three regeneration levels was approximately the same and within the expected range. Resins with greater porosity demonstrate a better performance for TOC removal [22]. Indeed, the macroporous SCAV4 seems to remove slightly more TOC compared to the gel IRA458, but the difference was merely 2%.

A relationship between the regeneration level and the NO_3^- volume weighted average concentration was noted. Lower regeneration levels led to lower NO_3^- removal for both resins. This lower NO_3^- removal at lower regeneration levels was caused by the higher NO_3^- baseline leakage. As explained earlier in sub-chapter 4.1.1, lower regeneration levels result to higher concentration of NO_3^- baseline leakage. The production of both resins was terminated at the same breakthrough concentration of 30 mg NO_3^-/L, hence the product water quality expressed by the volume weighted average concentration of the product samples was determined by the NO_3^- baseline leakage concentration.

Table 4.4: Volume weighted average product water quality at the three regeneration levels for Resin 1 (SCAV4)

Regeneration level (g NaCl/L_r)	120	100	80
HCO_3^- (mg/L)	181.75	109.70	104.80
SO_4^{2-} (mg/L)	< 5	< 5	< 5
NO_3^- (mg/L)	7.85	13.05	18.20
HPO_4^{2-}-P (mg/L)	0.10	< 0.02	< 0.02
TOC (mg/L)	3.30	2.65	2.40

Table 4.5: Volume weighted average product water quality at the three regeneration levels for Resin 2 (IRA458)

Regeneration level (g NaCl/L_r)	120	100	80
HCO_3^- (mg/L)	174.85	116.25	87.10
SO_4^{2-} (mg/L)	< 5	< 5	< 5
NO_3^- (mg/L)	11.10	15.60	23.05
HPO_4^{2-}-P (mg/L)	< 0.02	< 0.02	0.02
TOC (mg/L)	3.50	2.85	2.65

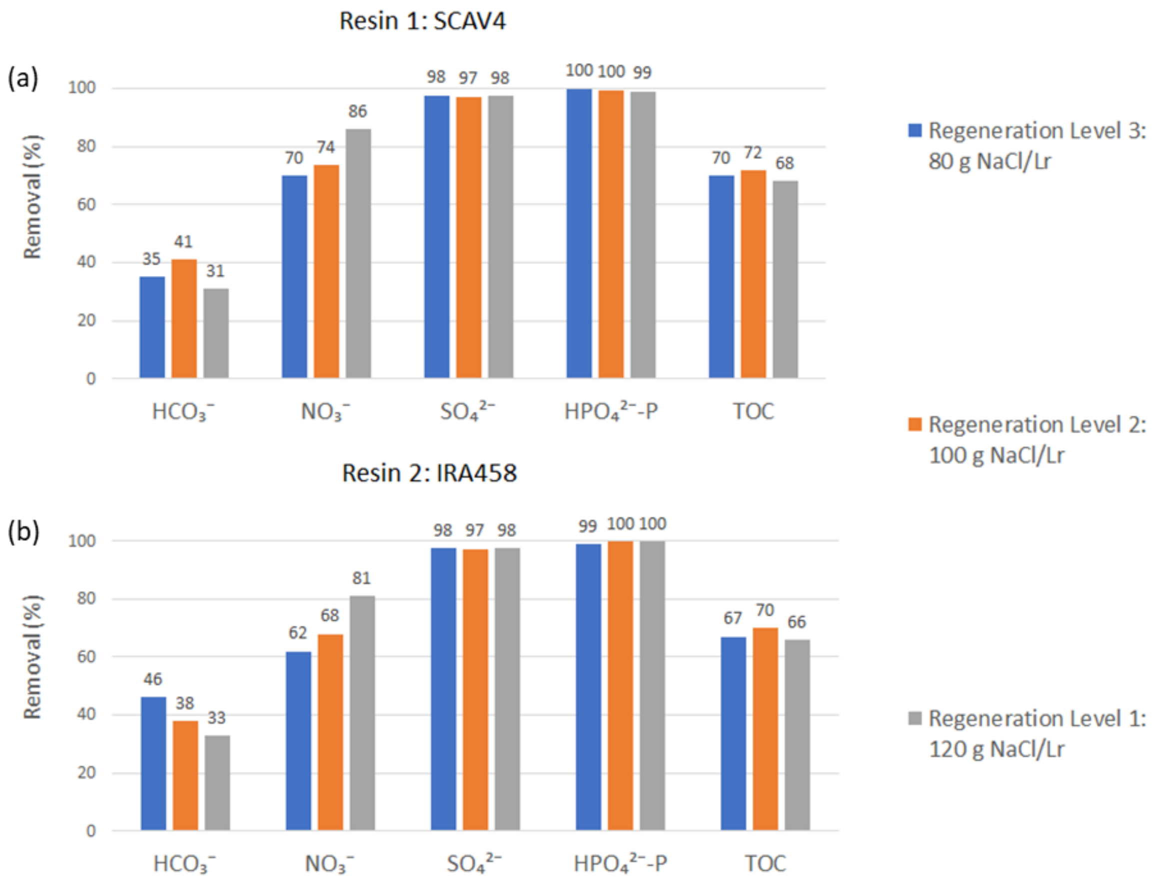

Figure 4.4: Removal of anion and TOC at the three regeneration levels by (a) resin 1 (SCAV4) and (b) resin 2 (IRA458)

4.1.4 Resins Performance at the Different Regeneration Levels

The best performing regeneration level for each resin was selected based on the removal of NO_3^-, SO_4^{2-}, HPO_4^{2-}-P and TOC, on the operational capacity and on the amount of chemicals used for regeneration. For both SCAV4 and IRA458 the removal of HPO_4^{2-}-P, SO_4^{2-} and TOC was similar at the three regeneration levels. The production was terminated at NO_3^- breakthrough concentration of 30 mg/L. It was found that HPO_4^{2}-P and SO_4^{2-} concentrations remained in low levels (below detection limit) up to the breakthrough point, therefore their removal was the same at all regeneration levels. As explained in sub-chapter 4.1.3, the removal of NO_3^- increased with increasing regeneration levels on account of lower NO_3^- baseline leakage after higher regenerant dosing. Thus, the lowest NO_3^- concentration in product water was achieved at regeneration level 1 and it was 7.85 mg/L and 11.10 mg/L for SCAV4 and IRA458, respectively. These concentrations of NO_3^- corresponds to a nitrogen (N) content in product water samples that is in excess for bacterial growth compared to phosphorus (P) and carbon (C) content of the product water samples, according to the C:N:P ratio of 100:20:1.7 required for bacterial growth [21]. On that account, even a higher NO_3^- concentration in the product water is expected to have a similar effect on the bacterial growth.

As discussed in sub-chapter 4.1.2, the operational capacity increased with an increasing regeneration level for SCAV4's regeneration levels 2 and 3. However, regeneration level 1 resulted in a lower operational capacity compared to regeneration level 2, which was the result of higher feed anions concentrations as explained before. If the feed anions concentrations were equal to the other two experiments, the computed operational capacity would be expected to be higher. For IRA458, the operational capacity increased with an increasing regeneration level for all three regeneration levels. Hence, the highest operational capacity was obtained at regeneration level 1.

All the above points are gathered in Figure 4.5 to facilitate the comparison between the three regeneration levels for each resin. Regeneration level 2 was chosen for both SCAV4 and IRA458. Even regeneration level 3 could have been a choice since the effect of the different regeneration levels on the product water quality and the operational capacity was found to be limited. But, the regeneration level that provides a balance between the used amount of regeneration chemicals, the product water quality and the operational capacity was chosen.

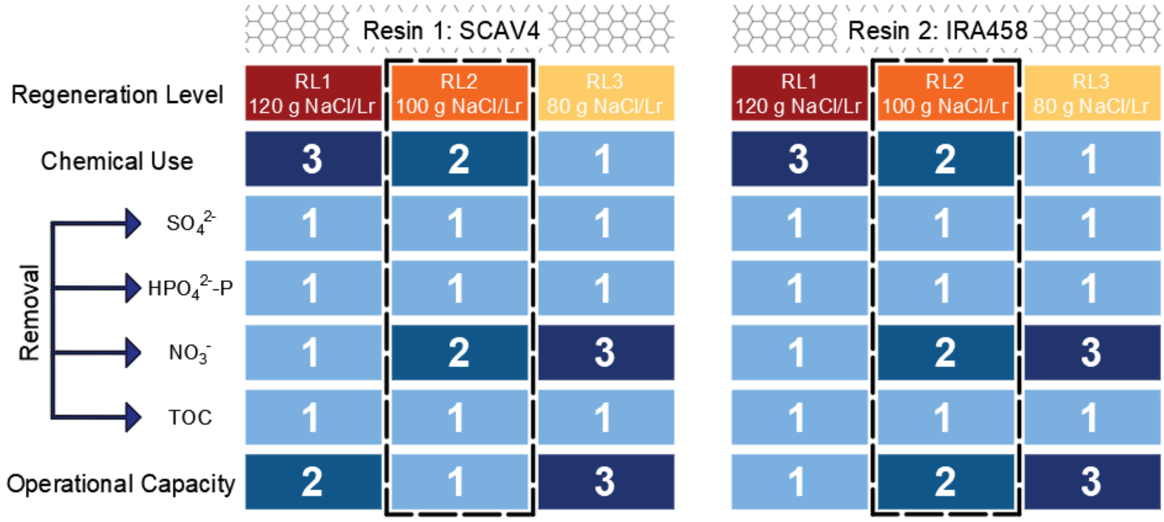

Resin	Regeneration Level	Chemical Use	SO_4^{2-}	HPO_4^{2-}-P	NO_3^-	TOC	Operational Capacity
Resin 1: SCAV4	RL1 120 g NaCl/Lr	3	1	1	1	1	2
	RL2 100 g NaCl/Lr	2	1	1	2	1	1
	RL3 80 g NaCl/Lr	1	1	1	3	1	3
Resin 2: IRA458	RL1 120 g NaCl/Lr	3	1	1	1	1	1
	RL2 100 g NaCl/Lr	2	1	1	2	1	2
	RL3 80 g NaCl/Lr	1	1	1	3	1	3

Figure 4.5: SCAV4 and IRA458 performance at the three regeneration levels comparison. No color gradient and the same number indicate no difference between the regeneration levels. The color gradients and the number indicate difference and the ranking of the three regeneration levels (darker color and higher number → worse value). The black dashed line indicates the chosen regeneration level for each resin.

4.2 Results Selectivity Order Experiments– SBA Resin Overrun

The experiments presented in sub-chapter 4.1.1 resulted in an anion selectivity order that complies with the generally accepted anion selectivity order for type I SBA resins ($HCO_3^- < NO_3^- < SO_4^{2-}$) [16, 22]. It was found that for both tested SBA resins HCO_3^- is less preferred than NO_3^-, which is less preferred than the divalent SO_4^{2-} and HPO_4^{2-}. The results of the SBA resins “overrun” experiments for the determination of the selectivity order between SO_4^{2-} and HPO_4^{2-} are presented in Figure 4.6. It can be seen that after NO_3^- breakthrough the next anion to breakthrough was HPO_4^{2-}-P for both resins. HPO_4^{2-} was the dominant phosphate species based on the pH of the samples. SO_4^{2-} concentration remained below detection limit (0.1 meq/L) in all product samples. The effluent NO_3^- concentrations rose above its influent concentration as HPO_4^{2-} ions displaced NO_3^- ions from the resin bed. Therefore, HPO_4^{2-}-P started being detected in product water samples at the point where NO_3^- reached its highest concentration. It is noteworthy that both HPO_4^{2-}-P and SO_4^{2-} remained below detection limit up to the point where NO_3^- concentration in product water was equal to feed NO_3^- concentration. Consequently, the same removal of HPO_4^{2-}-P and SO_4^{2-} can be achieved up to the that point, which results to a higher operational capacity with the same product water quality regarding HPO_4^{2-}-P and SO_4^{2-}, but higher NO_3^- concentration.

The anions selectivity order for both SCAV4 and IRA458 based on all experiments is the following:

$HCO_3^- < NO_3^- < HPO_4^{2-} < SO_4^{2-}$

The resulted selectivity order is in accordance with the expectation that the divalent SO_4^{2-} and HPO_4^{2-} are more preferred by SBA resins than the monovalent NO_3^- [24, 17]. Furthermore, HPO_4^{2-} was found to be less preferred than SO_4^{2-}. For ions having the same charge, their hydrated radius plays an important role in selectivity. Ions with smaller hydrated radius have higher affinity because they reduce the swelling pressure of the resins and are more tightly bound to the resin [24, 16]. SO_4^{2-} has a smaller hydrated radius compared to HPO_4^{2-} [44], which might have resulted to the latter's lower selectivity. The lower selectivity towards HPO_4^{2-} compared to SO_4^{2-} by SBA resins was also supported by Boari et al. (1976) [18] and Awual et al. (2015) [15], although opposed by Liberti et al. (1977) [14].

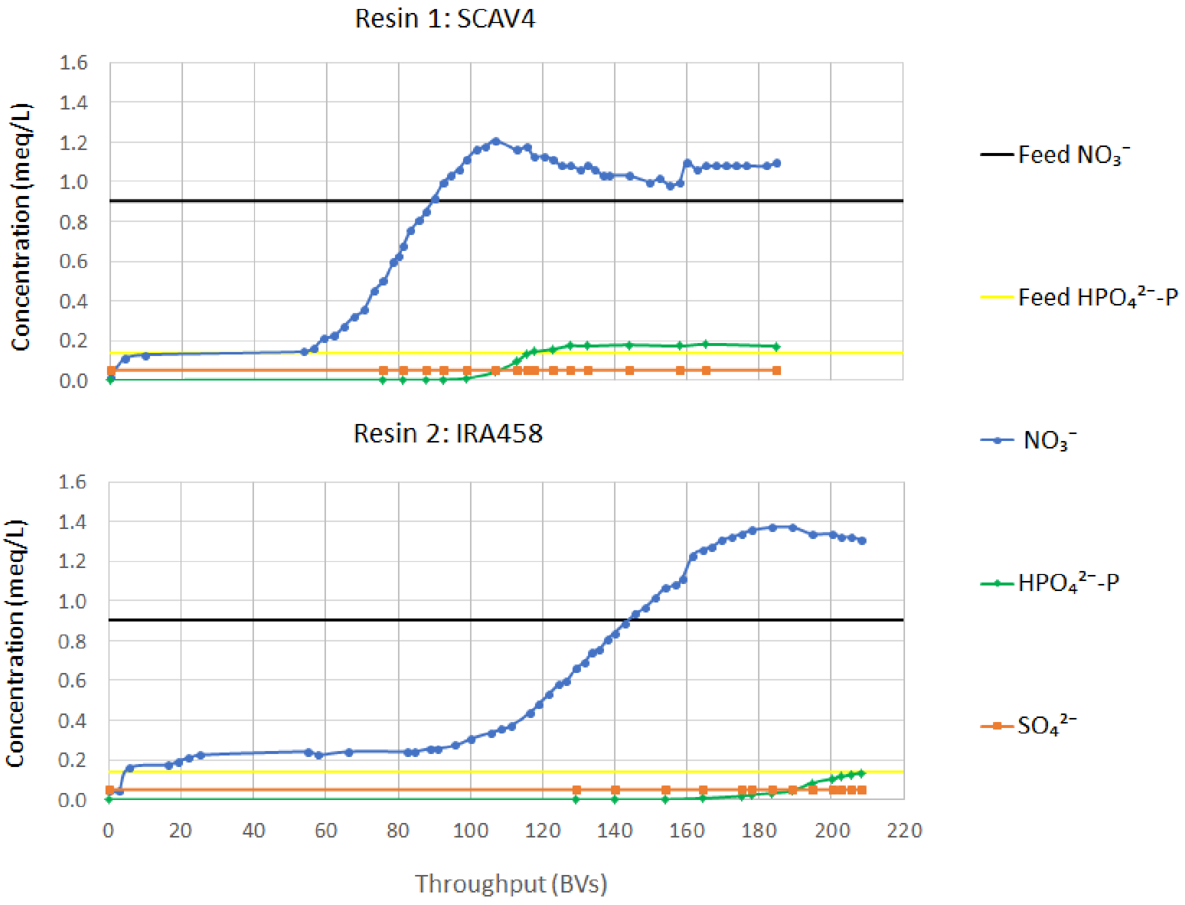

Figure 4.6: Overrun of resin 1 (SCAV4) and resin 2 (IRA458) to determine selectivity order of NO_3^-, HPO_4^{2-}-P and SO_4^{2-}

4.3 Results RO Performance Estimation Experiments

4.3.1 Bio-growth Potential Test

The effect of RO feed pretreatment with ion exchange on the RO biofouling potential was assessed based on three RO feed qualities. RO feed quality 1, referred as IX Feed, was municipal wastewater effluent pretreated with only an UF step. RO feed quality 2, referred as Product 1, was municipal wastewater effluent pretreated with an UF step and an ion exchange step consisting of the HPR8300 WAC resin and the SCAV4 SBA resin. RO feed quality 3, referred as Product 2, was municipal wastewater effluent pretreated with an UF step and an ion exchange step consisting of the HPR8300 WAC resin and the IRA458 SBA resin.

The concentrations of C, N, P and ATP in the three RO feed qualities are given in Table 4.6 (more measurements are available in Appendix H). Ion exchange treatment with both SBA resins resulted in

P, N and C removal of approximately 99%, 83% and 70%, respectively. Moreover, the ATP concentration was reduced after ion exchange treatment, which indicates that bacteria were retained in resin columns. In Figure 4.7, the net bacterial growth for the three RO feed qualities in the blank aliquots (no extra additives) are given. IX Feed (RO feed quality 1) supported bacterial growth up to 54 ± 1.5 × 10^6 cells/mL, while Product 1 (RO feed quality 2) and Product 2 (RO feed quality 3) supported bacterial growth up to 3.4 ± 0.3 × 10^6 cells/mL and to 1.25 ± 0.2 × 10^6 cells/mL, respectively. The reduction of bacterial growth potential between the IX Feed and Product 1 was 94%. The reduction of bacterial growth potential between the IX Feed and Product 2 was 98%. It can be concluded that lower amounts of nutrients were available for bacteria growth after ion exchange treatment with either SBA resin. Bacteria require nutrients to grow and produce EPS, thus form biofilms [6]. Limitation in nutrients availability is a proposed method for biofouling control [6, 11, 34, 35]. Subsequently, lower biofouling is expected in the RO modules by using feed water pretreated with UF and ion exchange with either SBA resin (Product 1 and 2) compared to feed water pretreated with only UF (IX Feed).

The water produced by IRA458 (Product 2) appears to have a lower bacterial growth potential compared to the water produced by SCAV4 (Product 1). Therefore, the bio-growth potential test allowed to visualize differences in the water quality of Product 1 and Product 2 that were not observed with the common physicochemical analyses of nutrients.

Table 4.6: C, N, P and ATP concentration in the three RO feed qualities

RO feed quality	1	2	3
Name	IX Feed	Product 1	Product 2
C (mg/L)	7.2	2.1	2.2
N (mg/L)	14.3	2.2	2.5
P (mg/L)	1.85	0.01	0.01
ATP (ng/L)	1400	31.40	82.10

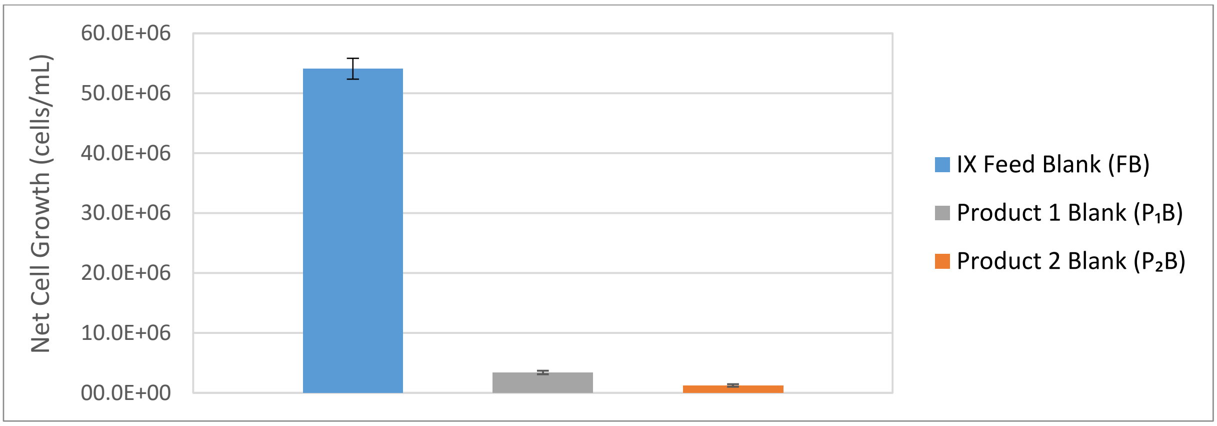

Figure 4.7: Net cell growth of blank samples IX Feed, Product 1 and Product 2 (three RO feed qualities). The error bars indicate the error on triplicate samples.

In microbial biomass, the C:N:P molar ratio is 100:20:1.7 [21], which corresponds to a mass ratio of 23:5:1. The C:N:P ratio for the three RO feed qualities is given in Table 4.7. In all RO feed qualities, the N content was in excess for bacterial growth compared to C and P content. Hence, the bacterial growth was expected to be C and/or P limited.

Table 4.7: C:N:P ratio in the three RO feed qualities

RO feed quality	1	2	3
Name	IX Feed	Product 1	Product 2
C:N:P	4:8:1	210:220:1	220:250:1

The limiting nutrient for bacterial growth of IX Feed (RO feed quality 1) was assessed based on the net cell growth of the different aliquots given in Figure 4.8. The extent of bacterial growth was not significantly affected by the addition of inorganic nutrients (N, trace elements and P). On the contrary, the addition of organic C (50 mg/L) resulted in a bacterial growth of 226 ± 38 × 10^6 cells/mL, which corresponds to a 320% increase. It can be concluded that the bacterial growth-limiting nutrient for IX Feed (RO feed quality 1) was organic C.

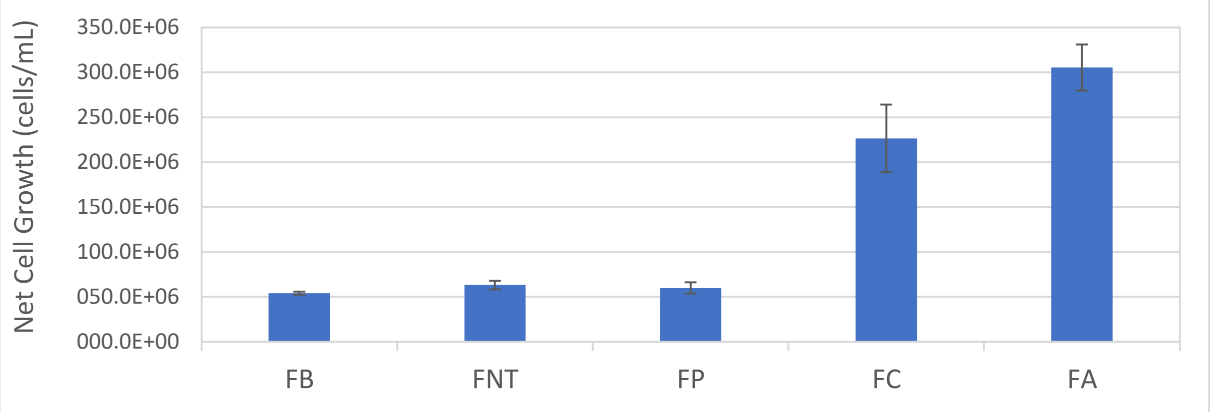

Figure 4.8: Net cell growth in the five types of IX Feed sample (RO feed quality 1).The error bars indicate the error on triplicate samples for each condition. (FB) no additives; (FNT) addition of N and trace elements; (FP) addition of P; (FC) addition of C; (FA) addition of N, trace elements, P and C.

The net cell growth of Products 1 and 2 (RO feed qualities 2 and 3) in the five conditions are given in Figures 4.9 and 4.10, respectively. For both products, N and trace elements addition and C addition had a negligible impact on the bacterial growth when compared to the blank aliquots. The addition of P, however, caused a bacterial growth increase of 215% in Product 1 and 865% in Product 2. Specifically, the net cell growth that corresponds to P addition (5 mg/L) in Product 1 and Product 2 were 10.7 ± 3.1 × 10^6 cells/mL and 12.1 ± 2.2 × 10^6 cells/mL, respectively. Therefore, the limiting nutrient for the bacterial growth after ion exchange treatment with either SBA resin (Product 1 and 2) was P. P limitation in water can restrict active bacterial cell growth [33, 45]. But, it can simultaneously enhance EPS production per active cell resulting in the formation of dense biofilm structures with high hydraulic resistance (given the same C content) [45]. In consequence, the limitation of P in the ion exchange products might cause a different biofilm composition, made of mainly EPS and less active biomass. Such impact should be further investigated. Nevertheless, the growth in Product 1 and Product 2 aliquots with P addition (5 mg/L) was 80% lower than the growth noted for the blank aliquot of IX Feed (54 ± 1.5 × 10^6 cells/mL) in which the P content was 2 mg/L. This difference indicates that a considerable fraction of AOC was removed by both SBA resins. Subsequently, despite the enhancing effect of EPS production potentially caused by P limitation, biofouling of RO modules is still expected to be strongly reduced as AOC is also removed by ion exchange pretreatment with either SBA resin. Additional RO experiments in lab or pilot scale are required to validate this outcome.

The bacterial growth, as expected, was not N limited. According to Desmond et al. (2018), N limitation could result in lower biofilm density and hence alleviates biofouling issues compared to P limiting conditions [45]. Further research is required to investigate if the proposed RO feed pretreatment method can be improved in order to remove N to the extent that N becomes limiting for bacterial growth.

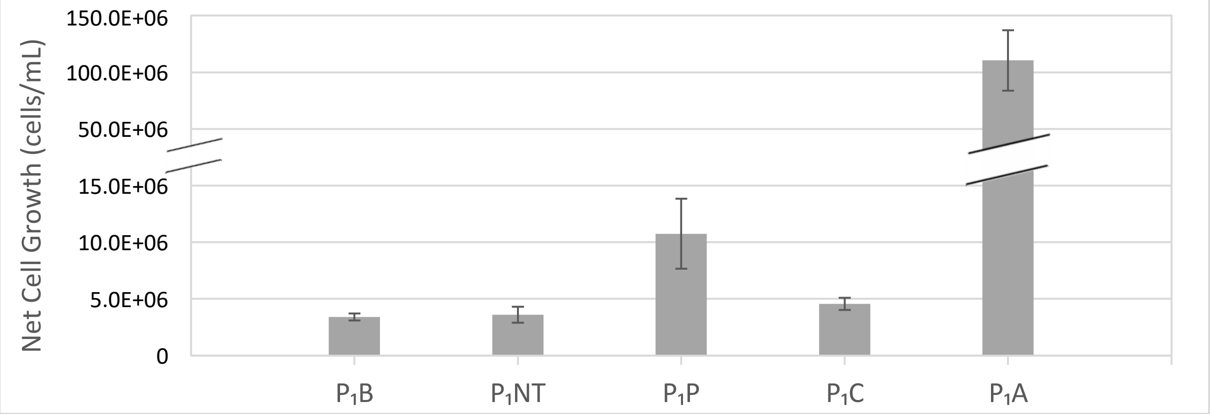

Figure 4.9: Net cell growth in the five types of Product 1 sample (RO feed quality 2).The error bars indicate the error on triplicate samples for each condition. (P_1B) no additives; (P_1NT) addition of N and trace elements; (P_1P) addition of P; (P_1C) addition of C; (P_1A) addition of N, trace elements, P and C. Note the y-axis breaks.

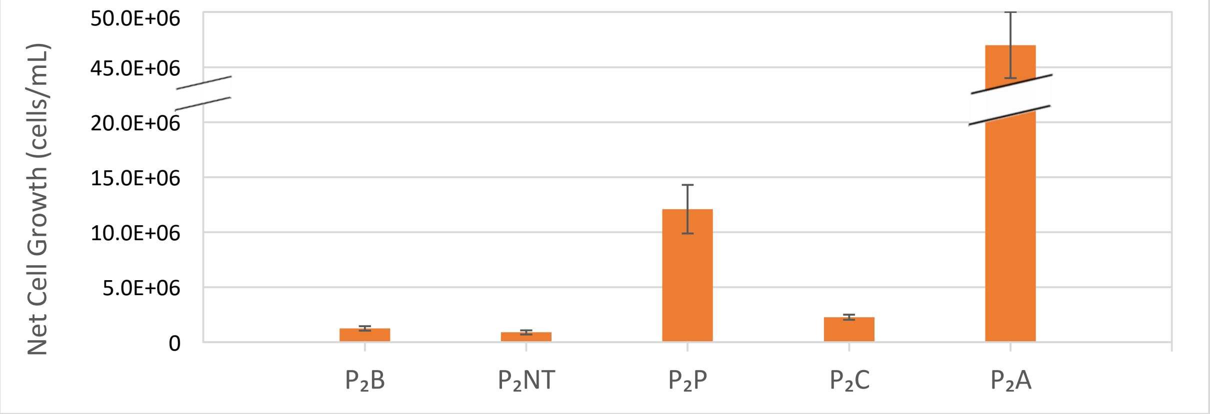

Figure 4.10: Net cell growth in the five types of Product 2 sample (RO feed quality 3).The error bars indicate the error on triplicate samples for each condition. (P_2B) no additives; (P_2NT) addition of N and trace elements; (P_2P) addition of P; (P_2C) addition of C; (P_2A) addition of N, trace elements, P and C. Note the y-axis breaks.

4.3.2 RO Scaling Experiments – Software Run Results

The RO concentrate water quality of the last RO stage for the three RO feed qualities (IX Feed, Product 1 and Product 2), obtained by WAVE design software is given in Table 4.8. The RO concentrate water quality would be responsible for scaling on the last stage. The RO concentrate of Product 1 and Product 2 contain in lower concentrations HPO_4^{2-}-P, SO_4^{2-}, Ca^{2+}, Mg^{2+}, Mn^{2+} and other scaling causing components compared to IX Feed (RO feed quality 1). Solubility warmings of WAVE design software were (i) “Anti-scalants may be required” for IX Feed (RO feed quality 1), (ii) “Anti-scalants may be required” for Product 1 (RO feed quality 2), (iii) “None” for Product 2 (RO feed quality 3).

Table 4.8: RO concentrate water quality from WAVE design software for the three RO feed qualities

RO concentrate for RO feed quality	1	2	3
Name	IX Feed	Product 1	Product 2
pH	8	9.4	8.3
HCO_3^- (mg/L)	1285	579.6	838.2
CO_3^{2-} (mg/L)	21.67	222.8	25.47
Cl^- (mg/L)	1353	2191	2137
SO_4^{2-} (mg/L)	573.8	16.55	16.55
NO_3^- (mg/L)	321.9	61.57	70.65
HPO_4^{2-}-P (mg P/L)	12.67	0.07	0.07
SiO_2 (mg Si/L)	30.05	26.96	27.44
F^- (mg/L)	1.31	1.31	1.31
Na^+ (mg/L)	919.1	1847	1754
K^+ (mg/L)	168.2	0.74	1.5
Ca^{2+} (mg/L)	4369	0.75	0.76
Mg^{2+} (mg/L)	116.9	0.38	0.38
Fe^{3+} (mg/L)	0.20	0.02	0.02
Mn^{2+} (mg/L)	0.56	0.001	0.001
NH_4^+ (mg/L)	26.54	0.18	0.37
Al^{3+} (mg/L)	0.04	0.02	0.01
Ba^{2+} (mg/L)	0.02	0.01	0.003
Sr^{2+} (mg/L)	2.04	0.003	0.003

More accurate predictions of the scaling potential were made based on the saturation indices (SI) produced by PHREEQC 3 software. The mineral that may cause scaling in at least one of the three RO feed qualities for either RO feed or RO concentrate water quality are presented in Table 4.9. The saturation index (SI) of more minerals can be found in Appendix H. It is observed that some scalant types that were sub-saturated (SI ≤ 0.2) in the feed stream become supersaturated (SI > 0.2) in the concentrate stream (85% recovery). Some examples are albite ($NaAlSi_3O_8$), chalcedony (SiO_2), chrysotile ($Mg_3Si_2O_5(OH)_4$) and other. The new scalant types that are introduced during RO operation may cause scaling in the final stage. Therefore, it is more valuable to evaluate scaling potential of the RO unit based on the saturation indices of the minerals in the concentrate stream.

High scaling potential for several silica-based scalants is noted for all RO feed qualities both in the feed and concentrate streams. This was expected since SBA resins in Cl^- form did not remove silica and its concentration in Product 1 and Product 2 were similar to that of IX Feed. For IX Feed, apart from silica scaling, scaling may occur also due to aragonite ($CaCO_3$), calcite ($CaCO_3$), dolomite ($CaMg(CO_3)_2$), gibbsite ($Al(OH)_3$), goethite ($FeOOH$), hematite (Fe_2O_3), hydroxyapatite ($Ca_5(PO_4)_3OH$) and rhodochrosite ($MnCO_3$). In both Product 1 and Product 2, the majority of these scalant types are not expected to occur. Specifically, the scaling potential of $CaCO_3$, $CaMg(CO_3)_2$, $Al(OH)_3$, $MnCO_3$ and $Ca_5(PO_4)_3OH$ was significantly reduced after ion exchange treatment with either SBA resin. Cation exchange is a widely applied pretreatment method to prevent scaling in RO membranes [5]. As expected, the WAC resin highly removed Ca^{2+}, Mg^{2+}, Al^{3+} and Mn^{2+} and the subsequent scaling potential was limited. For both Product 1 and Product 2, goethite ($FeOOH$) and hematite (Fe_2O_3) scaling is likely to occur (SI > 0.2). Moreover, several silica-based scalants have high scaling potential based on the PHREEQC 3 results (SI > 0.2). However, the standard industry guideline for maximum silica concentration in RO concentrate is 120 mg SiO_2/L (at 25°C) [46] and the silica concentration in Product 1 and 2 concentrate is approximately 58 mg SiO_2/L (27 mg Si/L in Table 4.8). Thus, further research with lab or pilot scale RO experiments is needed to determine if anti-scalant dosing is required. Between Product 1 and Product 2 no significant difference was observed in scaling potential, since both products had a similar water quality. The higher pH in Product 1 resulted in some saturation indices (e.g. Calcite) to be slightly higher compared to Product 2.

Table 4.9: Saturation index predictions by PHREEQC 3 of RO feed and RO concentrate for the three RO feed qualities

RO feed qualities	1		2		3	
Name	IX Feed		Product 1		Product 2	
Saturation index (SI) of	Feed	Concentrate	Feed	Concentrate	Feed	Concentrate
Albite ($NaAlSi_3O_8$)	-2.02	2.00	-2.70	1.25	-2.34	1.55
Aragonite ($CaCO_3$)	-0.04	1.65	-1.24	-0.06	-2.25	-0.89
Ca-Montmorillonite ($Ca_{0.165}Al_{2.33}Si_{3.67}O_{10}(OH)_2$)	0.52	4.65	-5.48	-0.64	-2.60	2.05
Calcite ($CaCO_3$)	0.11	1.80	-1.09	0.09	-2.10	-0.74
Chalcedony (SiO_2)	-0.18	0.65	-0.41	0.39	-0.23	0.60
Chlorite (14A) ($Mg_5Al_2Si_3O_{10}(OH)_8$)	-4.75	5.37	-2.38	4.27	-12.35	-5.62
Chrysotile ($Mg_3Si_2O_5(OH)_4$)	-4.94	0.85	-0.81	2.41	-8.11	-4.68
Dolomite ($CaMg(CO_3)_2$)	-0.07	3.31	-2.13	0.20	-4.17	-1.48
Gibbsite ($Al(OH)_3$)	0.49	0.87	-1.80	-1.03	-0.68	-0.03
Goethite (FeOOH)	7.30	8.17	5.71	6.58	6.26	7.16
Hematite (Fe_2O_3)	16.59	18.32	13.40	15.14	14.50	16.30
Hydroxyapatite ($Ca_5(PO_4)_3OH$)	4.24	10.15	-7.86	-3.43	-12.75	-7.83
Illite ($K_{0.6}Mg_{0.25}Al_{2.3}Si_{3.5}O_{10}(OH)_2$)	0.35	5.15	-5.57	-0.38	-3.56	1.42
K-feldspar ($KAlSi_3O_8$)	-0.35	3.65	-3.71	0.25	-3.01	0.88
K-mica ($KAl_3Si_3O_{10}(OH)_2$)	6.21	10.97	-1.73	3.78	1.22	6.40
Kaolinite ($Al_2Si_2O_5(OH)_4$)	2.32	4.72	-2.73	0.42	-0.12	2.84
Quartz (SiO_2)	0.27	1.09	0.03	0.84	0.22	1.04
Rhodochrosite ($MnCO_3$)	-0.39	0.95	-2.27	-1.54	-2.60	-1.70
Sepiolite ($Mg_2Si_3O_{7.5}OH\cdot3H_2O$)	-3.61	1.62	-1.25	2.23	-8.57	-2.15
Talc ($Mg_3Si_4O_{10}(OH)_2$)	-1.66	5.77	2.00	6.83	-4.93	0.15

Based on the saturation index results discussed above, a series of scalant types have high potential in IX Feed and anti-scalant dosing is probably required. In case of Product 1 and Product 2, anti-scalant dosing might be required merely due to the positive saturation index of some silica and iron based minerals. The scaling potential for the three RO feed qualities after anti-scalant dosing was evaluated with Advisor Ci software. The feed water quality of IX Feed, Product 1 and Product 2, the aiming recovery (85%) and the same amount of recommended anti-scalant was inserted in the software. The results of the minerals saturation state also referred as scaling tendency (%) produced by Advisor Ci software are shown in Figures 4.11, 4.12 and 4.13. For IX Feed with anti-scalant dosing, the scaling potential of all minerals processed by the software is moderated (saturation state < 60%) except of calcium phosphate. The saturation state of calcium phosphate was found to reach 120% (Figure 4.11), which indicates high scaling potential. Anti-scalants ineffectiveness to mitigate calcium phosphate scaling has been reported [5, 47]. Especially in cases when P based anti-scalants are used, the calcium phosphate scaling potential increases [8]. For Product 1 and Product 2 with anti-scalant dosing, the scaling potential of all scaling types processed by the software, including calcium phosphate, was found to be low (saturation state < 20%) as it can be seen in Figures 4.12 and 4.13.

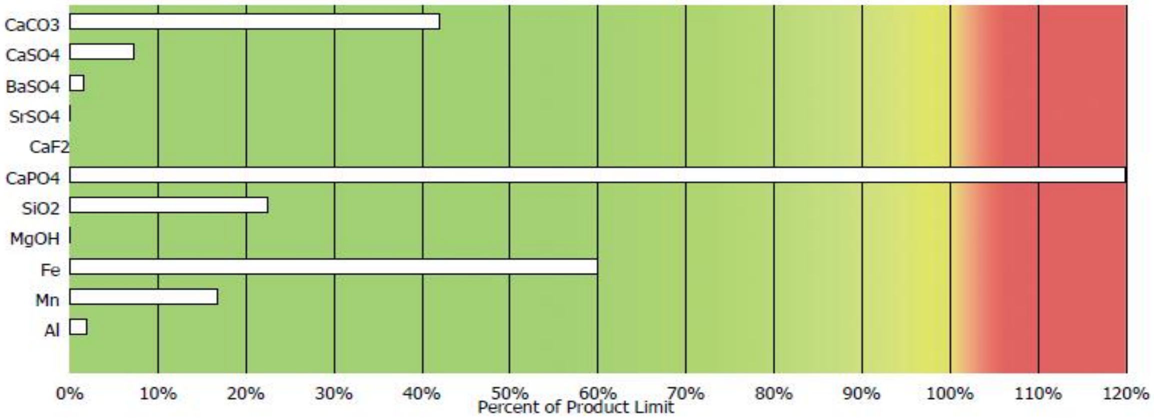

Figure 4.11: Minerals saturation state (%) results from Avista Ci software for IX Feed (RO feed quality 1). The "Percent of Product Limit" is the saturation state also known as scaling tendency (%). A value above 100% indicates high scaling potential (saturations out of product limits).

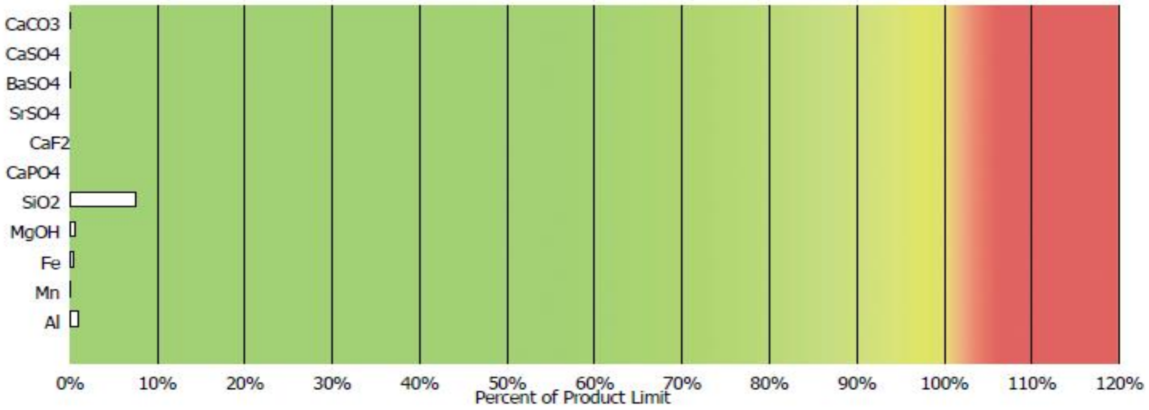

Figure 4.12: Minerals saturation state (%) results from Avista Ci software for Product 1 (RO feed quality 2). The "Percent of Product Limit" is the saturation state also known as scaling tendency (%). A value above 100% indicates high scaling potential (saturations out of product limits).

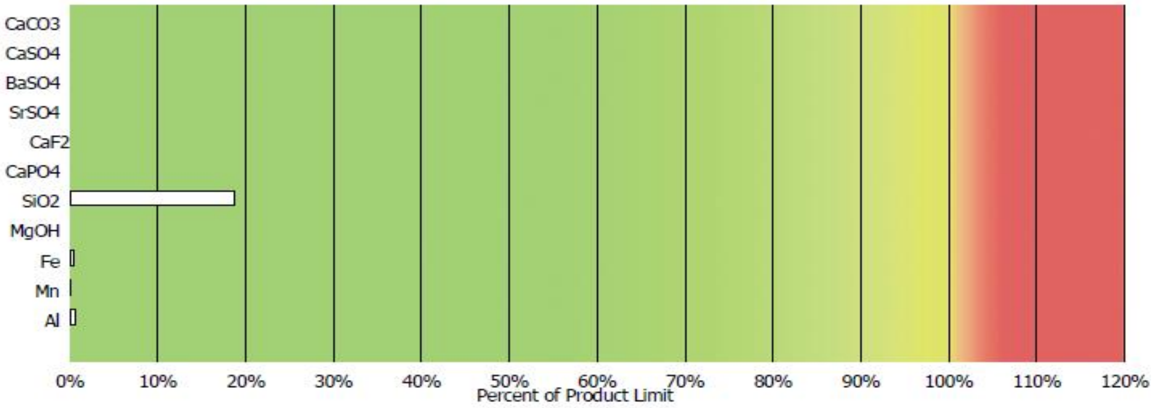

Figure 4.13: Minerals saturation state (%) results from Avista Ci software for Product 2 (RO feed quality 3. The "Percent of Product Limit" is the saturation state also known as scaling tendency (%). A value above 100% indicates high scaling potential (saturations out of product limits).

5. Conclusions

The objective of this thesis was to evaluate the effectiveness of ion exchange treatment with WAC and SBA resins columns in series for the pretreatment of municipal WWTP effluent (after UF treatment) in order to be used as RO feed water. The performance of two SBA resins, the Amberlite SCAV4 Cl (SCAV4) and the Amberlite IRA458 Cl (IRA458), for the removal of SO_4^{2-}, HPO_4^{2-}-P, NO_3^- and TOC was assessed at three regeneration levels (120, 100 and 80 g NaCl/L_r). The effect of the product water quality for the two SBA resin cases on the biofouling and scaling potential of a RO unit was investigated through indirect methods (no RO experiments). The biofouling was assessed with bio-growth potential tests and the scaling potential was based on theoretical predictions obtained with the use of WAVE design, PHREEQC 3 and Avista Ci software.

The NO_3^- concentration in product water (baseline leakage) depended on the regeneration level. For both SBA resins, a higher regeneration level resulted in a lower NO_3^- baseline leakage, hence to a higher NO_3^- removal. Both SCAV4 and IRA458 have higher selectivity towards HPO_4^{2-}-P and SO_4^{2-} compared to NO_3^-. The production was terminated on a chosen NO_3^- breakthrough concentration (30 mg NO_3^-/L). Therefore, the removal of HPO_4^{2-}-P and SO_4^{2-} up to NO_3^- breakthrough concentration was high (above 97%) regardless the regeneration level. In addition, TOC removal was stable and approximately equal to 70% for both SBA resins at all regeneration levels. Moreover, the operational capacity for both resins increased with increasing regeneration levels, but the difference was minor. The operational capacities achieved at each regeneration level for IRA458 were higher than those of SCAV4. It was concluded that the influence of the different regeneration levels to the product water quality and the operational exchange capacity is limited. The best performing regeneration level for both SBA resins was regeneration level 2 (100 g NaCl/L_r), which provides a balance between the used amount of regeneration chemicals, the product water quality and the operational capacity.

From the selectivity order experiments, where the water production did not stop at the NO_3^- breakthrough concentration but continued until a second anion in the product water reached its feed concentration, it was observed that the next anion to breakthrough after NO_3^- was HPO_4^{2-}-P for both SBA resins. HPO_4^{2-}-P breakthrough started at the point where NO_3^- in product water reached its highest concentration (greater than its feed concentration). Therefore, it was concluded that high removal of SO_4^{2-} and HPO_4^{2-}-P (above 97%) can be achieved up to the point where product NO_3^- concentration reaches its feed concentration. Thus, a higher amount of water (throughput) can be produced with the same water quality regarding SO_4^{2-} and HPO_4^{2-}-P.

The observed anion selectivity order for the two SBA resins was

$HCO_3^- < NO_3^- < HPO_4^{2-} < SO_4^{2-}$.

The ion selectivity increases with increasing valence, increasing atomic number and decreasing hydrated radius. HCO_3^- is less preferred than NO_3^- with respect to their hydrated radius [24, 16]. The divalent SO_4^{2-} and HPO_4^{2-} are more preferred by SBA resins than the monovalent NO_3^-. SO_4^{2-} has a smaller hydrated radius compared to HPO_4^{2-} [44], and thus is more preferred than HPO_4^{2-}.

The pretreatment of municipal WWTP effluent (after UF treatment) with ion exchange treatment consisting of a WAC resin and either SBA resin in series resulted in P, N and C removal of approximately 99%, 83% and 70%, respectively. The removal of nutrients led to a substantial reduction in the bacterial growth potential (above 90%). A switch in the growth-limiting nutrient from C to P was caused by ion exchange treatment with either SBA resin. Bio-growth test results also suggest that both SBA resins removed a considerable fraction of AOC. Both P limitation and AOC reduction lead to lower biofouling expectation in RO modules using feed water pretreated with UF and ion exchange with either SBA resin compared to RO modules fed with only UF pretreated water. The scaling potential assessed with PHREEQC 3 and Avista Ci software of the ion exchange product water with either SBA resin was low for several scalant types. Among them was calcium phosphate, which was found to have high scaling potential in RO feed without ion exchange treatment either with or without anti-scalant dosing. Still, anti-scalant dosing might be required after ion exchange treatment with either SBA resin due to the high scaling potential of some silica and iron based minerals. Further research is required to evaluate the extent of biofouling and scaling limitation by the proposed ion exchange treatment. Lab or pilot scale RO experiments can validate the lower biofouling and scaling potential that was found in this research and determine if anti-scalant dosing is required.

6. Recommendations

The pretreatment of municipal WWTP effluent (after UF treatment) with ion exchange treatment consisting of a WAC resin and either SBA resin in series resulted in substantial ions and TOC removal. The removal of these compounds, involved in fouling, resulted in lower scaling and biofouling potential. However, still a few questions are raised leading to the following recommendations for further research:

1. Statistical analyses of the results

The reproduction of the ion exchange experiments at least in triplicates for statistical validation of the results of this research would be interesting. Then, an analysis of variance (ANOVA) for the two SBA resins at the different regeneration levels could be performed in order to determine if differences noted in the removal of NO_3^- and the obtained operation capacity between groups (resin/regeneration level) are significant.

2. Further removal of nutrients

Any further removal of C, N and P would result into even lower biofouling potential in RO feed. The same treatment line of UF and ion exchange treatment with packed resin beds instead of non-packed resins bed is expected to reduced NO_3^- baseline leakage and thus reduce N content in RO feed. Moreover, the introduction of a constructed wetland treatment step prior to UF step can potentially reduce the content of TOC and N in the ion exchange feed and thus result in lower TOC and NO_3^- baseline leakage in ion exchange product (RO feed). Further research is required to investigate to what extent the TOC and N concentration can be reduced by these options and the subsequent effect on the biofouling potential in the RO feed.

The proposed pretreatment resulted in N concentration in the product water (RO feed) that is in excess compared to C and P for bacterial growth. The bacterial growth in ion exchange product water was P limited with either SBA resin. According to Desmond et al. (2018), N limitation reduces biofouling related issues compared to P limitation (given the same C content) [45]. The C:N:P mass ratio for biomass growth is 23:5:1 [21]. HPO_4^{2-} breaks through after NO_3^-. HPO_4^{2-}-P in product water was below the detection limit of 0.02 mg P/L. If assumed it is equal to 0.01 mg P/L (middle value between zero and the detection limit), to achieve N limitation the NO_3^--N baseline leakage should be below 0.05 mg N/L (0.22 mg NO_3^-/L). Such a low value seems not feasible considering that the lowest achieved concentration of NO_3^--N in this research was 1 mg N/L (4.6 mg NO_3^-/L). Subsequently, it is recommended to focus the research in further C, N and P removal rather than in N limitation with the same C content.

3. Lab or pilot scale RO experiments

The biofouling and scaling potential of the RO feed produced by either SBA resin was assessed with indirect methods (bio-growth potential tests and theoretical predictions with software). RO experiments are required to validate the lower biofouling and scaling potential that was concluded based on the findings of this research.

RO fouling (biofouling and scaling) causes increased pressure drop, decreased permeate flux, reduced salt rejection and gradual membrane biodegradation [6, 11]. The performance of pilot RO units fed with the ion exchange product water can be assessed by monitoring the pressure drop, the permeate flux and the salt rejection efficiency. In case severe fouling issues are noted, an autopsy on the membrane modules enables the characterization of foulants (destructive method).

Simultaneously, a lab scale RO unit (e.g. MFS) can be placed prior to the pilot RO and thus be fed with ion exchange product water (nutrient conditions A). Another lab scale RO unit fed with water pretreated only with UF can be placed in parallel (nutrient condition B). A third lab scale RO unit fed with ion exchange product water, where extra P is dosed can be placed in parallel (nutrient condition C). If MFS units are used, the fouling potential can be monitored with pressure drop measurements over the MFS unit, visual/ microscopic observations using the sight glass existing in the MFS unit and ATP analysis of the coupons sampled from the membrane sheet [40]. The proposed nutrient conditions are the following:

Conditions A - Growth-limiting Nutrient P

Use of the ion exchange product water as RO feed → TOC = 2.5 mg/L, N = 4 mg/L and P < 0.02 mg/L

Conditions B - Nutrients Enrich

Use of the UF permeate as RO feed → TOC = 7 mg/L, N = 10 mg/L and P = 2 mg/L

Conditions C - Growth-limiting Nutrient P and C

Use of the ion exchange product water with extra P addition so as the C:P mass ratio to be 23:1 as RO feed → TOC = 2.5 mg/L, N = 4 mg/L and P = 0.11 mg/L

Based on the results of this research it is expected that the biofouling caused by nutrient conditions A would be lower compared to nutrient condition B due to high P and AOC removal. Moreover, according to Desmond et al. (2018), nutrient conditions A will result to higher biofouling compared to C due to different biofilm composition under P limitated conditions. In this way, the impact of the P limitation in the ion exchange product water on biofouling can be assessed.

Moreover, it was found that in ion exchange product water with either one of the tested SBA resins, silica and iron based scaling might occur (SI > 0.2) and anti-scalant dosing might be required. However, initially the RO experiments (pilot scale) are recommended to be performed without antiscalant dosing. In case severe fouling issues are noted, a membrane autopsy can show if scaling is the cause and anti-scalant dosing is required. In that case, an alternative to P-based antiscalant might be needed to avoid increasing the P content of the water.

Bibliography

[1] X. Zhang, N. Qiu, W. Zhao, J. Tommy and H. An, "Water environment management at home and abroad research situation and enlightenment," in *Modelling and Computation in Engineering III*, Leiden, CRC Press/ Balkema, 2014, pp. 117-127.

[2] I. Katsoyiannis, P. Gkotsis, M. Castellana, F. Cartechini and A. Zouboulis, "Production of demineralized water for use in thermal power stations by advanced treatment of secondary wastewater effluent," *Journal of Environmental Management,* vol. 190, pp. 132-139, 29 December 2016.

[3] L. F. Greenlee, D. F. Lawler, B. D. Freeman, B. Marrot and P. Moulin, "Reverse osmosis desalination: Water sources, technology, and today's challenges," *Water Research,* vol. 43, pp. 2317-2348, 18 March 2009.

[4] F. Tang, H.-Y. Hu, L.-J. Sun, Q.-Y. Wu, Y.-M. Jiang, Y.-T. Guan and J.-J. Huang, "Fouling of reverse osmosis membrane for municipal wastewater reclamation: Autopsy results from a full scale plant," *Desalination,* vol. 349, pp. 73-79, 11 July 2014.

[5] A. Antony, J. H. Low, S. Gray, A. E. Childress, P. Le-Clech and G. Leslie, "Scale formation and control in high pressure membranes water treatment systems: A review," *Journal of Membrane Science,* vol. 383, pp. 1-16, 2 Septemeber 2011.

[6] A. Matin, Z. Khan, S. M. J. Zaidi and M. C. Boyce, "Biofouling in reverse osmosis membranes for seawater desalination: Phenomena and prevention," *Desalination,* vol. 281, pp. 1-16, 17 October 2011.

[7] M. Kumar, S. S. Adham and W. R. Pearce, "Investigation of seawater reverse osmosis fouling and its relationship to pretreatment type," *Environmental Science and Technology,* vol. 40, pp. 2037-2044, 8 February 2006.

[8] D. M. Warsinger, J. Swaminathan, E. Guillen-Burrieza, H. A. Arafat and J. H. Lienhard V, "Scaling and fouling in membrane distillation for desalination applications: A review," *Desalination,* vol. 356, pp. 294-313, 15 January 2015.

[9] M. P. del Pino and B. Durham, "Wastewater reuse through dual-membrane processes: opportunities for sustainable water resources," *Desalination,* vol. 124, pp. 271-277, 9 November 1999.

[10] P. C. Kamp, J. C. Kruithof and H. C. Folmer, "UF/RO treatment plant Heemskerk: from challenge to full scale application," *Desalination,* vol. 131, pp. 27-35, 17 July 2000.

[11] H. Maddah and A. Chogle, "Biofouling in reverse osmosis: phenomena, monitoring, controlling and remediation," *Applied Water Science,* vol. 7, pp. 2637-2651, 27 October 2017.

[12] M. K. Shahid, M. Pyo and Y.-G. Choi, "Inorganic fouling control in reverse osmosis wastewater reclamation by purging carbon dioxide," *Environmental Science and Pollution Research 26,* vol. 26, pp. 1094-1102, 21 April 2019.

[14] L. Liberti, G. Boari and R. Passino, "Selective renovation of eutrophic wastes phosphate/sulphate exchange," *Water Research,* vol. 11, pp. 517-523, 1977.

[15] M. R. Awual and A. Jyo, "Assessing of phosphorus removal by polymeric anion exchnagers," *Desalination,* vol. 281, pp. 111-117, 17 October 2011.

[16] J. C. Crittenden, R. R. Trussell, D. W. Hand, K. J. Howe and G. Tchobanoglous, MWH's Water Treatment Principles and Design, Third Edition, Hoboken: John Wiley & Sons, Inc, 2012.

[17] M. Zarrabi, M. N. Sepehr, M. M. Soori and A. Armane, "Removal of phosphorus by ion-exchange resins: Equilibrium, kinetic and thermodynamic studies," *Environmental Engineering and Management Journal,* vol. 13, pp. 891-903, 10 April 2014.

[18] G. Boari, L. Liberti and R. Passino, "Selective renovation of eutrophic wastes - phosphate removal," *Water Research,* vol. 10, pp. 421-428, 1976.

[19] A. Williams, "Ion Exchnage Nutrient Recovery from Municipal Wastewater," Milwaukee, 2013.

[20] D. Keulen, "Demin 2030, Report Research Intern," Evides Industry Water, Rotterdam, 2019.

[21] G. Tchobanoglous, F. L. Burton , H. D. Stensel and Metcalf & Eddy, Inc., Wastewater Engineering: Treatment and Reuses - 4th Edition, New York: McGraw-Hill Education, 2003.

[22] C. E. Harland, Ion Exchange: Theory and Practice - 2nd Edition, Cambridge: The Royal Society of Chemistry, 1994.

[23] F. de Dardel, "Ion exchange resin structure," 5 February 2019. [Online]. Available: http://dardel.info/IX/resin_structure.html. [Accessed 10 May 2019].

[24] A. D. Clifford, T. J. Sorg and G. L. Churye, Water Quality and Treatment: A Handbook on Drinking Water - 6th Edition, New York: American Water Works Association, 2011.

[25] D. Petruzzelli, L. De Florio, A. Dell'Erba, L. Liberti, M. Notarnicola and A. K. Sengupta, "A new phosphate-selective sorbent for the Rem Nut process. Laboratory investigation and field experience at a medium size wastewater treatment plant.," *Water Sci Technol,* vol. 48, pp. 179-184, 2003.

[26] D. van Halem, *Ion Exchange - Lecture Notes of TU Delft Course CIE4703,* Delft, 2017.

[27] A. A. Zagorodni, Ion Exchange Materials - Properties and Applicatios, Sweden: Elsevier Science, 2007.

[28] F. de Dardel, "Ion exchange capacity," 20 August 2018. [Online]. Available: http://dardel.info/IX/capacity.html. [Accessed 15 May 2019].

[29] C. S. Ruiz, "Ion Exchange (FS-TER-006)," Universidade Da Coruna & Inditex, Coruna, 2015.

[30] C. C. F. Michaud, "The Capacity of Ion Exchnage Resin," 20 March 2017. [Online]. Available: http://www.wcponline.com/2017/03/20/capacity-ion-exchange-resin/. [Accessed 10 09 2019].

[31] DuPont, "Tech Fact 177-03729: Recommended operating conditions for separate beds in water treatment," 3 October 2019. [Online]. Available:

https://www.dupont.com/content/dam/dupont/amer/us/en/water-solutions/public/documents/en/45-D01131-en.pdf. [Accessed 10 April 2020].

[32] R. Singh, Hybrid Membrane Systems for Water Purification, Elsevier Science, 2005.

[33] J. S. Vrouwenvelder, F. Beyer, K. Dahmani, N. Hasan, G. Galjaard, J. C. Kruithof and M. C. van Loosdrecht, "Phosphate limitation to control biofouling," *Water Research,* vol. 44, pp. 3454-3466, 27 March 2010.

[34] E. Filloux, J. Wang, M. Pidou, W. Gernjak and Z. Yuan, "Biofouling and scaling control of reverse osmosis membrane using one-step cleaning-potential of acidified nitrite solution as an agent," *Journal of Membrane Science,* vol. 495, pp. 276-283, 1 December 2015.

[35] T. Nguyen, F. A. Roddick and L. Fan, "Biofouling of water treatment membranes: a review of the underlying causes, monitoring techniques and control measures," *Membranes,* vol. 2, pp. 804-840, 21 November 2012.

[36] B. van Breukelen, *Module 5 Chemical Reactions - Lecture Notes of TU Delft Course CIE4495-13,* Delft, 2017.

[37] Avista_Technologies, "Advisor Ci - User Guide 4.5.0," 01 July 2018. [Online]. Available: http://www.avistaadvisor.com/advisorCiguide.pdf?fbclid=IwAR2HGd0Ranoqar43JR1glQerYCzJSTaKBL_oh7hJty5isWbLFy5hGfUkpcg. [Accessed 20 May 2020].

[38] E. I. Prest, F. Hammes, S. Kötzsch, M. C. M. van Loosdrecht and J. S. Vrouwenvelder, "A systematic approach for the assessment of bacterial growth-controlling factors linked to biological stability of drinking water in distribution systems.," *Water Science & Technology: Water Supply,* vol. 16, pp. 865-880, 5 January 2016.

[39] D. van der Kooij, "Potential for biofilm development in drinking water distribution systems," *Journal of Applied Microbiology,* vol. 85, pp. 39-44, 05 November 1999.

[40] J. S. Vrouwenvelder, J. A. M. van Paassen, L. P. Wessels, A. F. van Dam and S. M. Bakker, "The Membrane Fouling Simulator: A practical tool for fouling prediction and control," *Journal of Membrane Science,* no. 281, pp. 316-324, 15 September 2006.

[41] DUPONT-1, "Product Data Sheet: AMBERLITE™ HPR8300 H Ion Exchange Resin," July 2019. [Online]. Available: https://www.dupont.com/content/dam/dupont/amer/us/en/water-solutions/public/documents/en/45-D01239-en.pdf. [Accessed 20 April 2020].

[42] DUPONT-2, "Product Data Sheet: AMBERLITE™ SCAV4 Cl Ion Exchange Resin," June 2019. [Online]. Available: https://www.dupont.com/content/dam/dupont/amer/us/en/water-solutions/public/documents/en/45-D01262-en.pdf. [Accessed 20 April 2020].

[43] DUPONT-3, "Product Data Sheet: AMBERLITE™ IRA458 Cl Ion Exchange Resin," June 2019. [Online]. Available: https://www.dupont.com/content/dam/dupont/amer/us/en/water-solutions/public/documents/en/45-D01253-en.pdf. [Accessed 20 April 2020].

[44] M. Y. Kiriukhim and K. D. Collins, "Dynamic hyrdation numbers for biologically important ions," *Biophysical Chemistry,* vol. 99, pp. 155-168, 29 May 2002.

[45] P. Desmond, J. P. Best, E. Morgenroth and N. Derlon, "Linking composition of extracellular polymeric substances (EPS) to the physical structure and hydraulic resistance of membrane biofilms," *Water Research,* vol. 132, pp. 211-221, 27 December 2018.

[46] R. Sheikholeslami and S. Tan, "Effects of water quality on silica fouling of desalination plants," *Desalination,* vol. 126, pp. 267-280, 1995.

[47] G. Greenbeg, D. Hasson and R. Semiat, "Limits of RO recovery imposed by calcium phosphate precipitation," *Desalination,* vol. 183, pp. 273-288, 10 April 2005.

A. Appendix: Knowledge Gap Table

In Table A.1, the knowledge gap and the main research questions of this study are presented. In addition, a brief explanation of the methodology that was used to answer the research questions is provided. Finally, the last column of the table is name “Accomplished” and it was used in the end of the study to check whether the research questions have been answered. The available options are “yes” if the question has been fully answered, “partially “if more research is required and “no “ if the methodology followed was insufficient to answer the research question.

Table A.1: Knowledge gap and research questions table

Objective & Main research questions	Additional Research questions	Methodology		Accomplished (Yes/ Partly/ No)
The **objective** of this thesis was to investigate the effectiveness of ion exchange treatment with both cationic and anionic resin columns in series for the pretreatment of municipal WWTP effluent (after UF treatment) in order to be used as RO feed water. **Main research questions**: (i) what is the performance of two strong base anion (SBA) resins for the removal of sulfate (SO_4^{2-}), phosphate ($H_2PO_4^-$, HPO_4^{2-}, PO_4^{3-}), nitrate (NO_3^-) and total organic carbon (TOC) and (ii) what is the subsequent effect on the biofouling and scaling potential in a downstream RO membrane unit.	1. What is the removal efficiency of sulfate (SO_4^{2-}), phosphate ($H_2PO_4^-$, HPO_4^{2-}, PO_4^{3-}), nitrate (NO_3^-) and total organic carbon (TOC) by the two SBA resins at different regeneration levels?	Experiments with a pilot IX pilot that consist of a WAC resin column and a SBA resin column in series.	Test two SBA resins at three regeneration level for the removal of sulfate (SO_4^{2-}), phosphate ($H_2PO_4^-$, HPO_4^{2-}, PO_4^{3-}), nitrate (NO_3^-) and total organic carbon (TOC).	Yes
	2. How does the operational exchange capacity of the two SBA resins change at different regeneration levels?		Measurements of the operational exchange capacity of the two SBA resins at three regeneration levels.	Yes
	3. What phosphate ($H_2PO_4^-$, HPO_4^{2-}, PO_4^{3-}), sulfates (SO_4^{2-}) and total organic carbon (TOC) concentrations can be achieved in the product water (RO feed) by running ion exchange unit up to the breakthrough point of Nitrate (NO_3^-)?		Measure phosphate ($H_2PO_4^-$, HPO_4^{2-}, PO_4^{3-}), sulfates (SO_4^{2-}) and total organic carbon (TOC) concentrations during production up to and after the breakthrough point of the nitrate (NO_3^-).	Yes
	4. What is the selectivity order between sulfate (SO_4^{2-}), phosphate ($H_2PO_4^-$, HPO_4^{2-}, PO_4^{3-}) and nitrate (NO_3^-) for the two SBA resin?			Yes
	5. To what extent can the proposed ion exchange unit as a pretreatment step limit the RO biofouling potential?		Assess the RO biofouling potential with bio-growth potential test of the product water.	Partially
	6. To what extent can the proposed ion exchange unit as a pretreatment step limit the RO scaling potential?	Use water quality results of the above experiments as RO feed in membrane software.	Simulate the RO scaling potential with WAVE design, PHREEQC 3 and Advisor Ci.	Partially

B. Appendix: Pilot Equipment and Regeneration Chemicals Information

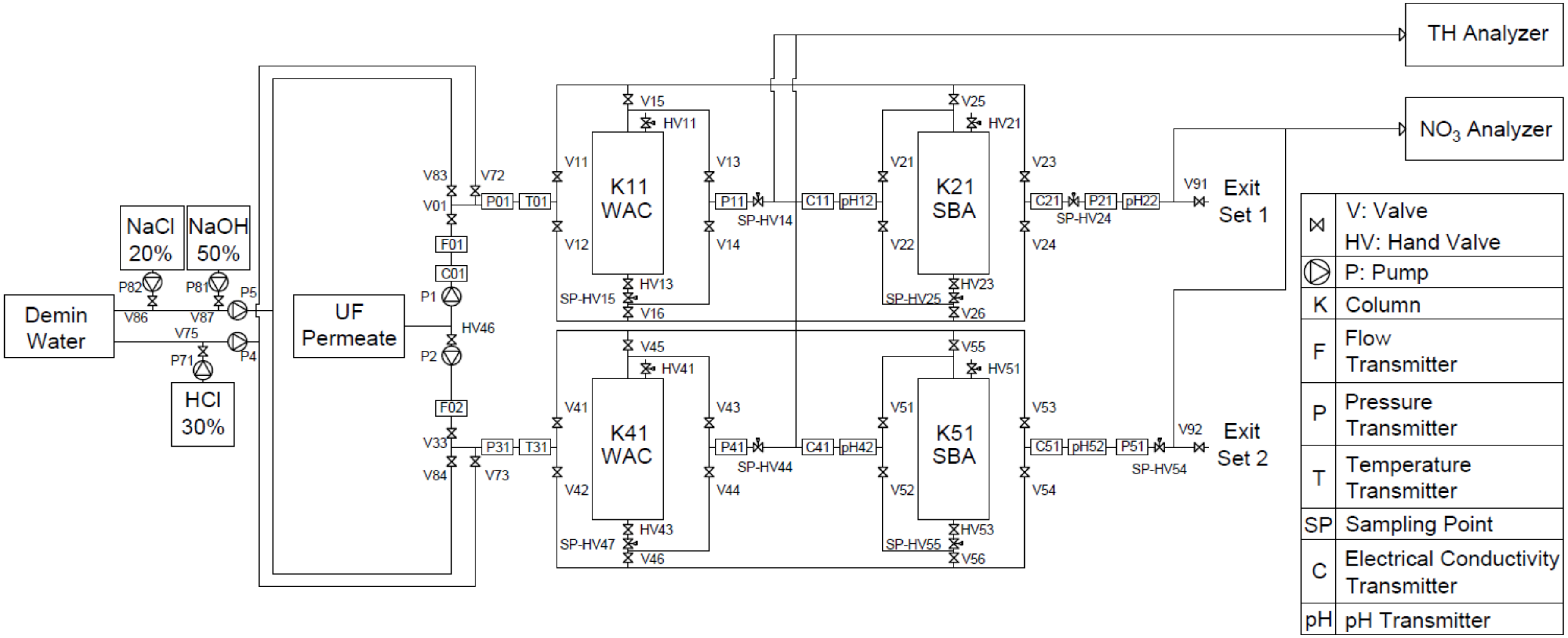

Figure B.1: Process and instrumentation diagram of the ion exchange pilot (IX pilot)

Table B.1: Monitoring equipment on IX pilot

Equipment	Number	Brand	Model
Feed water pumps	2	SONDERMANN, DE	BG 9/A
Demineralized water pumps	2	SONDERMANN, DE	BG 5/A
Chemical pumps	3	SERA, DE	DIAPHRAGM PUMP 409.2...e / 410.2...e
Flow transmitters	2	IFM, GB	SM6050
EC transmitters	5	JUMO, DE	ecoLine Lf-PVC
pH transmitters	4	JUMO, DE	labLine pH
Temperature transmitters	2	Profimess, DE	PT-01
Pressure transmitters	6	BD SENSORS, DE	DMP 331
TH analyzer	1	Testomat ECO, DE	Testomat EVO TH
NO_3 analyzer	1	TETHYS Instruments, FR	UV400

Table B.2: Regeneration chemicals brands

Chemical	Brand
30% HCl	Brenntag Nederland B.V., NL
50% NaOH	Brestedt Chemie B.V., NL
20% NaCl	Brenntag Nederland B.V., NL

C. Appendix: Feed Water Analyses

In Table C.1 the water quality of the IX pilot feed samples on the days of the experiments is given. In Table C.2, the water quality measurements are given expressed as meq/L in order the water balance of the samples to be checked. The CO_3^{2-} concentration in meq/L was calculated based on the HCO_3^- concentration and the pH. For the calculation of HPO_4^{2-}-P concentration in meq/L the pH was taken into account to determine the contributing ratios of $H_2PO_4^-$, HPO_4^{2-} and PO_4^{3-}. For SiO_2 on the days without measurement the average value of the existing measurements was used. For F only one measurement took place and it was used in all experiments.

Table C.1: Feed water quality in mg/L

Date		23-1-2020	4-2-2020	13-2-2020	24-2-2020	25-2-2020
Relevant tests		1.1 & 2.1	1.2 & 2.2	1.3 & 2.3	1.4 & 2.4	1.5 & 2.5
Turbidity	FTU	-	0.15	0.28	0.27	-
SS	mg/L	-	<2	<2	<2	-
EC	µS/cm	2000	1400	1400	1200	1200
pH	-	7.60	7.69	7.48	7.61	7.57
ATP	ng/L	220	260	1100	1400	1100
TOC	mg C/L	10	9.40	8	7.20	8
TP	mg P/L	-	-	-	-	2.20
HCO_3^-	mg/L	260	190	160	200	200
Cl^-	mg/L	410	250	240	210	200
SO_4^{2-}	mg/L	110	92	100	86	87
NO_3^-	mg/L	58	49	61	50	56
HPO_4^{2-}-P	mg P/L	7.6	2.1	2	1.90	2.20
SiO_2	mg Si/L	6.29	-	-	4.59	4.775
F^-	mg/L	-	-	-	-	<0.38
Na^+	mg/L	260	170	170	140	120
K^+	mg/L	45	28	27	25	24
Ca^{2+}	mg/L	85	59	62	64	65
Mg^{2+}	mg/L	30	18	19	17	16
Fe^{3+}	mg/L	0.06	0.05	0.05	0.03	0.04
Mn^{2+}	mg/L	0.11	0.09	0.11	0.084	0.086
NH_4^+	mg/L	4.20	4.00	4.40	4.00	4.00
Al^{3+}	mg/L	0.014	0.01	0.009	0.006	0.007
Ba^{2+}	mg/L	0.003	0.003	0.004	0.0035	0.003
Sr^{2+}	mg/L	0.37	0.26	0.27	0.28	0.27

Table C.2: Feed water balance

Date		23-1-2020	4-2-2020	13-2-2020	24-2-2020	25-2-2020
Relevant tests	Unit	1.1 & 2.1	1.2 & 2.2	1.3 & 2.3	1.4 & 2.4	1.5 & 2.5
HCO_3^-	meq/L	4.30	3.05	2.63	3.32	3.32
CO_3^{2-}	meq/L	0.01	0.01	0.01	0.01	0.01
Cl^-	meq/L	11.93	7.18	7.03	5.95	5.78
SO_4^{2-}	meq/L	2.27	1.91	2.14	1.80	1.80
NO_3^-	meq/L	0.93	0.79	0.98	0.80	0.91
HPO_4^{2-}-P	meq/L	0.49	0.13	0.13	0.12	0.14
SiO_2	meq/L	0.22	0.19	0.19	0.16	0.17
F^-	meq/L	0.01	0.01	0.01	0.01	0.01
Na^+	meq/L	11.13	7.57	7.58	5.95	5.20
K^+	meq/L	1.14	0.71	0.69	0.64	0.62
Ca^{2+}	meq/L	4.23	2.93	3.12	3.21	3.25
Mg^{2+}	meq/L	2.43	1.45	1.54	1.42	1.29
Fe^{3+}	meq/L	0.003	0.003	0.002	0.002	0.002
Mn^{2+}	meq/L	0.004	0.003	0.004	0.003	0.003
NH_4^+	meq/L	0.23	0.22	0.24	0.22	0.22
Al^{3+}	meq/L	0.002	0.001	0.001	0.001	0.001
Ba^{2+}	meq/L	0.00004	0.00004	0.00006	0.00005	0.00004
Sr^{2+}	meq/L	0.01	0.01	0.01	0.01	0.01
Sum anion	meq/L	20.18	13.27	13.11	12.18	12.13
Sum cation	meq/L	19.19	12.89	13.18	11.45	10.59
|Balance|	meq/L	0.99	0.37	0.06	0.73	1.54
Balance	%	2.51	1.43	0.24	3.08	6.78

D.Appendix: WAC Experiments Results

In order to choose the optimal regeneration level for the WAC resin to be used in the main experiments of this study, two preliminary experiments with different regeneration levels for the WAC regeneration were performed. Only the columns with the WAC resins of the IX pilot were operated. The same regeneration ratio was used for both HCl and NaOH regeneration. The two tested regeneration levels are based on the two regeneration ratios given in Table D.1. Based on DuPont Tech Fact 177-03729 [31] the recommended range of the regeneration ratio for WAC resin regeneration with HCl is 105-110%, while with NaOH is 110-160%. The lowest recommended regeneration ratio (105%) was compared to a higher regeneration ratio (135%) for both chemicals.

Table D.1: WAC regeneration levels

Regeneration ratio (%)	135	105
Load (eq)	51.85 (Table 3.4)	
Total regenerant passed (eq)	69.99	54.44
Total regenerant passed (g HCl)	2551.81	1984.74
Total regenerant passed (g NaOH)	2799.59	2177.46
WAC resin bed volume (H^+ form, L_r)	11 (Table 3.4)	
Regeneration level (H^+ form, g HCl/L_r)	231.33	179.92
Regeneration level (H^+ form, g NaOH/L_r)	253.79	197.39
Regeneration level (eq/L_r)	6.35	4.94

The total hardness of the product water during the experiments was monitored with the online total hardness analyzer Testomat EVO TH (Testomat ECO, DE). The production was stopped when the total hardness of the product water was different from zero. Specifically, the breakthrough point was chosen to be the lower detection limit of the analyzer (0.01 mmol/L). The operational capacity for the WAC resin was calculated based on the removal of Ca^{2+} and Mg^{2+} feed concentrations and the throughput. For each regeneration level four batches were performed. The results are given in Table D.2. The operational capacity obtained in both regeneration revels is approximately the same. Subsequently, the lower regeneration level 4.94 eq/L_r (105%) is sufficient for WAC resin regeneration. A higher regeneration level would result in the same operational capacity and to a higher chemical excess. For the main experiments of this study, the regeneration level 4.94 eq/L_r was chosen since the operational capacity obtained is sufficient and the excess of NaOH is expected to be limited.

Table D.2: WAC resin regeneration levels results

Regeneration level (eq/L_r)	6.35	4.94
Feed Ca^{2+} concentration (mg/L)	58.86	
Feed Mg^{2+} concentration (mg/L)	9.16	
Feed total hardness (meq/L)	3.69	
Batch 1 - Throughput (L)	11600	11800
Batch 2 - Throughput (L)	11300	10600
Batch 3 - Throughput (L)	11840	12000
Batch 4 - Throughput (L)	11000	10725
Batch 1 – Operational capacity (H^+ form, eq/L_r)	3.89	3.96
Batch 2 – Operational capacity (H^+ form, eq/L_r)	3.80	3.56
Batch 3 – Operational capacity (H^+ form, eq/Lr)	3.97	4.02
Batch 4 – Operational capacity (H^+ form, eq/L_r)	3.60	3.69

E. Appendix: Batches Results for all Experiments

The breakthrough curves for every batch of each experiment that were created based on NO_3^- measurements of the online analyzer are given in Figures E.1 to E.6. The feed concentrations of HPO_4^{2-}-P, SO_4^{2-} and NO_3^- used for the calculation of the operational capacity of each batch are available in Table E.1. The computed (simplified) operational capacities are available in Tables E.2 to E.7.

Table E.1: Feed concentrations of NO_3^-, SO_4^{2-} and HPO_4^{2-}-P in every batch

Feed concentrations (meq/L)	NO_3^-	SO_4^{2-}	HPO_4^{2-}-P	Sum
Experiments 1.1 & 2.1				
Batch 1	1.26	2.07	0.35	3.68
Batch 2	1.26	2.07	0.35	3.68
Batch 3	1.26	2.07	0.35	3.68
Batch 4	0.93	2.27	0.49	3.70
Experiments 1.2 & 2.2				
Batch 1	0.83	1.96	0.18	2.97
Batch 2	0.83	1.96	0.18	2.97
Batch 3	0.83	1.96	0.18	2.97
Batch 4	0.83	1.96	0.18	2.97
Batch 5	0.79	1.91	0.13	2.83
Experiments 1.3 & 2.3				
Batch 1	0.91	1.94	0.18	3.03
Batch 2	0.90	1.78	0.19	2.87
Batch 3	0.91	1.94	0.18	3.03
Batch 4	0.99	2.14	0.13	3.25

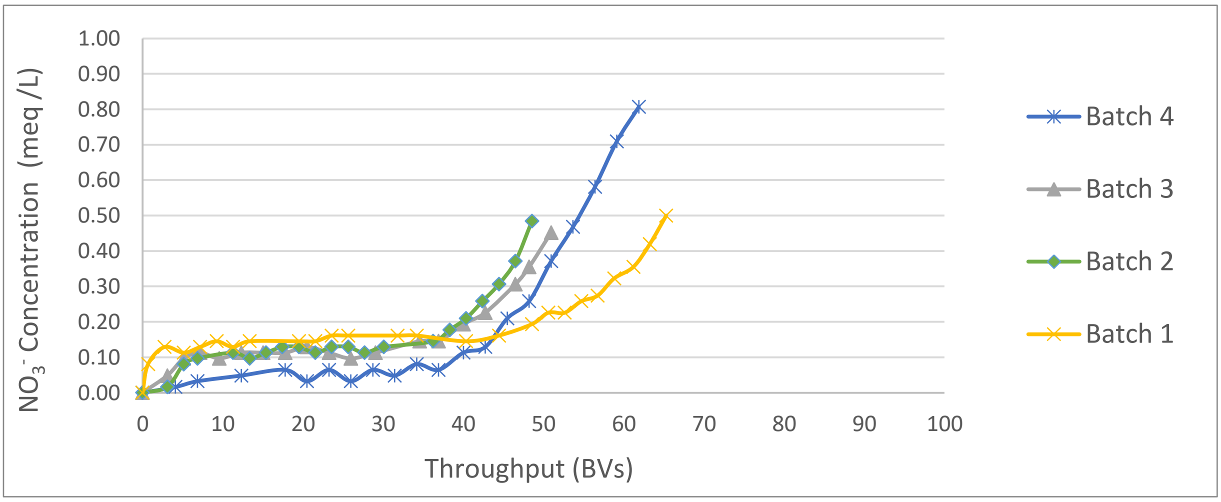

Figure E.1: Batches breakthrough curves – Experiment 1.1 – Resin 1 (SCAV4) at RL1 (120 g NaCl/L_r)

Table E.2: Operational capacity of batches – Experiment 1.1 – Resin 1 (SCAV4) at RL1 (120 g NaCl/L_r)

	Throughput (BVs)	Operational capacity (eq/L_r)	Operational capacity /Total capacity (%)
Batch 1	65.3	0.240	30.02
Batch 2	48.5	0.179	22.32
Batch 3	50.9	0.187	23.42
Batch 4	53.7	0.199	24.82

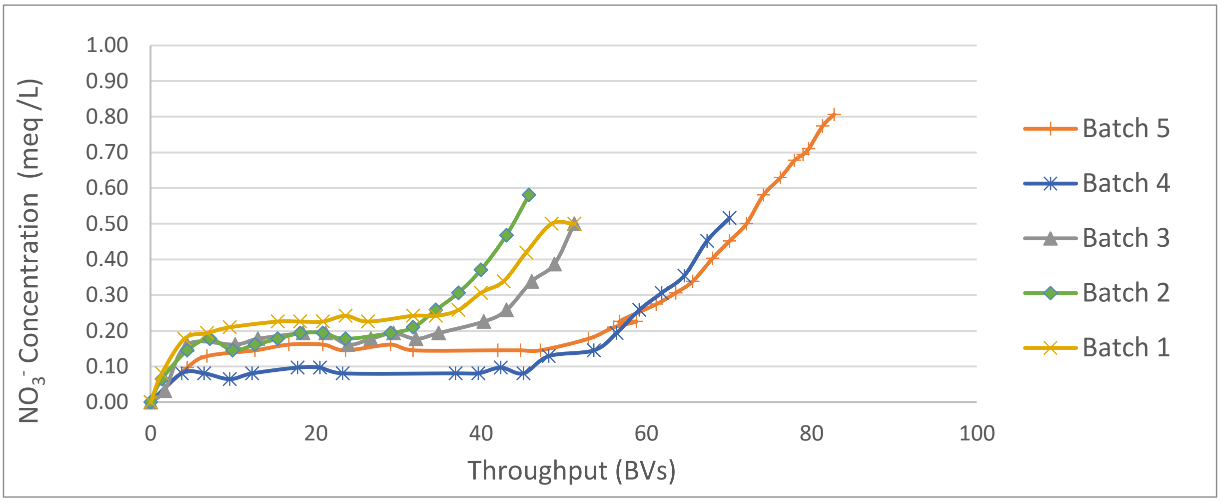

Figure E.2: Batches breakthrough curves – Experiment 1.2 – Resin 1 (SCAV4) at RL2 (100 g NaCl/L_r)

Table E.3: Operational capacity of batches – Experiment 1.2 – Resin 1 (SCAV4) at RL2 (100 g NaCl/L_r)

	Throughput (BVs)	Operational capacity (eq/L_r)	Operational capacity /Total capacity (%)
Batch 1	51.3	0.152	19.05
Batch 2	45.8	0.136	17.05
Batch 3	51.3	0.152	19.05
Batch 4	70.1	0.208	26.05
Batch 5	72.1	0.205	25.55

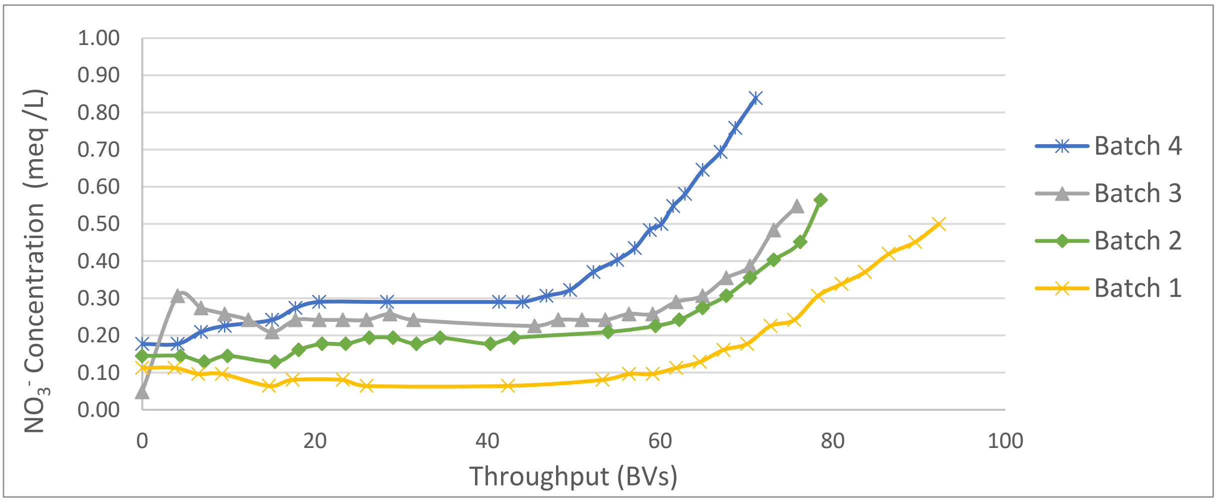

Figure E.3: Batches breakthrough curves – Experiment 1.3 – Resin 1 (SCAV4) at RL3 (80 g NaCl/L_r)

Table E.4: Operational capacity of batches – Experiment 1.3 – Resin 1 (SCAV4) at RL3 (80 g NaCl/L_r)

	Throughput (BVs)	Operational capacity (eq/L_r)	Operational capacity /Total capacity (%)
Batch 1	92.31	0.147	35.02
Batch 2	76.24	0.219	27.35
Batch 3	73.16	0.222	27.75
Batch 4	58.80	0.192	23.95

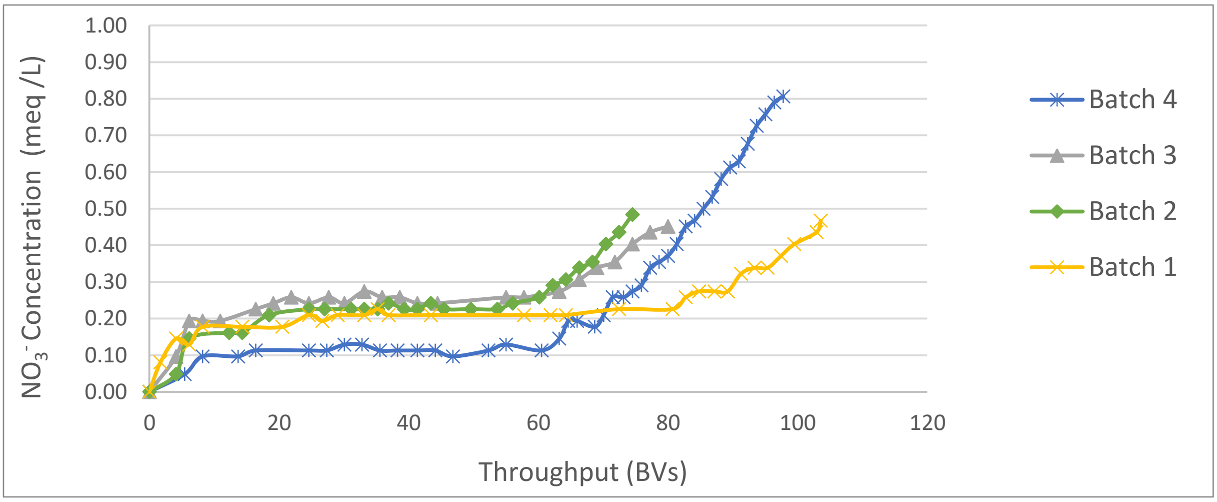

Figure E.4: Batches breakthrough curves – Experiment 2.1 – Resin 2 (IRA458) at RL1 (120 g NaCl/L_r)

Table E.5: Operational capacity of batches – Experiment 2.1 – Resin 2 (IRA458) at RL1 (120 g NaCl/L_r)

	Throughput (BVs)	Operational capacity (eq/L_r)	Operational capacity /Total capacity (%)
Batch 1	103.6	0.381	30.48
Batch 2	74.5	0.274	21.93
Batch 3	80.0	0.294	23.54
Batch 4	84.1	0.311	24.89

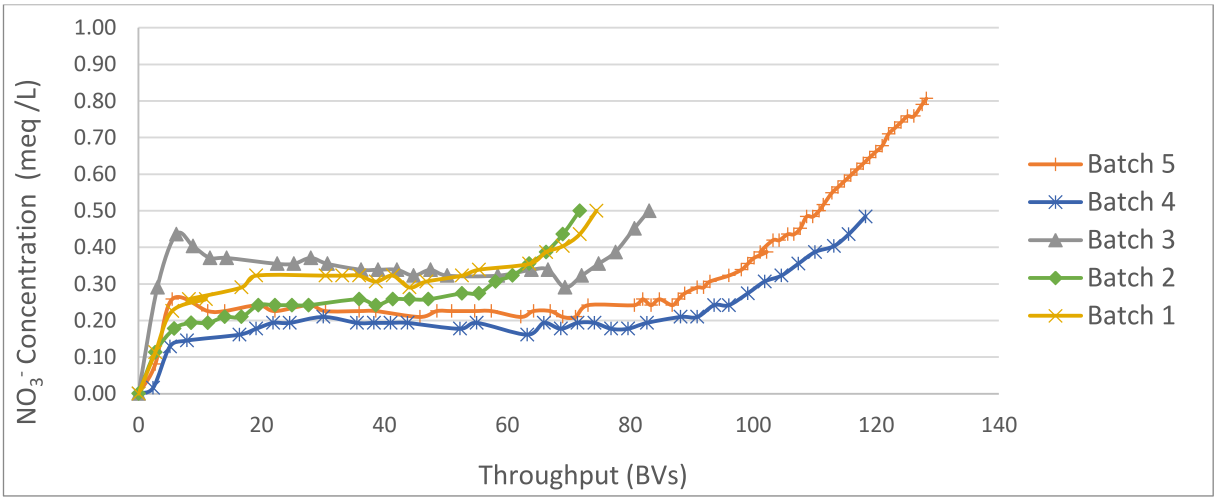

Figure E.5: Batches breakthrough curves – Experiment 2.2 – Resin 2 (IRA458) at RL2 (100 g NaCl/L_r)

Table E.6: Operational capacity of batches – Experiment 2.2 – Resin 2 (IRA458) at RL2 (100 g NaCl/L_r)

	Throughput (BVs)	Operational capacity (eq/L_r)	Operational capacity /Total capacity (%)
Batch 1	74.5	0.222	17.75
Batch 2	71.8	0.213	17.10
Batch 3	83.1	0.247	19.75
Batch 4	118.3	0.352	28.15
Batch 5	108.7	0.308	24.65

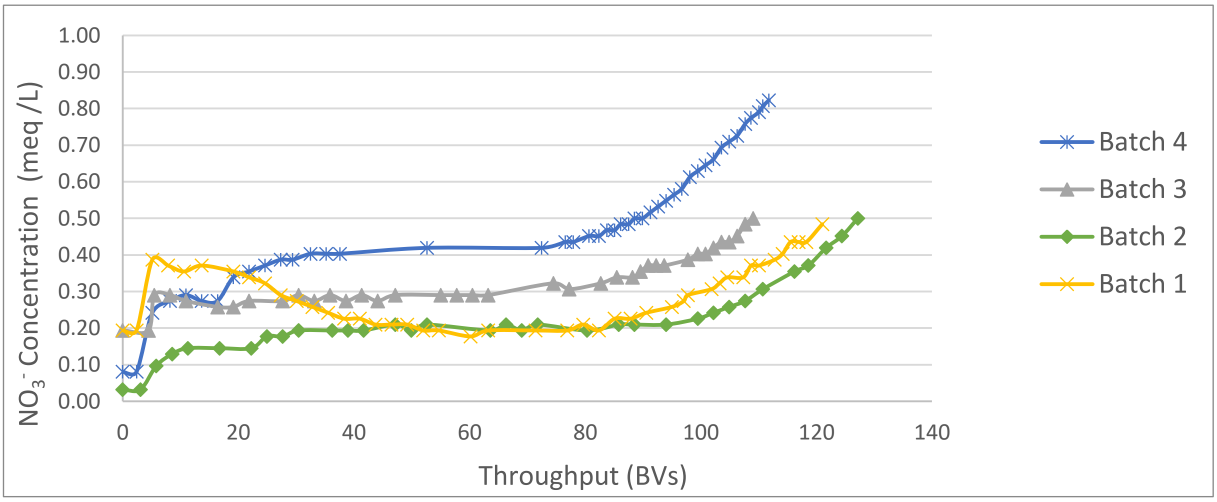

Figure E.6: Batches breakthrough curves – Experiment 2.3 – Resin 2 (IRA458) at RL3 (80 g NaCl/L_r)

Table E.7: Operational capacity of batches – Experiment 2.3 – Resin 2 (IRA458) at RL3 (80 g NaCl/L_r)

	Throughput (BVs)	Operational capacity (eq/L_r)	Operational capacity /Total capacity (%)
Batch 1	121.03	0.367	29.39
Batch 2	127.18	0.365	29.19
Batch 3	109.06	0.331	26.48
Batch 4	86.15	0.281	22.45

F. Appendix: Results Details Experiments 1.1, 1.2, 1.3, 2.1, 2.2 and 2.3

Experiment 1.1

In Tables F.1 to F.8 and in Figures F.1 to F.3 detailed results of the measurements and the calculations for Experiment 1.1 are given. Some comments and clarifications are included.

Some ion measurements were below detection limit. In those cases, the middle value between zero and the detection limit was used for the calculations. The CO_3^{2-} concentration in meq/L was calculated based on the HCO_3^- concentration and the pH. For the calculation of HPO_4^{2-}-P concentration in meq/L the pH was taken into account to determine the contributing ratios of $H_2PO_4^-$, HPO_4^{2-} and PO_4^{3-}. SiO_2 and F concentrations weren't measured in most product samples due to measuring issues. It was assumed that their concentration in the product samples was equal to that of the feed samples, thus that the SBA resins did not remove them. The difference of cations and anions equivalents over the total equivalents (balance percentage) in all samples was below 10%.

Table F.1: Product samples water quality – Experiment 1.1

Sample	Unit	1	2	3	4	5	6	7	8
EC	µS/cm	2332.44	2254.32	2176.2	2148.3	2139.37	2130.44	2127.1	2120.4
pH	-	8.04	8.18	8.19	8.21	8.22	8.22	8.24	8.26
ATP	ng/L	2.20	2.80	3.00	2.90	3.70	3.40	-	3.10
TOC	mg C/L	2.31	3.25	3.49	3.49	3.55	3.58	3.67	3.74
HCO_3^-	mg/L	9.87	87.42	224.82	264.93	275.05	280.37	283.02	285.05
Cl^-	mg/L	746.41	687.32	590.73	567.95	560.62	545.67	549.03	532.88
SO_4^{2-}	mg/L	< 5.00	< 5.00	< 5.00	< 5.00	< 5.00	< 5.00	< 5.00	< 5.00
NO_3^-	mg/L	3.47	3.70	3.65	5.98	9.66	17.89	24.35	36.44
HPO_4^{2-}-P	mg P/L	0.11	0.12	0.11	0.11	0.11	0.11	0.11	0.12
Na^+	mg/L	467.90	460.70	447.70	450.30	448.90	445.70	449.60	455.00
K^+	mg/L	< 0.30	< 0.30	< 0.30	< 0.30	< 0.30	< 0.30	< 0.30	0.56
Ca^{2+}	mg/L	< 3.00	< 3.00	< 3.00	< 3.00	< 3.00	< 3.00	< 3.00	< 3.00
Mg^{2+}	mg/L	< 0.40	< 0.40	< 0.40	< 0.40	< 0.40	< 0.40	< 0.40	< 0.40
Fe^{3+}	mg/L	< 0.005	< 0.005	< 0.005	< 0.005	< 0.005	< 0.005	< 0.005	< 0.005
Mn^{2+}	mg/L	< 0.0004	< 0.0004	< 0.0004	< 0.0004	< 0.0004	< 0.0004	< 0.0004	< 0.0004
NH_4^+	mg/L	< 0.05	< 0.05	< 0.05	< 0.05	< 0.05	< 0.05	< 0.05	< 0.05
Al^{3+}	mg/L	0.0016	0.0028	0.0029	0.0035	0.0030	0.0031	0.0029	0.0031
Ba^{2+}	mg/L	< 0.001	< 0.001	< 0.001	< 0.001	< 0.001	< 0.001	< 0.001	< 0.001
Sr^{2+}	mg/L	< 0.012	< 0.012	< 0.012	< 0.012	< 0.012	< 0.012	< 0.012	< 0.012

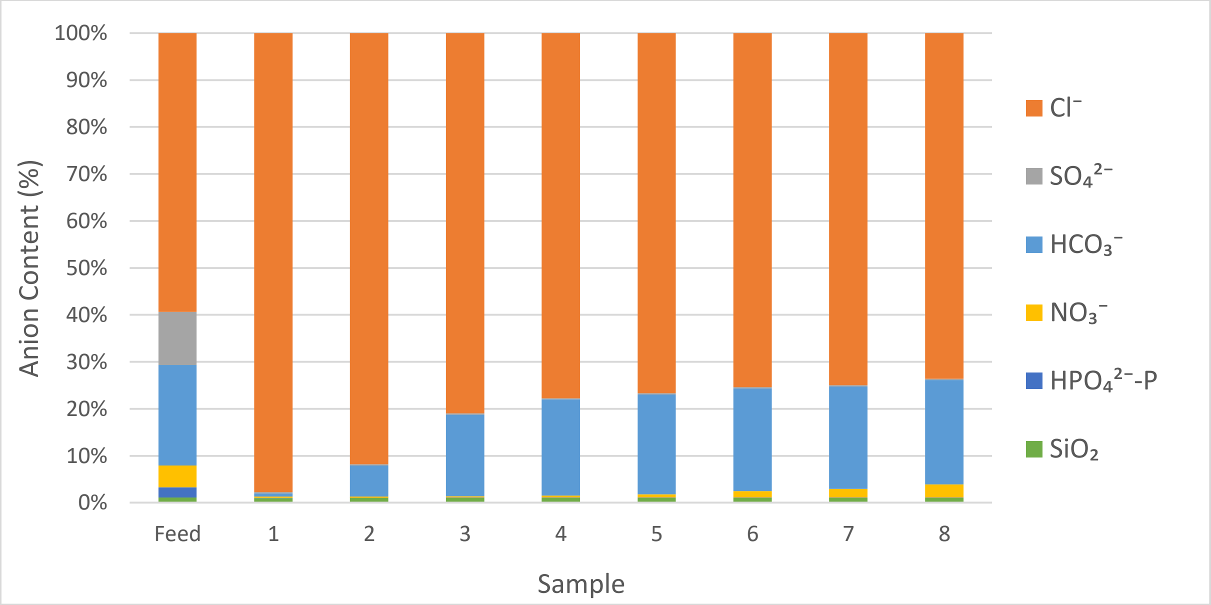

Figure F.1: Product water quality – Anion content (%) – Experiment 1.1

Table F.2: Product samples water balance – Experiment 1.1

Production started at		10:40							
Sample		1	2	3	4	5	6	7	8
Sampling time		10:57	11:42	12:12	12:37	12:47	13:02	13:12	13:27
Throughput	BVs	6.0	21.4	31.6	40.2	43.6	48.7	52.1	57.3
TOC	mmol/L	0.19	0.27	0.29	0.29	0.30	0.30	0.31	0.31
HCO_3^-	meq/L	0.16	1.43	3.68	4.34	4.51	4.60	4.64	4.67
CO_3^{2-}	meq/L	0.00	0.01	0.04	0.05	0.05	0.05	0.05	0.06
Cl^-	meq/L	21.67	19.95	17.15	16.49	16.27	15.84	15.94	15.47
SO_4^{2-}	meq/L	0.05	0.05	0.05	0.05	0.05	0.05	0.05	0.05
NO_3^-	meq/L	0.06	0.06	0.06	0.10	0.16	0.29	0.39	0.59
HPO_4^{2-}-P	meq/L	0.01	0.01	0.01	0.01	0.01	0.01	0.01	0.01
SiO_2	meq/L	0.22	0.22	0.22	0.22	0.22	0.22	0.22	0.22
F^-	meq/L	0.02	0.02	0.02	0.02	0.02	0.02	0.02	0.02
Na^+	meq/L	20.35	20.04	19.47	19.59	19.53	19.39	19.56	19.79
K^+	meq/L	0.004	0.004	0.004	0.004	0.004	0.004	0.004	0.014
Ca^{2+}	meq/L	0.005	0.005	0.005	0.005	0.005	0.005	0.005	0.005
Mg^{2+}	meq/L	0.008	0.008	0.008	0.008	0.008	0.008	0.008	0.008
Fe^{3+}	meq/L	0.0001	0.0001	0.0001	0.0001	0.0001	0.0001	0.0001	0.0001
Mn^{2+}	meq/L	0.00001	0.00001	0.00001	0.00001	0.00001	0.00001	0.00001	0.00001
NH_4^+	meq/L	0.001	0.001	0.001	0.001	0.001	0.001	0.001	0.001
Al^{3+}	meq/L	0.0002	0.0003	0.0003	0.0004	0.0003	0.0003	0.0003	0.0003
Ba^{2+}	meq/L	0.00001	0.00001	0.00001	0.00001	0.00001	0.00001	0.00001	0.00001
Sr^{2+}	meq/L	0.0001	0.0001	0.0001	0.0001	0.0001	0.0001	0.0001	0.0001
Sum anion	meq/L	22.19	21.76	21.23	21.27	21.29	21.07	21.32	21.08
Sum cation	meq/L	20.37	20.06	19.49	19.61	19.54	19.41	19.58	19.82
|Balance|	meq/L	1.82	1.70	1.74	1.67	1.74	1.67	1.75	1.26
Balance	%	4.27	4.07	4.26	4.07	4.27	4.12	4.27	3.09

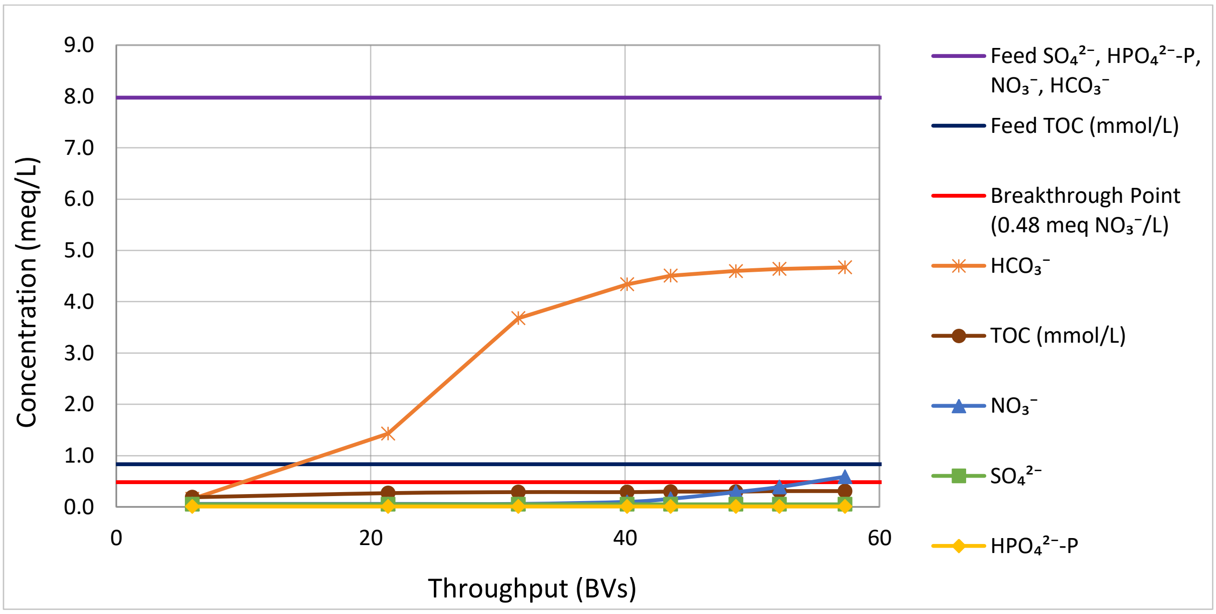

Figure F.2: Breakthrough curves – Experiment 1.1

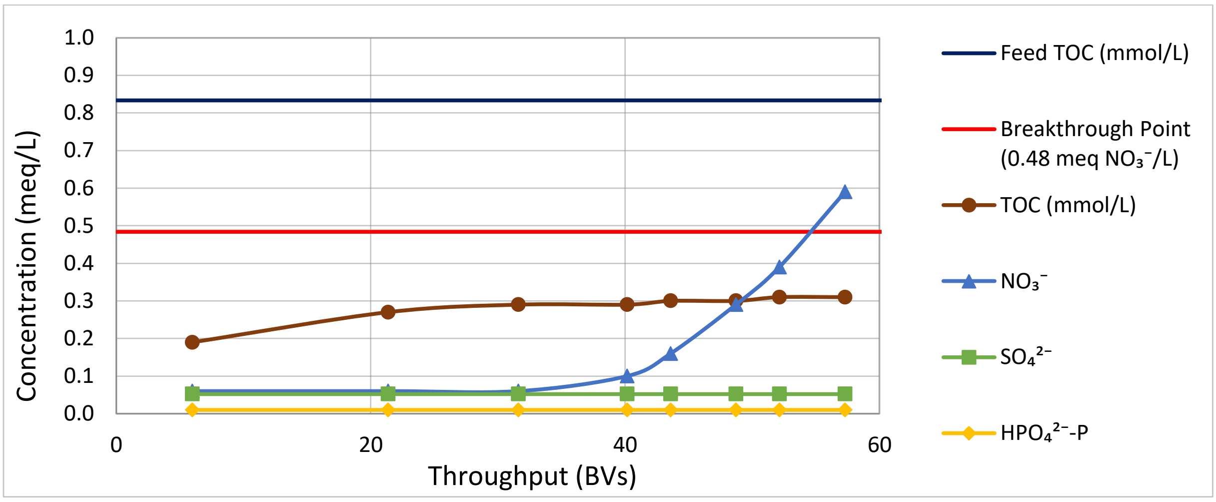

Figure F.3: Breakthrough curves – Experiment 1.1 – Zoom in

The NO_3^- concentration of sample 8 was above the breakthrough concentration. The point "8^-" of Table F.3 was acquired with linear interpolation between the measurements of samples 7 and 8.

Table F.3: SBA Operational capacity – Experiment 1.1

Sample	Feed	1	2	3	4	5	6	7	8^-
Throughput (L)	-	117	417	617	783	850	950	1016	1047
HCO_3^- (meq/L)	4.30	0.16	1.43	3.68	4.34	4.51	4.60	4.64	4.64
SO_4^{2-} (meq/L)	2.27	0.05	0.05	0.05	0.05	0.05	0.05	0.05	0.05
NO_3^- (meq/L)	0.93	0.06	0.06	0.06	0.10	0.16	0.29	0.39	0.48
HPO_4^{2-}-P (meq/L)	0.44	0.01	0.01	0.01	0.01	0.01	0.01	0.01	0.01
Anions removed (meq/L)	-	7.67	6.40	4.15	3.45	3.23	3.01	2.86	2.75
Anions removed (meq)	-	895	2815	3644	4219	4435	4735	4926	5008
Operational capacity (eq/L_r)				0.257					
Operational capacity /Total capacity (%)				32					

TOC is negatively charged and during ion exchange treatment is partially removed by exchange and partially by adsorption. The equivalents of TOC removed based on the measurements of TOC concentration is the product samples is not possible, since TOC charge is not known. However, when TOC is removed is replaced by Cl^- ions in equivalent amounts. The excess Cl^-, which is the extra amount of Cl^- in the product samples that cannot be attributed to HCO_3^-, NO_3^-, HPO_4^{2-}-P and SO_4^{2-} exchange, was calculated in Table F.4 based on the water quality measurements of the product samples. The equivalents of excess Cl^- in the product samples, which was considered to be the result of TOC removal due to ion exchange, was taken into account in the calculation of the operational capacity in Tables F.5.

Table F.4: Removed TOC and excess Cl^- – Experiment 1.1

Sample	Feed	1	2	3	4	5	6	7	8^-
Anions removed (meq/L) Table F.3	-	7.67	6.40	4.15	3.45	3.23	3.01	2.86	2.75
Cl^- (meq/L)	11.93	21.67	19.95	17.15	16.49	16.27	15.84	15.94	15.47
$\lvert\Delta Cl^-\rvert$(meq/L)	-	9.73	8.02	5.22	4.55	4.34	3.91	4.00	3.54
Cl^- excess (meq/L)	-	2.06	1.62	1.07	1.10	1.11	0.90	1.15	0.78
TOC (mmol/L)	0.86	0.19	0.27	0.29	0.29	0.30	0.30	0.31	0.31
Removed TOC (mmol/L)	-	0.67	0.59	0.57	0.57	0.56	0.56	0.55	0.55

Table F.5: SBA operational capacity with TOC into account – Experiment 1.1

Sample	1	2	3	4	5	6	7	8^-
Throughput (L)	117	417	617	783	850	950	1016	1047
Anions removed (meq) Table F.3	895	2815	3644	4219	4435	4735	4926	5008
Cl^- excess (meq/L)	2.06	1.62	1.07	1.10	1.11	0.90	1.15	0.78
Cl^- excess (meq)	241	727	941	1124	1198	1288	1364	1388
Total removed (meq)	1136	3542	4585	5343	5633	6023	6290	6396
Operational capacity (eq/L_r)			0.328					
Operational capacity/Total capacity (%)			41					

Table F.6: WAC operational capacity – Experiment 1.1

Sample	1	2	3	4	5	6	7	8
Cations removed (meq/L)	8.04	8.04	8.04	8.04	8.04	8.04	8.04	8.03
Cations removed (meq)	938	3350	4959	6299	6835	7639	8175	8978
WAC operational capacity (eq/L_r)		0.816						
Operational capacity/Total capacity (%)		17						

Table F.7: Volume weighted average and removal – Experiment 1.1

Parameter	VW average	VW average	Feed	Removal
Unit	meq/L	mg/L	mg/L	%
ATP (ng/L)	-	2.93	216.60	99
TOC (mmol/L)	0.28	3.32	10.33	68
HCO_3^-	2.98	181.75	262.53	31
Cl^-	18.06	622.07	411.07	-51
SO_4^{2-}	0.05	2.50	109.16	98
NO_3^-	0.13	7.86	57.74	86
HPO_4^{2-}-P	0.01	0.11	7.62	99
SiO_2	0.22	6.29	6.29	0
F^-	0.02	0.35	0.35	0
Na^+	19.75	454.15	255.80	-78
K^+	0.004	0.15	44.58	100
Ca^{2+}	0.005	0.10	84.85	100
Mg^{2+}	0.01	0.10	29.59	100
Fe^{3+}	0.0001	0.003	0.06	95
Mn^{2+}	0.00001	0.0002	0.11	100
NH_4^+	0.001	0.03	4.21	99
Al^{3+}	0.0003	0.003	0.01	79
Ba^{2+}	0.00001	0.001	0.003	83
Sr^{2+}	0.0001	0.01	0.37	98

A few water samples of the stream after the WAC resin and before the SBA resin were collected along production to ensure that ions, TOC, and ATP were removed as expected (Table F.8).

Table F.8: Samples after WAC before SBA water quality – Experiment 1.1

Sample	Unit	M1	M2	M3
Sampling time	-	11:52	12:27	12:57
Throughput	BVs in H form	44	65.2	83.3
EC	µS/cm	2124.86	2110.36	2104.78
pH	-	9.17	9.03	8.95
ATP	ng/L	-	149.90	-
TOC	mg C/L	10.18	10.23	10.14
HCO_3^-	mg/L	255.06	262.15	265.44
CO_3^{2-}	mg/L	24.88	18.04	14.68
Cl^-	mg/L	410.43	407.13	409.06
SO_4^{2-}	mg/L	107.71	108.10	108.15
NO_3^-	mg/L	54.67	57.21	57.99
HPO_4^{2-}-P	mg/L	2.48	2.44	2.41
Na^+	mg/L	457.00	444.80	450.40
K^+	mg/L	< 0.30	< 0.30	< 0.30
Ca^{2+}	mg/L	< 3.00	< 3.00	< 3.00
Mg^{2+}	mg/L	< 0.40	< 0.40	< 0.40
Fe^{3+}	mg/L	0.05	0.05	0.05
Mn^{2+}	mg/L	0.001	0.001	0.001
NH_4^+	mg/L	< 0.05	< 0.05	< 0.05
Al^{3+}	mg/L	0.005	0.005	0.005
Ba^{2+}	mg/L	< 0.001	< 0.001	< 0.001
Sr^{2+}	mg/L	< 0.012	< 0.012	< 0.012

In following tables and figures details for the results of experiments 1.2, 1.3, 2.1, 2.2 and 2.3 are given. The same assumptions and procedures explained above for experiment 1.1 were followed for these experiments, too.

Experiment 1.2

Table F.9: Product samples water quality – Experiment 1.2

Sample	Unit	1	2	3	4	5	6	7	8
EC	µS/cm	1736.50	1620.43	1553.47	1509.95	1493.21	1465.31	1457.50	1445.22
pH	-	8.85	8.38	8.31	8.24	8.24	8.26	8.16	8.27
ATP	ng/L	6.80	13.20	18.05	22.90	22.00	30.00	30.50	31.00
TOC	mg C/L	1.92	2.62	2.72	2.68	2.74	2.81	2.91	2.82
HCO_3^-	mg/L	7.08	22.33	86.52	142.27	165.00	179.75	181.52	184.68
CO_3^{2-}	mg/L	< 5	< 5	-	-	-	-	-	-
Cl^-	mg/L	532.09	484.68	434.73	407.42	378.37	359.83	350.75	343.14
SO_4^{2-}	mg/L	< 5	< 5	< 5	< 5	< 5	< 5	< 5	< 5
NO_3^-	mg/L	9.84	9.76	9.16	8.80	9.17	13.44	19.41	29.94
HPO_4^{2-}-P	mg P/L	< 0.02	< 0.02	< 0.02	< 0.02	< 0.02	< 0.02	< 0.02	0.022
Na^+	mg/L	342.22	302.92	283.47	301.78	299.30	299.85	297.52	294.14
K^+	mg/L	< 0.1	< 0.1	< 0.1	< 0.1	< 0.1	< 0.1	< 0.1	0.11
Ca^{2+}	mg/L	<0.2	<0.2	<0.2	<0.2	<0.2	<0.2	<0.2	<0.2
Mg^{2+}	mg/L	<0.1	<0.1	<0.1	<0.1	<0.1	<0.1	<0.1	<0.1
Fe^{3+}	mg/L	< 0.005	< 0.005	< 0.005	< 0.005	< 0.005	< 0.005	< 0.005	< 0.005
Mn^{2+}	mg/L	< 0.0004	< 0.0004	< 0.0004	< 0.0004	< 0.0004	< 0.0004	< 0.0004	< 0.0004
NH_4^+	mg/L	0.05	0.07	0.06	0.06	0.05	0.06	0.09	0.06
Al^{3+}	mg/L	0.004	0.006	0.007	0.007	0.007	0.007	0.007	0.007
Ba^{2+}	mg/L	< 0.001	< 0.001	< 0.001	< 0.001	< 0.001	< 0.001	< 0.001	< 0.001
Sr^{2+}	mg/L	< 0.001	< 0.001	< 0.001	< 0.001	< 0.001	< 0.001	< 0.001	< 0.001

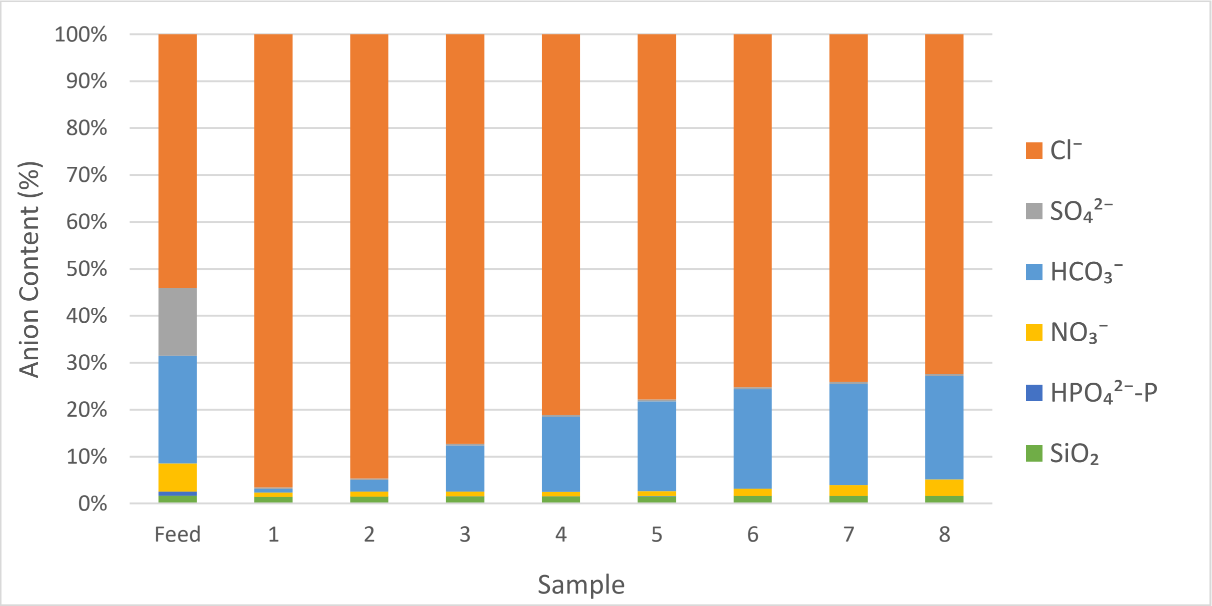

Figure F.4: Product water quality – Anion content (%) – Experiment 1.2

Table F.10: Product samples water balance – Experiment 1.2

Production started at		9:00							
Sample		1	2	3	4	5	6	7	8
Samling time		9:22	10:07	10:37	11:02	11:17	11:52	12:10	12:32
Throughput	BVs	8.0	23.4	33.7	42.2	47.4	59.3	65.3	73
TOC	mmol/L	0.16	0.22	0.23	0.22	0.23	0.23	0.24	0.24
HCO_3^-	meq/L	0.12	0.37	1.42	2.33	2.70	2.95	2.97	3.03
CO_3^{2-}	meq/L	0.01	0.01	0.02	0.03	0.03	0.03	0.03	0.04
Cl^-	meq/L	15.45	14.07	12.62	11.83	10.98	10.44	10.18	9.96
SO_4^{2-}	meq/L	0.05	0.05	0.05	0.05	0.05	0.05	0.05	0.05
NO_3^-	meq/L	0.16	0.16	0.15	0.14	0.15	0.22	0.31	0.48
HPO_4^{2-}-P	meq/L	0.0006	0.0006	0.0006	0.0006	0.0006	0.0006	0.0006	0.001
SiO_2	meq/L	0.22	0.22	0.22	0.22	0.22	0.22	0.22	0.22
F^-	meq/L	0.02	0.02	0.02	0.02	0.02	0.02	0.02	0.02
Na^+	meq/L	14.89	13.18	12.33	13.13	13.02	13.04	12.94	12.79
K^+	meq/L	0.003	0.003	0.003	0.003	0.003	0.003	0.003	0.003
Ca^{2+}	meq/L	0.005	0.005	0.005	0.005	0.005	0.005	0.005	0.005
Mg^{2+}	meq/L	0.01	0.01	0.01	0.01	0.01	0.01	0.01	0.01
Fe^{3+}	meq/L	0.0001	0.0001	0.0001	0.0001	0.0001	0.0001	0.0001	0.0001
Mn^{2+}	meq/L	0.00001	0.00001	0.00001	0.00001	0.00001	0.00001	0.00001	0.00001
NH_4^+	meq/L	0.003	0.004	0.003	0.003	0.003	0.003	0.005	0.004
Al^{3+}	meq/L	0.000	0.001	0.001	0.001	0.001	0.001	0.001	0.001
Ba^{2+}	meq/L	0.00001	0.00001	0.00001	0.00001	0.00001	0.00001	0.00001	0.00001
Sr^{2+}	meq/L	0.00001	0.00001	0.00001	0.00001	0.00001	0.00001	0.00001	0.00001
Sum anion	meq/L	16.02	14.89	14.49	14.62	14.16	13.93	13.79	13.80
Sum cation	meq/L	14.90	13.20	12.35	13.15	13.04	13.06	12.96	12.81
|Balance|	meq/L	1.11	1.69	2.14	1.47	1.12	0.87	0.83	0.98
Balance	%	3.60	6.03	7.99	5.30	4.11	3.22	3.08	3.70

Table F.11: SBA operational capacity – Experiment 1.2

Sample	Feed	1	2	3	4	5	6	7	8
Throughput (L)	-	157	457	657	823	923	1157	1273	1423
HCO_3^- (meq/L)	3.05	0.12	0.37	1.42	2.33	2.70	2.95	2.97	3.03
SO_4^{2-} (meq/L)	1.91	0.05	0.05	0.05	0.05	0.05	0.05	0.05	0.05
NO_3^- (meq/L)	0.79	0.16	0.16	0.15	0.14	0.15	0.22	0.31	0.48
HPO_4^{2-}-P (meq/L)	0.12	0.0006	0.0006	0.0006	0.0006	0.0006	0.0006	0.0006	0.001
Anions removed (meq/L)	-	5.54	5.29	4.25	3.34	2.97	2.66	2.53	2.31
Anions removed (meq)	-	868	2457	3307	3865	4161	4781	5076	5422
Operational capacity (eq/L_r)				0.278					
Operational capacity/Total capacity (%)				35					

Table F.12: Removed TOC and excess Cl^- – Experiment 1.2

Sample	Feed	1	2	3	4	5	6	7	8
Anions removed (meq/L) Table F.11	-	5.54	5.29	4.25	3.34	2.97	2.66	2.53	2.31
Cl^- (meq/L)	7.18	15.45	14.07	12.62	11.83	10.98	10.44	10.18	9.96
$\lvert \Delta Cl^- \rvert$(meq/L)	-	8.27	6.89	5.44	4.65	3.80	3.27	3.00	2.78
Cl^- excess (meq/L)	-	2.72	1.59	1.20	1.32	0.86	0.63	0.49	0.50
TOC (mmol/L)	0.79	0.16	0.22	0.23	0.22	0.23	0.23	0.24	0.24
Removed TOC (mmol/L)	-	0.63	0.57	0.56	0.56	0.56	0.55	0.54	0.55

Table F.13: SBA operational capacity with TOC into account – Experiment 1.2

Sample	1	2	3	4	5	6	7	8
Throughput (L)	157	457	657	823	923	1157	1273	1423
Anions removed (meq) Table F.11	868	2457	3307	3865	4161	4781	5076	5422
Cl^- excess (meq/L)	2.72	1.59	1.20	1.32	0.86	0.63	0.49	0.50
Cl^- excess (meq)	427	904	1144	1363	1449	1597	1653	1728
Total removed (meq)	1295	3361	4451	5228	5610	6378	6729	7150
Operational capacity (eq/L_r)			0.367					
Operational capacity/Total capacity (%)			46					

Table F.14: WAC operational capacity – Experiment 1.2

Sample	1	2	3	4	5	6	7	8
Cations removed (meq/L)	5.31	5.31	5.31	5.31	5.31	5.31	5.31	5.31
Cations removed (meq)	832	2424	3485	4370	4901	6139	6758	7554
WAC operational capacity (eq/L_r)			0.687					
Operational capacity/Total capacity (%)			15					

Table F.15: Volume weighted average and removal – Experiment 1.2

Parameter	VW average	VW average	Feed	Removal
Unit	meq/L	mg/L	mg/L	%
ATP (ng/L)	-	21.02	260	92
TOC (mmol/L)	0.22	2.65	9.42	72
HCO_3^-	1.80	109.70	186.07	41
Cl^-	12.19	420.00	247.33	-70
SO_4^{2-}	0.05	2.50	91.58	97
NO_3^-	0.21	13.05	49.26	74
HPO_4^{2-}-P	0.0006	0.01	2.07	100
SiO_2	0.22	6.18	6.18	0
F^-	0.02	0.35	0.35	0
Na^+	13.15	302.25	173.97	-74
K^+	0.003	0.10	27.88	100
Ca^{2+}	0.005	0.10	58.70	100
Mg^{2+}	0.008	0.10	17.64	99
Fe^{3+}	0.0001	0.003	0.05	95
Mn^{2+}	0.00001	0.0002	0.09	100
NH_4^+	0.003	0.06	3.98	98
Al^{3+}	0.0007	0.007	0.01	37
Ba^{2+}	0.00001	0.0005	0.003	81
Sr^{2+}	0.00001	0.0005	0.27	100

Table F.16: Samples after WAC before SBA water quality – Experiment 1.2

Sample	Unit	M1	M2
Sampling time	-	9:57	10:47
Throughput	BVs in H form	35.45	65.7
EC	µS/cm	1506.6	1465.31
pH	-	9.61	9.5
ATP	ng/L	-	128.7
TOC	mg C/L	9.43	9.35
HCO_3^-	mg/L	159.25	161.19
CO_3^{2-}	mg/L	41.42	35.01
Cl^-	mg/L	258.15	257.56
SO_4^{2-}	mg/L	97.55	99.63
NO_3^-	mg/L	54.71	49.29
HPO_4^{2-}-P	mg P/L	2.26	2.02
Na^+	mg/L	308.146	309.841
K^+	mg/L	< 0.1	< 0.1
Ca^{2+}	mg/L	<0.2	<0.2
Mg^{2+}	mg/L	<0.1	<0.1
Fe^{3+}	mg/L	< 0.005	< 0.005
Mn^{2+}	mg/L	< 0.0004	< 0.0004
NH_4^+	mg/L	< 0.05	< 0.05
Al^{3+}	mg/L	0.010	0.009
Ba^{2+}	mg/L	< 0.001	< 0.001
Sr^{2+}	mg/L	< 0.001	< 0.001

Experiment 1.3

Table F.17: Product samples water quality – Experiment 1.3

Sample	Unit	1	2	3	4	5	6	7
EC	µS/cm	1841.4	1627.13	1517.76	1501.02	1497.67	1494.32	1487.63
pH	-	11.30	10.20	8.42	8.40	8.41	8.41	8.44
ATP	ng/L	89.50	82.30	760	760	773	786	861
TOC	mg C/L	1.17	2.35	2.63	2.66	2.68	2.72	2.79
HCO_3^-	mg/L	< 5	< 5	141.15	163.76	167.79	170.13	175.46
CO_3^{2-}	mg/L	< 5	5.37	< 5	< 5	< 5	< 5	< 5
Cl^-	mg/L	441.05	466.09	382.55	368.00	360.85	357.46	344.11
SO_4^{2-}	mg/L	< 5	< 5	< 5	< 5	< 5	< 5	< 5
NO_3^-	mg/L	13.36	15.73	16.93	23.29	26.50	30.77	44.74
HPO_4^{2-}-P	mg P/L	< 0.02	< 0.02	< 0.02	< 0.02	< 0.02	< 0.02	< 0.02
Na^+	mg/L	346.95	339.857	326.752	332.495	332.058	331.936	329.178
K^+	mg/L	0.10	0.12	0.12	0.10	0.11	0.11	0.12
Ca^{2+}	mg/L	<0.2	<0.2	<0.2	<0.2	<0.2	<0.2	<0.2
Mg^{2+}	mg/L	<0.1	<0.1	<0.1	<0.1	<0.1	<0.1	<0.1
Fe^{3+}	mg/L	< 0.005	< 0.005	< 0.005	< 0.005	< 0.005	< 0.005	< 0.005
Mn^{2+}	mg/L	< 0.0005	< 0.0005	< 0.0005	< 0.0005	< 0.0005	< 0.0005	< 0.0005
NH_4^+	mg/L	< 0.05	< 0.05	< 0.05	< 0.05	< 0.05	< 0.05	< 0.05
Al^{3+}	mg/L	<0.003	0.003	0.003	0.004	0.004	0.004	0.004
Ba^{2+}	mg/L	< 0.001	< 0.001	< 0.001	< 0.001	< 0.001	< 0.001	< 0.001
Sr^{2+}	mg/L	< 0.001	< 0.001	< 0.001	< 0.001	< 0.001	< 0.001	< 0.001

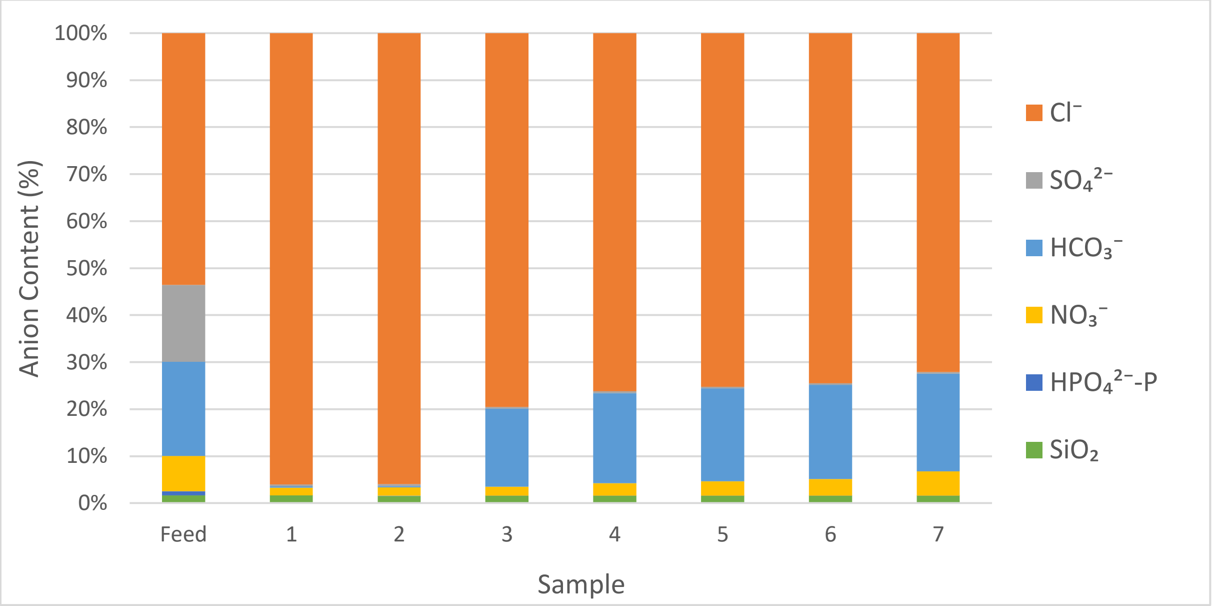

Figure F.5: Product water quality – Anion content (%) – Experiment 1.3

Table F.18: Product samples water balance – Experiment 1.3

Production started at		8:12						
Sample		1	2	3	4	5	6	7
Samling time		8:35	9:07	10:32	10:58	11:07	11:15	11:40
Throughput	BVs	7.8	19.0	48.1	56.9	59.8	62.6	71.1
TOC	mmol/L	0.10	0.20	0.22	0.22	0.22	0.23	0.23
HCO_3^-	meq/L	0.04	0.04	2.31	2.68	2.75	2.79	2.88
CO_3^{2-}	meq/L	0.53	0.04	0.04	0.04	0.05	0.05	0.05
Cl^-	meq/L	12.80	13.53	11.10	10.68	10.47	10.38	9.99
SO_4^{2-}	meq/L	0.05	0.05	0.05	0.05	0.05	0.05	0.05
NO_3^-	meq/L	0.22	0.25	0.27	0.38	0.43	0.50	0.72
HPO_4^{2-}-P	meq/L	0.0006	0.0006	0.0006	0.0006	0.0006	0.0006	0.0006
SiO_2	meq/L	0.22	0.22	0.22	0.22	0.22	0.22	0.22
F^-	meq/L	0.02	0.02	0.02	0.02	0.02	0.02	0.02
Na^+	meq/L	15.09	14.78	14.21	14.46	14.44	14.44	14.32
K^+	meq/L	0.003	0.003	0.003	0.003	0.003	0.003	0.003
Ca^{2+}	meq/L	0.005	0.005	0.005	0.005	0.005	0.005	0.005
Mg^{2+}	meq/L	0.01	0.01	0.01	0.01	0.01	0.01	0.01
Fe^{3+}	meq/L	0.0001	0.0001	0.0001	0.0001	0.0001	0.0001	0.0001
Mn^{2+}	meq/L	0.00001	0.00001	0.00001	0.00001	0.00001	0.00001	0.00001
NH_4^+	meq/L	0.001	0.001	0.001	0.001	0.001	0.001	0.001
Al^{3+}	meq/L	0.0002	0.0004	0.0004	0.0004	0.0004	0.0004	0.0004
Ba^{2+}	meq/L	0.00001	0.00001	0.00001	0.00001	0.00001	0.00001	0.00001
Sr^{2+}	meq/L	0.00001	0.00001	0.00001	0.00001	0.00001	0.00001	0.00001
Sum anion	meq/L	13.88	14.16	14.02	14.08	13.99	14.00	13.93
Sum cation	meq/L	15.11	14.80	14.23	14.48	14.46	14.46	14.34
|Balance|	meq/L	1.23	0.64	0.21	0.40	0.47	0.46	0.41
Balance	%	4.24	2.22	0.74	1.41	1.66	1.61	1.44

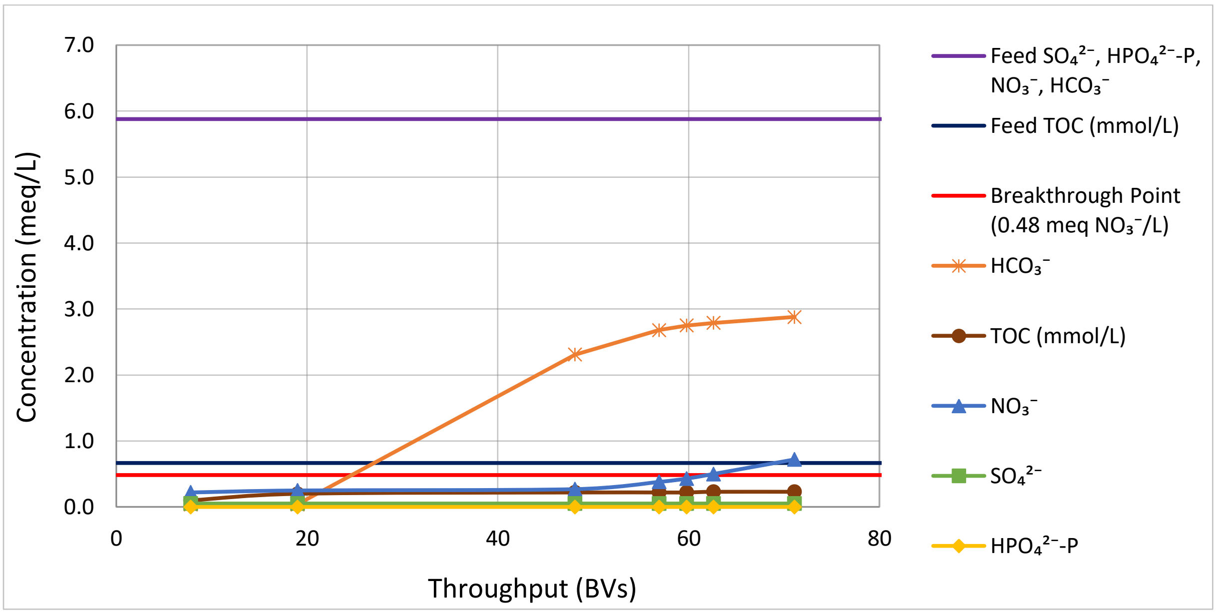

Figure F.6: Breakthrough curves – Experiment 1.3

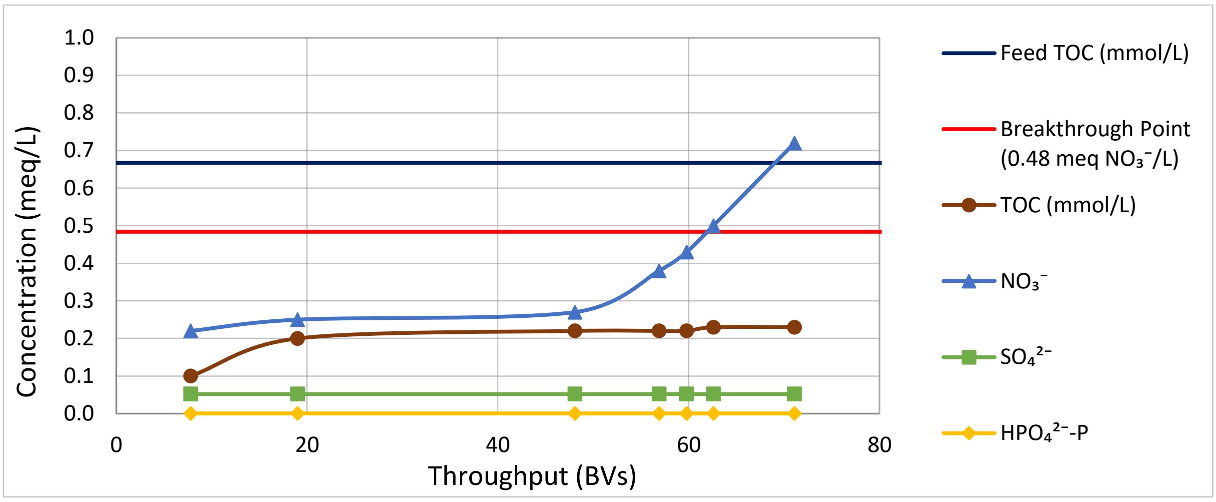

Figure F.7: Breakthrough curves – Experiment 1.3 – Zoom in

TableF.19: SBA operational capacity – Experiment 1.3

Sample	Feed	1	2	3	4	5	6
Throughput (L)	-	153	370	937	1110	1167	1220
HCO_3^- (meq/L)	2.63	0.04	0.04	2.31	2.68	2.75	2.79
SO_4^{2-} (meq/L)	2.14	0.05	0.05	0.05	0.05	0.05	0.05
NO_3^- (meq/L)	0.99	0.22	0.25	0.27	0.38	0.43	0.50
HPO_4^{2-}-P (meq/L)	0.12	0.0006	0.0006	0.0006	0.0006	0.0006	0.0006
Anions removed (meq/L)	-	5.56	5.52	3.23	2.76	2.64	2.53
Anions removed (meq)	-	853	2049	3880	4358	4508	4643
Operational capacity (eq/L_r)			0.238				
Operational capacity /Total capacity (%)			30				

Table F.20: Removed TOC and excess Cl^- – Experiment 1.3

Sample	Feed	1	2	3	4	5	6
Anions removed (meq/L) Table F.19	-	5.56	5.52	3.23	2.76	2.64	2.53
Cl^- (meq/L)	7.03	12.80	13.53	11.10	10.68	10.47	10.38
$\lvert\Delta Cl^-\rvert$(meq/L)	-	5.77	6.50	4.07	3.65	3.44	3.35
Cl^- excess (meq/L)	-	0.21	0.98	0.84	0.89	0.80	0.81
TOC (mmol/L)	0.66	0.10	0.20	0.22	0.22	0.22	0.23
Removed TOC (mmol/L)	-	0.56	0.47	0.44	0.44	0.44	0.44

Table F.21: SBA operational capacity with TOC into account – Experiment 1.3

Sample	1	2	3	4	5	6
Throughput (L)	153	370	937	1110	1167	1220
Anions removed (meq) Table F.20	853	2049	3880	4358	4508	4643
Cl^- excess (meq/L)	0.21	0.98	0.84	0.89	0.80	0.81
Cl^- excess (meq)	32	245	721	875	921	964
Total removed (meq)	885	2294	4601	5233	5429	5607
Operational capacity (eq/L_r)	0.287					
Operational capacity/Total capacity (%)	36					

Table F.22: WAC operational capacity – Experiment 1.3

Sample	1	2	3	4	5	6	7
Cations removed (meq/L)	5.59	5.58	5.59	5.59	5.59	5.59	5.58
Cations removed (meq)	856	2067	5231	6199	6516	6814	7745
WAC operational capacity (eq/L_r)	0.704						
Operational capacity/Total capacity (%)	15						

Table F.23: Volume weighted average and removal – Experiment 1.3

Parameter	VW average	VW average	Feed	Removal
Unit	meq/L	mg/L	mg/L	%
ATP (ng/L)	-	557	1125	50
TOC (mmol/L)	0.20	2.41	7.95	70
HCO_3^-	1.72	104.82	160.38	35
Cl^-	11.63	400.57	242.20	-65
SO_4^{2-}	0.05	2.50	102.78	98
NO_3^-	0.29	18.22	61.07	70
HPO_4^{2-}-P	0.0006	0.01	2.01	100
SiO_2	0.22	6.18	6.18	0
F^-	0.02	0.35	0.35	0
Na^+	14.48	332.91	174.15	-91
K^+	0.003	0.11	26.82	100
Ca^{2+}	0.005	0.10	62.49	100
Mg^{2+}	0.008	0.10	18.75	99
Fe^{3+}	0.0001	0.003	0.05	95
Mn^{2+}	0.00001	0.0003	0.11	100
NH_4^+	0.001	0.03	4.37	99
Al^{3+}	0.0004	0.003	0.01	64
Ba^{2+}	0.00001	0.001	0.004	89
Sr^{2+}	0.00001	0.001	0.27	100

Table F.24: Samples after WAC before SBA water quality – Experiment 1.3

Sample	Unit	M1	M2
Sampling time	-	8:52	10:47
Throughput	BVs in H form	24.5	94.3
EC	µS/cm	1513.30	1464.19
pH	-	9.79	9.45
ATP	ng/L	-	352
TOC	mg C/L	7.82	7.96
HCO_3^-	mg/L	120.87	150.11
CO_3^{2-}	mg/L	53.04	31.19
Cl^-	mg/L	239.95	246.14
SO_4^{2-}	mg/L	99.46	100.06
NO_3^-	mg/L	58.71	57.37
HPO_4^{2-}-P	mg P/L	2.03	2.02
Na^+	mg/L	341.43	333.49
K^+	mg/L	0.11	0.11
Ca^{2+}	mg/L	<0.2	<0.2
Mg^{2+}	mg/L	<0.1	<0.1
Fe^{3+}	mg/L	< 0.005	< 0.005
Mn^{2+}	mg/L	0.0006	0.0006
NH_4^+	mg/L	< 0.05	< 0.05
Al^{3+}	mg/L	0.005	0.005
Ba^{2+}	mg/L	< 0.001	< 0.001
Sr^{2+}	mg/L	< 0.001	< 0.001

Experiment 2.1

Table F.25: Product samples water quality – Experiment 2.1

Sample	Unit	1	2	3	4	5	6	7	8
EC	µS/cm	2365.92	2321.28	2209.68	2171.74	2157.23	2146.07	2144.95	2144.95
pH	-	8.82	8.68	8.5	8.46	8.46	8.46	8.46	8.45
ATP	ng/L	1.7	2.00	1.90	2.20	2.30	2.30	-	2.90
TOC	mg C/L	3.70	3.72	3.26	2.54	3.68	3.63	3.90	3.99
HCO_3^-	mg/L	6.71	9.62	178.39	242.79	261.13	269.48	277.33	279.35
CO_3^{2-}	mg/L	< 5	< 5	< 5	< 5	< 5	< 5	< 5	< 5
Cl^-	mg/L	743.72	730.65	626.96	582.33	567.54	559.37	552.76	551.51
SO_4^{2-}	mg/L	< 5	< 5	< 5	< 5	< 5	< 5	< 5	< 5
NO_3^-	mg/L	6.11	7.27	8.38	7.85	9.16	11.35	15.95	19.73
HPO_4^{2-}-P	mg P/L	< 0.02	< 0.02	< 0.02	< 0.02	< 0.02	< 0.02	< 0.02	< 0.02
Na^+	mg/L	473.3	464.9	450.6	458.9	448.6	445.2	451.5	443.7
K^+	mg/L	< 0.3	< 0.3	< 0.3	0.349	1.011	2.157	5.118	7.03
Ca^{2+}	mg/L	< 3	< 3	< 3	< 3	< 3	< 3	< 3	< 3
Mg^{2+}	mg/L	< 0.4	< 0.4	< 0.4	< 0.4	< 0.4	< 0.4	< 0.4	< 0.4
Fe^{3+}	mg/L	< 0.005	< 0.005	< 0.005	< 0.005	< 0.005	< 0.005	< 0.005	< 0.005
Mn^{2+}	mg/L	< 0.0004	< 0.0004	< 0.0004	< 0.0004	< 0.0004	< 0.0004	< 0.0004	< 0.0004
NH_4^+	mg/L	< 0.05	< 0.05	< 0.05	< 0.05	< 0.05	< 0.05	< 0.05	0.052
Al^{3+}	mg/L	0.0017	0.0028	0.0031	0.0030	0.0031	0.0033	0.0030	0.0030
Ba^{2+}	mg/L	< 0.001	< 0.001	< 0.001	< 0.001	< 0.001	< 0.001	< 0.001	< 0.001
Sr^{2+}	mg/L	< 0.012	< 0.012	< 0.012	< 0.012	< 0.012	< 0.012	< 0.012	< 0.012

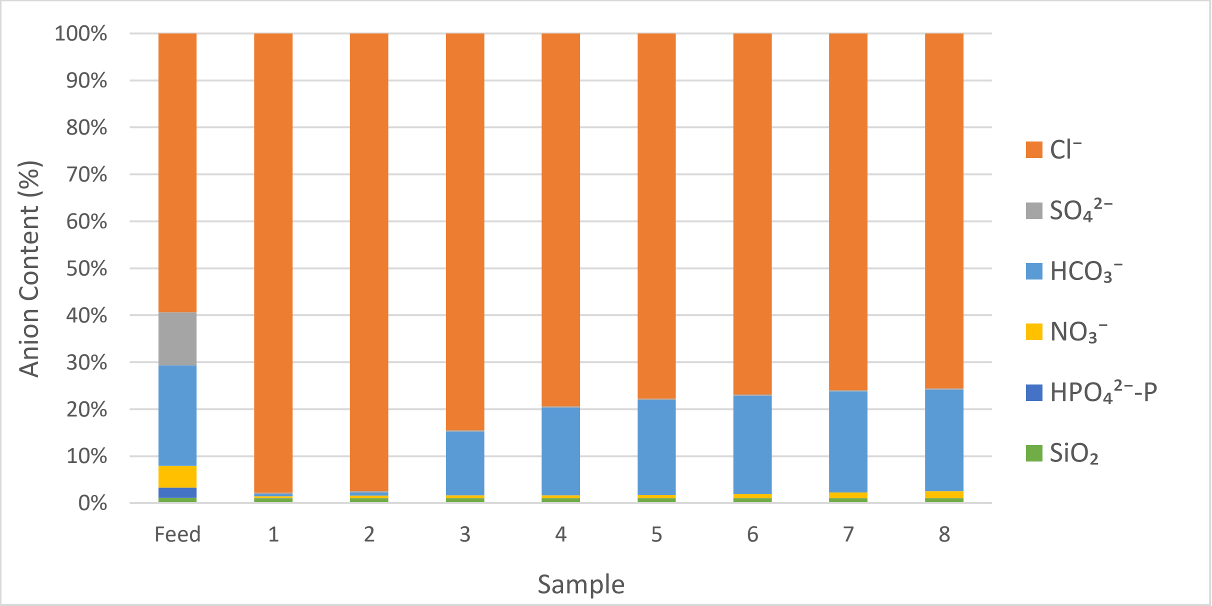

Figure F.8: Product water quality – Anion content (%) – Experiment 2.1

Table F.26: Product samples water balance – Experiment 2.1

Production started at		10:40							
Sample		1	2	3	4	5	6	7	8
Samling time		10:57	11:42	12:57	13:27	13:47	14:02	14:19	14:27
Throughput	BVs	6.0	21.4	47.0	57.3	64.1	69.2	74.9	77.8
TOC	mmol/L	0.31	0.31	0.27	0.21	0.31	0.30	0.33	0.33
HCO_3^-	meq/L	0.11	0.16	2.92	3.98	4.28	4.42	4.55	4.58
CO_3^{2-}	meq/L	0.00	0.00	0.06	0.07	0.08	0.08	0.08	0.08
Cl^-	meq/L	21.59	21.21	18.20	16.90	16.47	16.24	16.05	16.01
SO_4^{2-}	meq/L	0.05	0.05	0.05	0.05	0.05	0.05	0.05	0.05
NO_3^-	meq/L	0.10	0.12	0.135	0.13	0.15	0.18	0.26	0.32
HPO_4^{2-}-P	meq/L	0.0006	0.0006	0.0006	0.0006	0.0006	0.0006	0.0006	0.0006
SiO_2	meq/L	0.22	0.22	0.22	0.22	0.22	0.22	0.22	0.22
F^-	meq/L	0.02	0.02	0.02	0.02	0.02	0.02	0.02	0.02
Na^+	meq/L	20.59	20.22	19.60	19.96	19.51	19.36	19.64	19.30
K^+	meq/L	0.004	0.004	0.004	0.009	0.026	0.055	0.131	0.180
Ca^{2+}	meq/L	0.005	0.005	0.005	0.005	0.005	0.005	0.005	0.005
Mg^{2+}	meq/L	0.01	0.01	0.01	0.01	0.01	0.01	0.01	0.01
Fe^{3+}	meq/L	0.0001	0.0001	0.0001	0.0001	0.0001	0.0001	0.0001	0.0001
Mn^{2+}	meq/L	0.00001	0.00001	0.00001	0.00001	0.00001	0.00001	0.00001	0.00001
NH_4^+	meq/L	0.001	0.001	0.001	0.001	0.001	0.001	0.001	0.003
Al^{3+}	meq/L	0.0002	0.0003	0.0003	0.0003	0.0003	0.0004	0.0003	0.0003
Ba^{2+}	meq/L	0.00001	0.00001	0.00001	0.00001	0.00001	0.00001	0.00001	0.00001
Sr^{2+}	meq/L	0.0001	0.0001	0.0001	0.0001	0.0001	0.0001	0.0001	0.0001
Sum anion	meq/L	22.10	21.78	21.61	21.38	21.28	21.21	21.23	21.28
Sum cation	meq/L	20.61	20.24	19.62	19.99	19.55	19.44	19.79	19.50
|Balance|	meq/L	1.49	1.54	1.99	1.39	1.72	1.78	1.44	1.79
Balance	%	3.5	3.7	4.8	3.4	4.2	4.4	3.5	4.4

The NO_3^- concentration of the last sample was below the breakthrough concentration of 0.48 meq/L. The point "8^+" was based on the online NO_3^- analyzer measurements.

Table F.27: SBA operational capacity – Experiment 2.1

Sample	Feed	1	2	3	4	5	6	7	8^+
Throughput (L)	-	117	417	917	1117	1250	1350	1460	1667
HCO_3^- (meq/L)	4.30	0.11	0.16	2.92	3.98	4.28	4.42	4.55	4.58
SO_4^{2-} (meq/L)	2.27	0.05	0.05	0.05	0.05	0.05	0.05	0.05	0.05
NO_3^- (meq/L)	0.93	0.10	0.12	0.14	0.13	0.15	0.18	0.26	0.5
HPO_4^{2-}-P (meq/L)	0.44	0.0006	0.0006	0.0006	0.0006	0.0006	0.0006	0.0006	0.0006
Anions removed (meq/L)	-	7.69	7.62	4.84	3.79	3.47	3.30	3.09	3.00
Anions removed (meq)	-	897	3184	5603	6361	6823	7153	7494	8086
Operational capacity (eq/L_r)				0.415					
Operational capacity/Total capacity (%)				33					

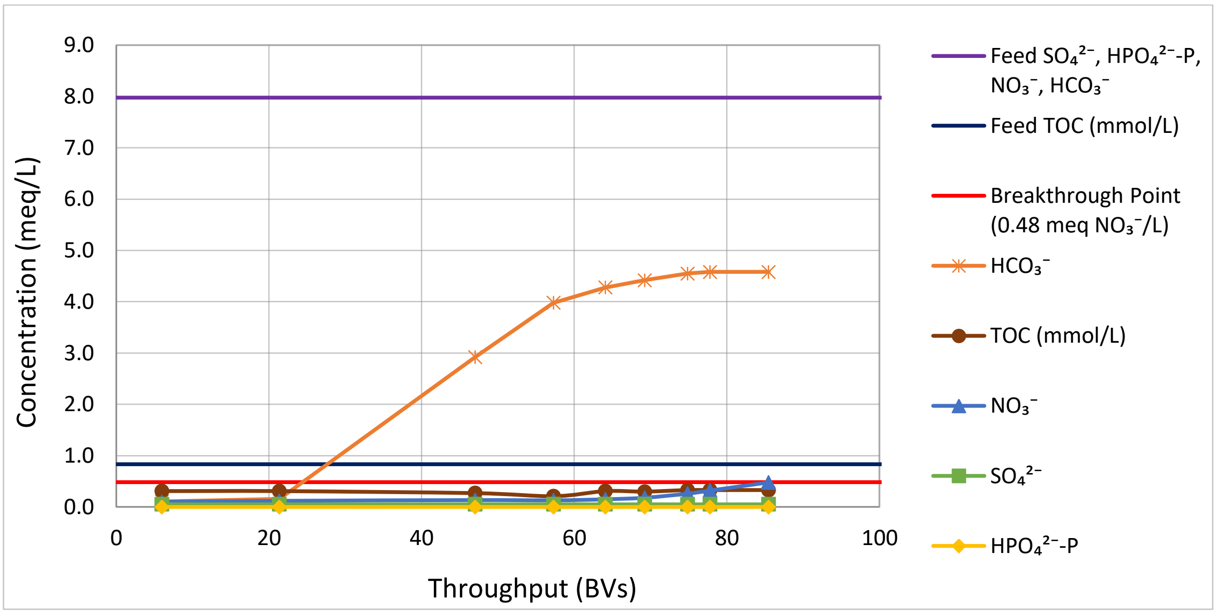

Figure F.9: Breakthrough curves – Experiment 2.1

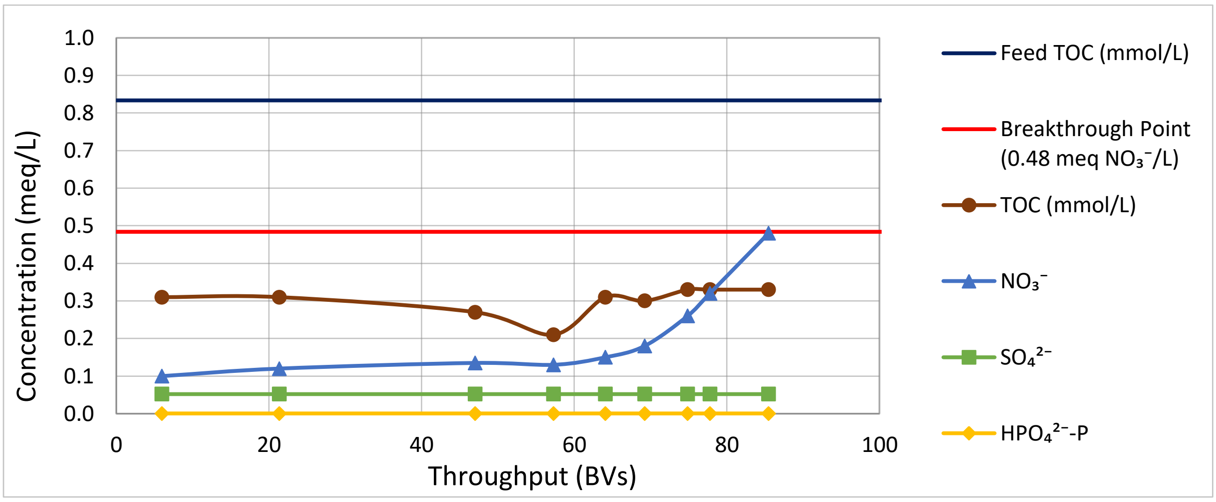

Figure F.10: Breakthrough curves – Experiment 2.1 – Zoom in

Table F.28: Removed TOC and excess Cl^- – Experiment 2.1

Sample	Feed	1	2	3	4	5	6	7	8$^+$
Anions removed (meq/L) Table F.27	-	7.69	7.62	4.84	3.79	3.47	3.30	3.09	3.00
Cl^- (meq/L)	11.93	21.59	21.21	18.20	16.90	16.47	16.24	16.05	16.01
$\|\Delta Cl^-\|$(meq/L)	-	9.66	9.28	6.27	4.97	4.54	4.30	4.11	4.08
Cl^- excess (meq/L)	-	1.97	1.65	1.43	1.18	1.07	1.01	1.02	1.08
TOC (mmol/L)	0.86	0.31	0.31	0.27	0.21	0.31	0.30	0.33	0.33
Removed TOC (mmol/L)	-	0.55	0.55	0.59	0.65	0.55	0.56	0.54	0.53

Table F.29: SBA operational capacity with TOC into account – Experiment 2.1

Sample	1	2	3	4	5	6	7	8^+
Throughput (L)	117	417	917	1117	1250	1350	1460	1667
Anions removed (meq) Table F.27	897	3184	5603	6361	6823	7153	7494	8086
Cl^- excess (meq/L)	1.97	1.65	1.43	1.18	1.07	1.01	1.02	1.08
Cl^- excess (meq)	230	725	1440	1676	1819	1920	2032	2256
Total removed (meq)	1127	3909	7043	8037	8642	9073	9526	10342
Operational capacity (eq/L_r)	0.530							
Operational capacity/Total capacity (%)	42							

Table F.30: WAC operational capacity – Experiment 2.1

Sample	1	2	3	4	5	6	7	8
Cations removed (meq/L)	8.04	8.04	8.04	8.04	8.02	7.99	7.91	7.86
Cations removed (meq)	938	3350	7371	8978	10047	10846	11717	12162
WAC operational capacity (eq/L_r)	1.106							
Operational capacity/Total capacity (%)	24							

Table F.31: Volume weighted average and removal – Experiment 2.1

Parameter	VW average	VW average	Feed	Removal
Unit	meq/L	mg/L	mg/L	%
ATP (ng/L)	-	2.19	216.60	99
TOC (mmol/L)	0.29	3.48	10.33	66
HCO_3^-	2.87	174.86	262.53	33
Cl^-	18.15	625.38	411.07	-52
SO_4^{2-}	0.05	2.50	109.16	98
NO_3^-	0.18	11.12	57.74	81
HPO_4^{2-}-P	0.0006	0.01	7.62	100
SiO_2	0.22	6.29	6.29	0
F^-	0.02	0.35	0.35	0
Na^+	19.77	454.48	255.80	-78
K^+	0.04	1.54	44.58	97
Ca^{2+}	0.005	0.10	84.85	100
Mg^{2+}	0.01	0.10	29.59	100
Fe^{3+}	0.0001	0.00	0.06	95
Mn^{2+}	0.00001	0.00	0.11	100
NH_4^+	0.002	0.03	4.21	99
Al^{3+}	0.0003	0.00	0.01	79
Ba^{2+}	0.00001	0.00	0.003	83
Sr^{2+}	0.0001	0.01	0.37	98

Table F.32: Samples after WAC before SBA water quality – Experiment 2.1

Sample	Unit	M1	M2	M3
Sampling time	-	11:52	13:37	14:02
Throughput	BVs in H form	43.8	107.6	122.7
EC	µS/cm	2148.30	2115.94	2111.47
pH	-	9.37	9.13	9.1
ATP	ng/L	-	-	150.3
TOC	mg C/L	10.22	10.50	10.09
HCO_3^-	mg/L	241.90	257.09	258.35
CO_3^{2-}	mg/L	37.95	23.14	21.28
Cl^-	mg/L	406.05	402.63	409.83
SO_4^{2-}	mg/L	108.31	107.232	107.609
NO_3^-	mg/L	55.90	57.48	58.51
HPO_4^{2-}-P	mg P/L	2.41	7.22	2.36
Na^+	mg/L	457.80	451.80	450.40
K^+	mg/L	0.15	0.93	2.97
Ca^{2+}	mg/L	< 3	< 3	< 3
Mg^{2+}	mg/L	< 0.4	< 0.4	< 0.4
Fe^{3+}	mg/L	0.05	0.05	0.05
Mn^{2+}	mg/L	0.001	0.001	0.008
NH_4^+	mg/L	0.03	0.03	0.04
Al^{3+}	mg/L	0.01	0.01	0.01
Ba^{2+}	mg/L	< 0.001	< 0.001	< 0.001
Sr^{2+}	mg/L	< 0.012	< 0.012	< 0.012

Experiment 2.2

Table F.33: Product samples water quality – Experiment 2.2

Sample	Unit	1	2	3	4	5	6	7	8
EC	µS/cm	1912.82	1655.03	1485.4	1450.8	1438.52	1428.48	1425.13	1421.78
pH	-	11.3	10.4	8.69	8.62	8.6	8.6	8.61	8.60
ATP	ng/L	2.40	4.70	37.70	37.70	35.80	39.40	39.20	36.50
TOC	mg C/L	1.89	2.85	2.95	2.96	2.98	2.95	2.99	2.98
HCO_3^-	mg/L	< 5	< 5	127.5	165.58	171.4	174.31	176.33	178.1
CO_3^{2-}	mg/L	9.7	10.7	< 5	< 5	< 5	< 5	< 5	< 5
Cl^-	mg/L	485.52	475.47	380.33	357.12	350.51	352.04	336.13	335.22
SO_4^{2-}	mg/L	< 5	< 5	< 5	< 5	< 5	< 5	< 5	< 5
NO_3^-	mg/L	17.36	14.56	12.79	14.79	16.56	20.20	22.35	25.34
HPO_4^{2-}-P	mg P/L	0.162	0.321	0.192	0.16	0.161	0.16	0.15	0.16
Na^+	mg/L	307.84	309.73	292.22	273.66	286.77	275.82	278.21	256.86
K^+	mg/L	0.12	0.10	0.10	0.28	0.46	0.78	1.24	1.75
Ca^{2+}	mg/L	<0.2	<0.2	<0.2	<0.2	<0.2	<0.2	<0.2	<0.2
Mg^{2+}	mg/L	<0.1	<0.1	<0.1	<0.1	<0.1	<0.1	<0.1	<0.1
Fe^{3+}	mg/L	< 0.005	< 0.005	< 0.005	< 0.005	< 0.005	< 0.005	< 0.005	< 0.005
Mn^{2+}	mg/L	0.0003	0.0003	0.0018	0.0009	0.0008	0.0011	0.0006	0.0006
NH_4^+	mg/L	0.05	0.07	0.06	0.06	0.05	0.06	0.09	0.06
Al^{3+}	mg/L	0.005	0.005	0.007	0.007	0.006	0.007	0.007	0.007
Ba^{2+}	mg/L	< 0.001	< 0.001	< 0.001	< 0.001	< 0.001	< 0.001	< 0.001	< 0.001
Sr^{2+}	mg/L	0.001	< 0.001	< 0.001	< 0.001	< 0.001	< 0.001	< 0.001	< 0.001

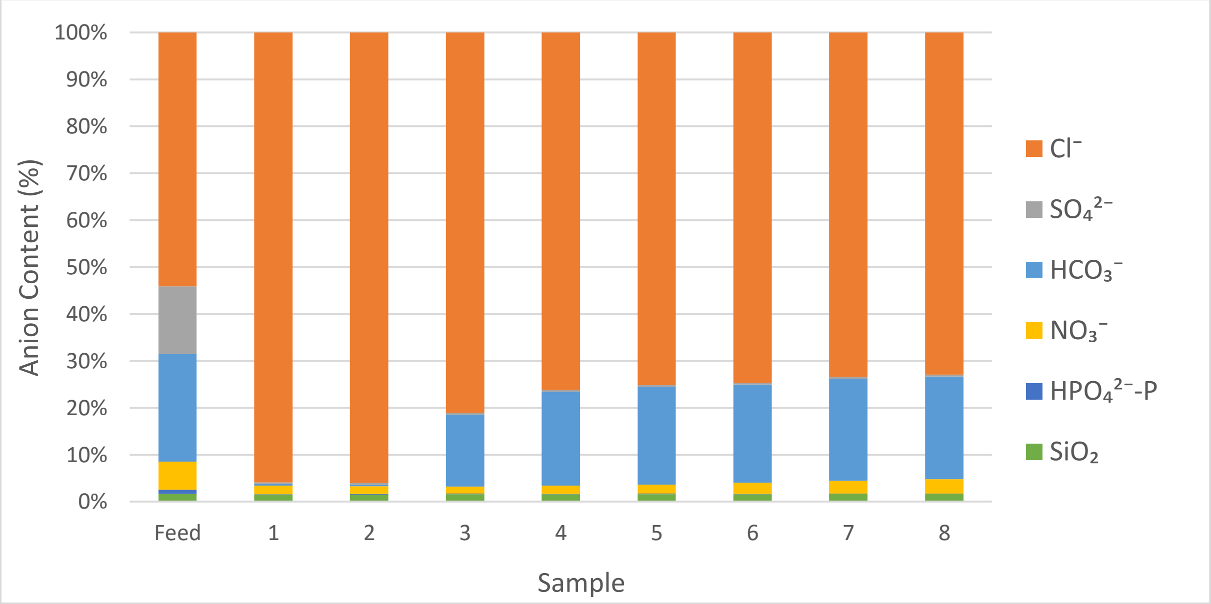

Figure F.11: Product water quality – Anion content (%) – Experiment 2.2

Table F.34: Product samples water balance – Experiment 2.2

Production started at		9:00							
Sample		1	2	3	4	5	6	7	8
Samling time		9:22	10:07	12:22	13:12	13:27	13:43	13:57	14:07
Throughput	BVs	8.0	23.4	69.6	86.7	91.8	97.3	102.1	105.3
TOC	mmol/L	0.16	0.24	0.25	0.25	0.25	0.25	0.25	0.25
HCO_3^-	meq/L	0.04	0.04	2.09	2.71	2.81	2.86	2.89	2.92
CO_3^{2-}	meq/L	0.53	0.07	0.07	0.07	0.07	0.07	0.08	0.08
Cl^-	meq/L	14.09	13.80	11.04	10.37	10.17	10.22	9.76	9.73
SO_4^{2-}	meq/L	0.05	0.05	0.05	0.05	0.05	0.05	0.05	0.05
NO_3^-	meq/L	0.28	0.23	0.21	0.24	0.27	0.33	0.36	0.41
HPO_4^{2-}-P	meq/L	0.01	0.02	0.01	0.01	0.01	0.01	0.01	0.01
SiO_2	meq/L	0.22	0.22	0.22	0.22	0.22	0.22	0.22	0.22
F^-	meq/L	0.02	0.02	0.02	0.02	0.02	0.02	0.02	0.02
Na^+	meq/L	13.39	13.47	12.71	11.90	12.47	12.00	12.10	11.17
K^+	meq/L	0.003	0.003	0.002	0.007	0.012	0.020	0.032	0.045
Ca^{2+}	meq/L	0.005	0.005	0.005	0.005	0.005	0.005	0.005	0.005
Mg^{2+}	meq/L	0.01	0.01	0.01	0.01	0.01	0.01	0.01	0.01
Fe^{3+}	meq/L	0.0001	0.0001	0.0001	0.0001	0.0001	0.0001	0.0001	0.0001
Mn^{2+}	meq/L	0.00001	0.00001	0.00007	0.00003	0.00003	0.00004	0.00002	0.00002
NH_4^+	meq/L	0.003	0.004	0.003	0.003	0.003	0.003	0.005	0.004
Al^{3+}	meq/L	0.0006	0.0005	0.0007	0.0008	0.0007	0.0007	0.0008	0.0007
Ba^{2+}	meq/L	0.00001	0.00001	0.00001	0.00001	0.00001	0.00001	0.00001	0.00001
Sr^{2+}	meq/L	0.00003	0.00001	0.00001	0.00001	0.00001	0.00001	0.00001	0.00001
Sum anion	meq/L	15.24	14.45	13.70	13.69	13.62	13.78	13.38	13.43
Sum cation	meq/L	13.41	13.49	12.73	11.93	12.50	12.03	12.15	11.24
|Balance|	meq/L	1.83	0.96	0.97	1.76	1.12	1.74	1.23	2.20
Balance	%	6.4	3.4	3.7	6.9	4.3	6.7	4.8	8.9

The HPO_4^{2-}-P concentration in the product water samples given in Table F.34 are above the detection limit of 0.02 mg/L. However, experiments 2.4 and 2.5 were performed with the same conditions of experiment 2.2 (resin 2 at regeneration level 2), since the latter was selected as the best performing regeneration level for resin 2. In those two experiments, HPO_4^{2-}-P concentration was found to be below detection limit. For this reason the concentration of HPO_4^{2-}-P for the calculations of the operational capacity, the volume weighted average and the removal in experiment 2.2 was considered to be below the detection limit 0.02 mg/L.

Table F.35: SBA operational capacity – Experiment 2.2

Sample	Feed	1	2	3	4	5	6	7	8^+
Throughput (L)	-	157	457	1357	1690	1790	1897	1990	2120
HCO_3^- (meq/L)	3.05	0.04	0.04	2.09	2.71	2.81	2.86	2.89	2.92
SO_4^{2-} (meq/L)	1.91	0.05	0.05	0.05	0.05	0.05	0.05	0.05	0.05
NO_3^- (meq/L)	0.79	0.28	0.23	0.21	0.24	0.27	0.33	0.36	0.48
HPO_4^{2-}-P (meq/L)	0.12	0.0006	0.0006	0.0006	0.0006	0.0006	0.0006	0.0006	0.0006
Anions removed (meq/L)	-	5.50	5.55	3.52	2.87	2.74	2.63	2.57	2.42
Anions removed (meq)	-	863	2528	5696	6651	6925	7206	7445	7760
Operational capacity (eq/L_r)	0.398								
Operational capacity/Total capacity (%)	32								

Table F.36: Removed TOC and excess Cl^- – Experiment 2.2

Sample	Feed	1	2	3	4	5	6	7	8^+
Anions removed (meq/L) Table F.35	-	5.50	5.55	3.52	2.87	2.74	2.63	2.57	2.42
Cl^- (meq/L)	7.18	14.09	13.80	11.04	10.37	10.17	10.22	9.76	9.73
$\lvert \Delta Cl^- \rvert$(meq/L)	-	6.91	6.62	3.86	3.19	2.99	3.04	2.58	2.55
Cl^- excess(meq/L)	-	1.41	1.07	0.34	0.32	0.25	0.41	0.01	0.13
TOC (mmol/L)	0.79	0.16	0.24	0.25	0.25	0.25	0.25	0.25	0.25
Removed TOC (mmol/L)	-	0.63	0.55	0.54	0.54	0.54	0.54	0.54	0.54

Table F.37: SBA operational capacity with TOC into account – Experiment 2.2

Sample	1	2	3	4	5	6	7	8^+
Throughput (L)	157	457	1357	1690	1790	1897	1990	2120
Anions removed (meq) Table F.36	863	2528	5696	6651	6925	7206	7445	7760
Cl^- excess (meq/L)	1.41	1.07	0.34	0.32	0.25	0.41	0.01	0.13
Cl^- excess (meq)	221	542	848	955	980	1024	1025	1042
Total removed (meq)	1084	3070	6544	7606	7905	8230	8470	8802
Operational capacity (eq/L_r)	0.451							
Operational capacity/Total capacity (%)	36							

Table F.38: WAC operational capacity – Experiment 2.2

Sample	1	2	3	4	5	6	7	8
Cations removed (meq/L)	5.31	5.31	5.31	5.30	5.30	5.29	5.28	5.26
Cations removed (meq)	832	2424	7200	8968	9498	10062	10555	10888
WAC operational capacity (eq/L_r)	0.990							
Operational capacity/Total capacity (%)	21							

Table F.39: Volume weighted average and removal – Experiment 2.2

Parameter	VW average	VW average	Feed	Removal
Unit	meq/L	mg/L	mg/L	%
ATP (ng/L)	-	30.41	260	88
TOC (mmol/L)	0.24	2.86	9.42	70
HCO_3^-	1.91	116.24	186.07	38
Cl^-	11.33	390.38	247.33	-58
SO_4^{2-}	0.05	2.50	91.58	97
NO_3^-	0.25	15.57	49.26	68
HPO_4^{2-}-P	0.0006	0.01	2.07	100
SiO_2	0.22	6.18	6.18	0
F^-	0.02	0.35	0.35	0
Na^+	12.57	289.07	173.97	-66
K^+	0.01	0.33	27.88	99
Ca^{2+}	0.005	0.10	58.70	100
Mg^{2+}	0.01	0.10	17.64	99
Fe^{3+}	0.0001	0.003	0.05	95
Mn^{2+}	0.00004	0.001	0.09	99
NH_4^+	0.003	0.06	3.98	98
Al^{3+}	0.001	0.01	0.01	40
Ba^{2+}	0.00001	0.001	0.003	81
Sr^{2+}	0.00001	0.001	0.27	100

Table F.40: Samples after WAC before SBA water quality – Experiment 2.2

Sample	Unit	M1	M2
Sampling time	-	9:57	13:02
Throughput	BVs in H form	35.5	147.6
EC	µS/cm	1523.34	1417.32
pH	-	9.71	9.44
ATP	ng/L	-	137.30
TOC	mg C/L	9.47	8.86
HCO_3^-	mg/L	151.03	161.03
CO_3^{2-}	mg/L	49.26	28.61
Cl^-	mg/L	255.78	243.63
SO_4^{2-}	mg/L	98.329	96.7002
NO_3^-	mg/L	255.78	52.07
HPO_4^{2-}-P	mg P/L	2.06	1.98
Na^+	mg/L	312.82	296.05
K^+	mg/L	0.12	0.25
Ca^{2+}	mg/L	<0.2	<0.2
Mg^{2+}	mg/L	<0.1	<0.1
Fe^{3+}	mg/L	< 0.005	< 0.005
Mn^{2+}	mg/L	0.0007	0.0008
NH_4^+	mg/L	< 0.05	< 0.05
Al^{3+}	mg/L	0.010	0.009
Ba^{2+}	mg/L	< 0.001	< 0.001
Sr^{2+}	mg/L	< 0.001	< 0.001

Experiment 2.3

Table F.41: Product samples water quality – Experiment 2.3

Sample	Unit	1	2	3	4	5	6	7
EC	µS/cm	1862.6	1772.21	1621.55	1600.34	1506.6	1487.63	1475.35
pH	-	11.3	11.2	10.2	9.57	8.62	8.55	8.57
ATP	ng/L	73	131.8	209.9	288	638.5	989	864
TOC	mg C/L	1.41	2.29	2.53	2.71	2.85	2.96	2.97
HCO_3^-	mg/L	< 5	< 5	< 5	< 5	141.80	161.03	179.36
CO_3^{2-}	mg/L	5.11	5.88	5.5	6.01	3.45	3.83	4.22
Cl^-	mg/L	443.97	416.71	469.33	466.91	373.54	360.69	336.32
SO_4^{2-}	mg/L	< 5	< 5	< 5	< 5	< 5	< 5	< 5
NO_3^-	mg/L	15.53	18.65	21.42	23.92	23.96	27.44	44.79
HPO_4^{2-}-P	mg P/L	< 0.02	< 0.02	0.018	0.027	0.024	0.023	0.032
Na^+	mg/L	349.24	347.39	342.88	335.46	329.04	331.14	322.04
K^+	mg/L	0.09	0.10	0.11	0.11	0.16	0.36	3.16
Ca^{2+}	mg/L	<0.2	<0.2	<0.2	<0.2	<0.2	<0.2	<0.2
Mg^{2+}	mg/L	<0.1	<0.1	<0.1	<0.1	<0.1	<0.1	<0.1
Fe^{3+}	mg/L	< 0.005	< 0.005	< 0.005	< 0.005	< 0.005	< 0.005	< 0.005
Mn^{2+}	mg/L	< 0.0005	< 0.0005	< 0.0005	< 0.0005	< 0.0005	< 0.0005	< 0.0005
NH_4^+	mg/L	< 0.05	< 0.05	< 0.05	< 0.05	0.0535	0.072	0.1072
Al^{3+}	mg/L	0.003	0.003	0.003	0.005	0.003	0.004	0.004
Ba^{2+}	mg/L	< 0.001	< 0.001	< 0.001	< 0.001	< 0.001	< 0.001	< 0.001
Sr^{2+}	mg/L	< 0.001	< 0.001	< 0.001	< 0.001	< 0.001	< 0.001	< 0.001

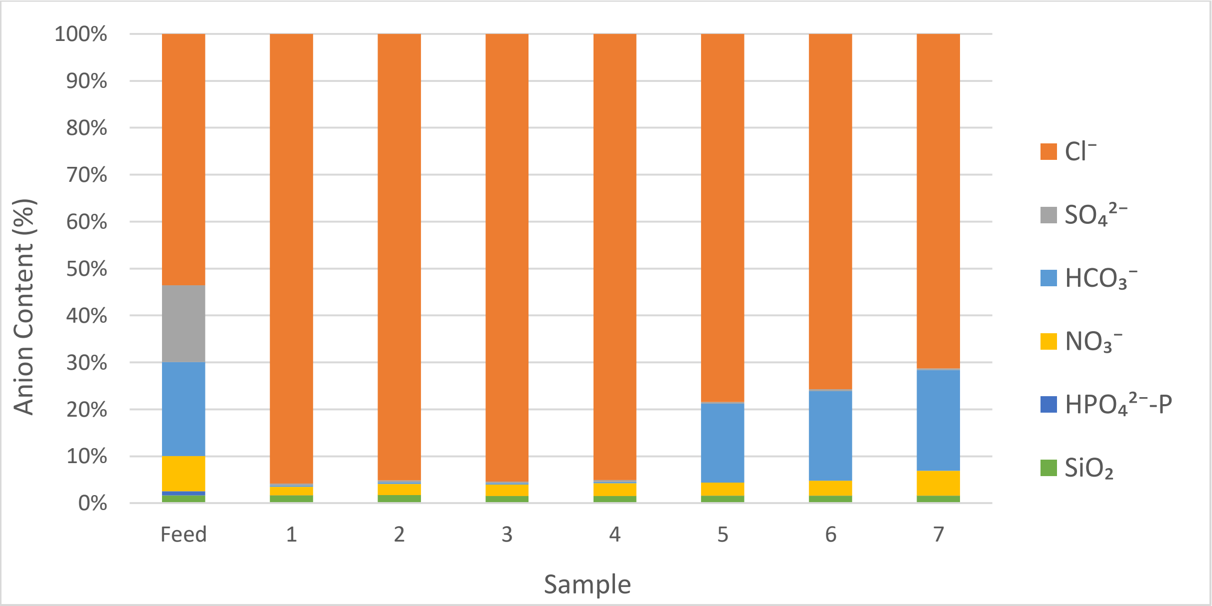

Figure F.12: Product water quality – Anion content (%) – Experiment 2.3

Table F.42: Product samples water balance – Experiment 2.3

Production started at		8:12						
Sample		1	2	3	4	5	6	7
Sampling time		8:35	9:07	9:24	10:03	12:02	12:30	13:38
Throughput	BVs	7.8	19.0	24.8	38.1	78.8	88.4	111.4
TOC	mmol/L	0.12	0.19	0.21	0.23	0.24	0.25	0.25
HCO_3^-	meq/L	0.04	0.04	0.04	0.04	2.32	2.64	2.94
CO_3^{2-}	meq/L	0.53	0.42	0.04	0.01	0.06	0.06	0.07
Cl^-	meq/L	12.89	12.10	13.62	13.55	10.84	10.47	9.76
SO_4^{2-}	meq/L	0.05	0.05	0.05	0.05	0.05	0.05	0.05
NO_3^-	meq/L	0.25	0.30	0.35	0.39	0.39	0.44	0.72
HPO_4^{2-}-P	meq/L	0.0006	0.0006	0.001	0.002	0.002	0.002	0.002
SiO_2	meq/L	0.22	0.22	0.22	0.22	0.22	0.22	0.22
F^-	meq/L	0.02	0.02	0.02	0.02	0.02	0.02	0.02
Na^+	meq/L	15.19	15.11	14.91	14.59	14.31	14.40	14.01
K^+	meq/L	0.002	0.003	0.003	0.003	0.004	0.009	0.08
Ca^{2+}	meq/L	0.005	0.005	0.005	0.005	0.005	0.005	0.005
Mg^{2+}	meq/L	0.01	0.01	0.01	0.01	0.01	0.01	0.01
Fe^{3+}	meq/L	0.0001	0.0001	0.0001	0.0001	0.0001	0.0001	0.0001
Mn^{2+}	meq/L	0.00001	0.00001	0.00001	0.00001	0.00001	0.00001	0.00001
NH_4^+	meq/L	0.001	0.001	0.001	0.001	0.003	0.004	0.006
Al^{3+}	meq/L	0.0003	0.0003	0.0003	0.0005	0.0004	0.0004	0.0004
Ba^{2+}	meq/L	0.00001	0.00001	0.00001	0.00001	0.00001	0.00001	0.00001
Sr^{2+}	meq/L	0.00001	0.00001	0.00001	0.00001	0.00001	0.00001	0.00001
Sum anion	meq/L	14.00	13.15	14.34	14.28	13.91	13.90	13.79
Sum cation	meq/L	15.21	15.13	14.93	14.61	14.33	14.43	14.11
|Balance|	meq/L	1.21	1.98	0.59	0.33	0.43	0.53	0.32
Balance	%	4.1	7.0	2.0	1.1	1.5	1.9	1.2

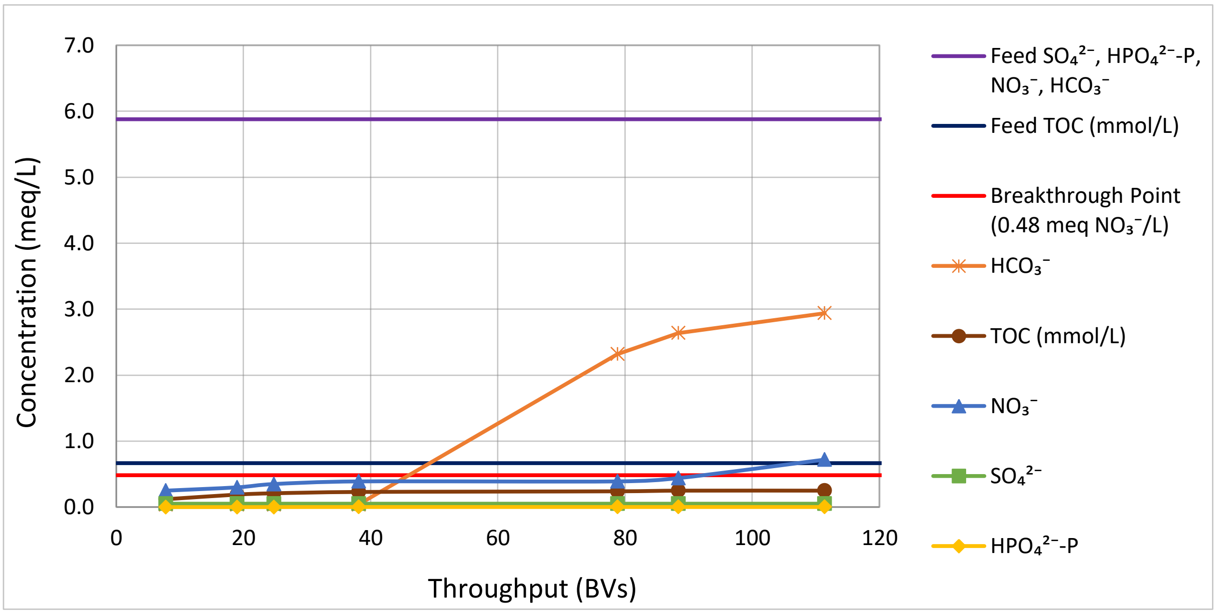

Figure F.13: Breakthrough curves – Experiment 2.3

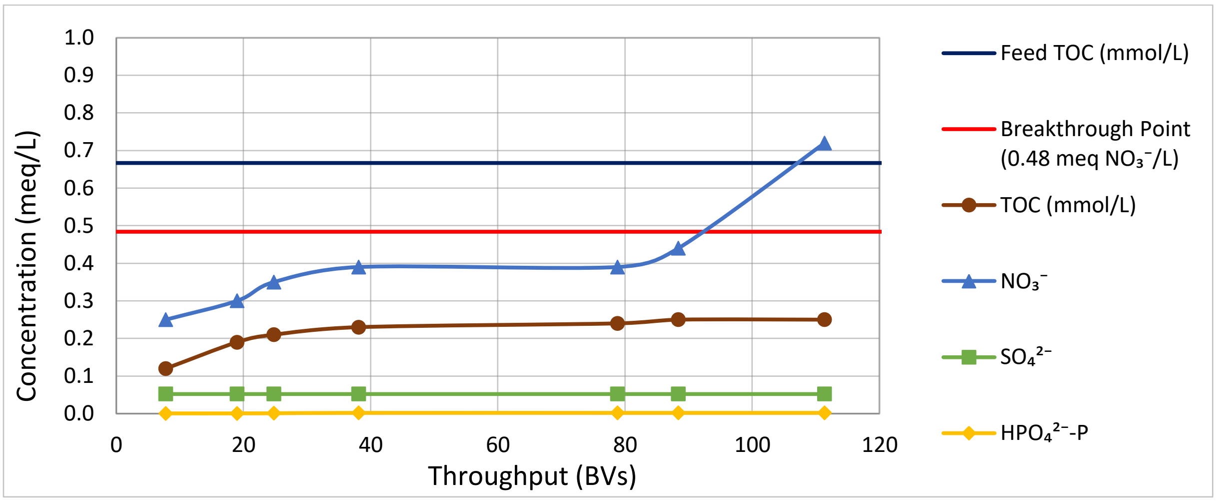

Figure F.14: Breakthrough curves – Experiment 2.3 – Zoom in

Table F.43: SBA operational capacity – Experiment 2.3

Sample	Feed	1	2	3	4	5	6	7^-
Throughput (L)	-	153	370	483	743	1537	1723	1800
HCO_3^- (meq/L)	2.63	0.04	0.04	0.04	0.04	2.32	2.64	2.64
SO_4^{2-} (meq/L)	2.14	0.05	0.05	0.05	0.05	0.05	0.05	0.05
NO_3^- (meq/L)	0.99	0.25	0.30	0.35	0.39	0.39	0.44	0.48
HPO_4^{2-}-P (meq/L)	0.12	0.0006	0.0006	0.001	0.002	0.002	0.002	0.002
Anions removed (meq/L)	-	5.53	5.48	5.43	5.39	3.11	2.74	2.70
Anions removed (meq)	-	847	2034	2649	4051	6515	7026	7232
Operational capacity (eq/L_r)			0.371					
Operational capacity/Total capacity (%)			30					

Table F.44: Removed TOC and excess Cl^- – Experiment 2.3

Sample	Feed	1	2	3	4	5	6	7^-
Anions removed (meq/L) Table F.42	-	5.53	5.48	5.43	5.39	3.11	2.74	2.70
Cl^- (meq/L)	7.03	12.89	12.10	13.62	13.55	10.84	10.47	9.76
$\|\Delta Cl^-\|$(meq/L)	-	5.86	5.07	6.59	6.52	3.81	3.44	2.73
Cl^- excess (meq/L)	-	0.33	0	1.16	1.13	0.71	0.70	0.03
TOC (mmol/L)	0.66	0.12	0.19	0.21	0.23	0.24	0.25	0.25
Removed TOC (mmol/L)	-	0.55	0.47	0.45	0.44	0.43	0.42	0.42

Table F.45: SBA operational capacity with TOC into account – Experiment 2.3

Sample	1	2	3	4	5	6	7^-
Throughput (L)	153	370	483	743	1537	1723	1800
Anions Removed (meq) Table F.43	847	2034	2649	4051	6515	7026	7232
Cl^- excess (meq/L)	0.33	0	1.16	1.13	0.71	0.70	0.03
Cl^- excess (meq)	50	50	182	475	1039	1169	1172
Total removed (meq)	897	2084	2831	4526	7554	8195	8404
Operational capacity (eq/L_r)			0.431				
Operational capacity/Total capacity (%)			34.5				

Table F.46: WAC operational capacity – Experiment 2.3

Sample	1	2	3	4	5	6	7
Cations removed (meq/L)	5.59	5.59	5.59	5.59	5.58	5.58	5.50
Cations removed (meq)	856	2067	2700	4152	8580	9621	12097
WAC operational capacity (eq/L_r)			1.100				
Operational capacity/Total capacity (%)			23				

Table F.47: Volume weighted average and removal – Experiment 2.3

Parameter	VW average	VW average	Feed	Removal
Unit	meq/L	mg/L	mg/L	%
ATP (ng/L)	-	498	1125	56
TOC (mmol/L)	0.22	2.63	7.95	67
HCO_3^-	1.43	160.38	160.38	46
Cl^-	11.68	242.20	242.20	-66
SO_4^{2-}	0.05	102.78	102.78	98
NO_3^-	0.37	61.07	61.07	62
HPO_4^{2-}-P	0.001	2.01	2.01	99
SiO_2	0.22	6.18	6.18	0
F^-	0.02	0.35	0.35	0
Na^+	14.57	174.15	174.15	-92
K^+	0.004	26.82	26.82	99
Ca^{2+}	0.005	62.49	62.49	100
Mg^{2+}	0.008	18.75	18.75	99
Fe^{3+}	0.0001	0.05	0.05	95
Mn^{2+}	0.00001	0.11	0.11	100
NH_4^+	0.002	4.37	4.37	99
Al^{3+}	0.0004	0.01	0.01	61
Ba^{2+}	0.00001	0.004	0.004	89
Sr^{2+}	0.00001	0.27	0.27	100

Table F.48: Samples after WAC before SBA water quality – Experiment 2.3

Sample	Unit	M1	M2
Sampling time	-	8:52	9:38
Throughput	BVs in H form	13.9	29.6
EC	µS/cm	1521.11	1488.74
pH	-	9.83	9.64
ATP	ng/L	-	28
TOC	mg C/L	7.71	7.76
HCO_3^-	mg/L	118.53	137.9
CO_3^{2-}	mg/L	55.22	41.54
Cl^-	mg/L	244.34	242.73
SO_4^{2-}	mg/L	102.48	98.04
NO_3^-	mg/L	59.87	56.81
HPO_4^{2-}-P	mg P/L	2.03	1.89
Na^+	mg/L	341.23	339.01
K^+	mg/L	0.11	0.10
Ca^{2+}	mg/L	<0.2	<0.2
Mg^{2+}	mg/L	<0.1	<0.1
Fe^{3+}	mg/L	< 0.005	< 0.005
Mn^{2+}	mg/L	0.0006	0.0006
NH_4^+	mg/L	< 0.05	< 0.05
Al^{3+}	mg/L	0.006	0.007
Ba^{2+}	mg/L	< 0.001	< 0.001
Sr^{2+}	mg/L	< 0.001	< 0.001

G.Appendix: Results Details Experiments 1.4 and 2.4

Table G.1: Product samples water quality – Experiment 1.4

Sample	Unit	1	2	3	4
EC	µS/cm	1324.69	1313.53	1293.44	1283.4
pH	-	8.35	9.36	9.73	9.69
ATP	ng/L	-	-	-	11.9
TOC	mg C/L	-	2.03	-	2.7
HCO_3^-	mg/L	213.18	201.42	188.88	191.72
CO_3^{2-}	mg/L	-	31.53	61.54	57.34
Cl^-	mg/L	288.02	234.76	208.45	206.30
SO_4^{2-}	mg/L	< 5 mg/L	< 5 mg/L	< 5 mg/L	< 5 mg/L
NO_3^-	mg/L	36.86	72.37	58.63	60.68
HPO_4^{2-}-P	mg P/L	< 0.02	2.07	2.678	2.67
SiO_2	mg Si/L	4.41	4.49	4.58	4.72
F^-	mg/L	220.603	246.65	223.356	226.659
Na^+	mg/L	0.11	2.32	18.87	27.52
K^+	mg/L	<0.2	<0.2	<0.2	<0.2
Ca^{2+}	mg/L	<0.1	<0.1	<0.1	<0.1
Mg^{2+}	mg/L	< 0.005	< 0.005	< 0.005	< 0.005
Fe^{3+}	mg/L	< 0.0005	< 0.0005	< 0.0005	0.0005
Mn^{2+}	mg/L	< 0.05	0.077	0.2885	0.6482
NH_4^+	mg/L	0.004	0.003	0.005	0.005
Al^{3+}	mg/L	< 0.001	< 0.001	< 0.001	< 0.001
Ba^{2+}	mg/L	< 0.001	< 0.001	< 0.001	< 0.001
Sr^{2+}	mg/L	< 0.001	< 0.001	< 0.001	< 0.001

Table G.2: Product samples water balance – Experiment 1.4

Production started at		7:14			
Sample		1	2	3	4
Sampling time		11:15	12:55	15:02	16:10
Throughput	BVs	82.4	116.6	160	183.3
TOC	mmol/L	0.19	0.26	0.26	0.27
HCO_3^-	meq/L	3.49	3.30	3.10	3.14
CO_3^{2-}	meq/L	0.05	0.49	1.08	1.00
Cl^-	meq/L	8.36	6.81	6.05	5.99
SO_4^{2-}	meq/L	0.05	0.05	0.05	0.05
NO_3^-	meq/L	0.594	1.167	0.946	0.98
HPO_4^{2-}-P	meq/L	0.0006	0.1270	0.1643	0.1638
SiO_2	meq/L	0.16	0.16	0.16	0.17
F^-	meq/L	0.01	0.01	0.01	0.01
Na^+	meq/L	9.60	10.73	9.72	9.86
K^+	meq/L	0.003	0.059	0.483	0.704
Ca^{2+}	meq/L	0.005	0.005	0.005	0.005
Mg^{2+}	meq/L	0.01	0.01	0.01	0.01
Fe^{3+}	meq/L	0.0001	0.0001	0.0001	0.0001
Mn^{2+}	meq/L	0.00001	0.00001	0.00001	0.00002
NH_4^+	meq/L	0.001	0.001	0.001	0.001
Al^{3+}	meq/L	0.0004	0.0004	0.0006	0.0005
Ba^{2+}	meq/L	0.00001	0.00001	0.00001	0.00001
Sr^{2+}	meq/L	0.00001	0.00001	0.00001	0.00001
Sum anion	meq/L	12.72	12.12	11.56	11.50
Sum cation	meq/L	9.61	10.80	10.21	10.58
|Balance|	meq/L	3.11	1.32	1.34	0.92
Balance	%	13.9	5.7	6.2	4.2

Table G.3: HPO_4^{2-}-P measurements on product water samples – Experiment 1.4

Sampling time	Volume (BVs)	HPO_4^{2-}-P (mg P/L)	HPO_4^{2-}-P (meq/L)
10:56	75.9	0.01	0.0006
11:31	87.9	0.025	0.002
11:45	92.6	0.054	0.003
12:03	98.8	0.17	0.01
12:27	107.0	0.67	0.04
12:44	112.8	1.49	0.10
12:58	117.6	2.23	0.14
13:14	123.1	2.45	0.16
13:28	127.9	2.71	0.17
13:42	132.6	2.68	0.17
14:15	143.9	2.77	0.18
15:18	165.5	2.82	0.18

Table G.4: Product samples water quality – Experiment 2.4

Sample	Unit	1	2	3	4
EC	µS/cm	1326.92	1312.42	1303.49	1294.56
pH	-	8.47	8.56	8.97	9.23
ATP	ng/L	-	-	-	10.6
TOC	mg C/L	2.69	2.61	3.11	3.03
HCO_3^-	mg/L	217.06	211.37	206.2	200.64
CO_3^{2-}	mg/L	2.67	4.07	13.1	23.39
Cl^-	mg/L	273.06	251.44	240.61	233.27
SO_4^{2-}	mg/L	< 5 mg/L	< 5 mg/L	< 5 mg/L	< 5 mg/L
NO_3^-	mg/L	49.04	80.30	81.45	78.44
HPO_4^{2-}-P	mg P/L	< 0.02	0.28	1.29	2.12
SiO_2	mg Si/L	4.44	4.42	4.47	4.52
Na^+	mg/L	295.58	240.06	220.63	222.13
K^+	mg/L	7.91	23.10	28.38	30.47
Ca^{2+}	mg/L	<0.2	<0.2	<0.2	<0.2
Mg^{2+}	mg/L	<0.1	<0.1	<0.1	<0.1
Fe^{3+}	mg/L	< 0.005	< 0.005	< 0.005	< 0.005
Mn^{2+}	mg/L	< 0.0005	< 0.0005	< 0.0005	0.0005
NH_4^+	mg/L	0.153	0.460	0.857	1.095
Al^{3+}	mg/L	0.005	0.006	0.005	0.004
Ba^{2+}	mg/L	< 0.001	< 0.001	< 0.001	< 0.001
Sr^{2+}	mg/L	< 0.001	< 0.001	< 0.001	< 0.001

Table G.5: Product samples water balance – Experiment 2.4

Production started at		7:14			
Sample		1	2	3	4
Sampling time		14:03	15:46	16:43	17:23
Throughput	BVs	139.8	175	194.5	208.2
TOC	mmol/L	0.22	0.22	0.26	0.25
HCO_3^-	meq/L	3.56	3.46	3.38	3.29
CO_3^{2-}	meq/L	0.09	0.14	0.44	0.78
Cl^-	meq/L	7.93	7.30	6.98	6.77
SO_4^{2-}	meq/L	0.05	0.05	0.05	0.05
NO_3^-	meq/L	0.79	1.30	1.31	1.27
HPO_4^{2-}-P	meq/L	0.0006	0.02	0.08	0.13
SiO_2	meq/L	0.16	0.16	0.16	0.16
F^-	meq/L	0.01	0.01	0.01	0.01
Na^+	meq/L	12.86	10.44	9.60	9.66
K^+	meq/L	0.202	0.591	0.726	0.779
Ca^{2+}	meq/L	0.005	0.005	0.005	0.005
Mg^{2+}	meq/L	0.01	0.01	0.01	0.01
Fe^{3+}	meq/L	0.0001	0.0001	0.0001	0.0001
Mn^{2+}	meq/L	0.00001	0.00001	0.00001	0.00002
NH_4^+	meq/L	0.008	0.026	0.048	0.061
Al^{3+}	meq/L	0.0006	0.0006	0.0005	0.0005
Ba^{2+}	meq/L	0.00001	0.00001	0.00001	0.00001
Sr^{2+}	meq/L	0.00001	0.00001	0.00001	0.00001
Sum anion	meq/L	12.58	12.43	12.41	12.46
Sum cation	meq/L	13.08	11.07	10.38	10.52
|Balance|	meq/L	0.50	1.36	2.03	1.94
Balance	%	1.9	5.8	8.9	8.4

Table G.6: HPO_4^{2-}-P measurements on product water samples – Experiment 2.4

Sampling time	Volume (BVs)	HPO_4^{2-}-P (mg P/L)	HPO_4^{2-}-P (meq/L)
13:32	129.2	0.01	0.0006
14:44	153.85	0.025	0.002
15:14	164.1	0.107	0.007
15:54	177.8	0.389	0.025
16:10	183.25	0.525	0.03
16:27	189.1	0.71	0.05
16:59	200.0	1.65	0.11
17:07	202.7	1.8	0.12
17:15	205.5	1.95	0.13

H.Appendix: Results Details Experiments 1.5 and 2.5

Mixing Ratios & Water Quality

Representative product water samples of 4 L were produced for both SBA resins by mixing proportionally product water collected in jerrycans.

The computation of the mixing ratios for Product 1 and Product 2 are given in Tables H.1 and H.2, respectively. In Table H.3 the water quality measurements of the two product samples and the feed sample of the IX pilot are given.

Table H.1: Mixing ratios – Experiment 1.5 – Product 1

Jerrycan	Throughput (BVs)	Throughput (L)	ΔVolume (L)	Mixing ratios (%)	Volume of water for 4 L sample
1st	55.4	1080	1080	78	3116
2nd	65.3	1273	193	14	558
3rd (Production end)	71.1	1387	113	8	326
Total volume of sample "Product 1"					4000

Table H.2: Mixing ratios – Experiment 2.5 – Product 2

Jerrycan	Throughput (BVs)	Throughput (L)	ΔVolume (L)	Mixing ratios (%)	Volume of water for 4 L sample
1st	74.9	1460	1460	60	2400
2nd	98.8	1927	467	19	767
3rd (Production end)	124.8	2433	506	21	832
Total volume of sample "Product 1"					4000

Table H.3: IX Feed, Product 1 and Product 2 samples water quality – Experiments 1.5 and 2.5

Date		24-2-2020	24-2-2020	24-2-2020
RO feed quality		1	2	3
Relevant tests 1.5 and 2.5		IX Feed	Product 1	Product 2
EC	µS/cm	1200	1374	1300
pH	-	7.610	9.60	8.30
ATP	ng/L	1400	31.40	82.10
TOC	mg C/L	7.20	2.10	2.20
HCO_3^-	mg/L	200	92	132
Cl^-	mg/L	210	332	324
SO_4^{2-}	mg/L	86	< 5	< 5
NO_3^-	mg/L	50	9.50	11
HPO_4^{2-}-P	mg P/L	1.90	< 0.02	< 0.02
SiO_2	mg Si/L	4.59	3.87	4.18
Na^+	mg/L	140.00	248.78	232.15
K^+	mg/L	25	0.1	0.2
Ca^{2+}	mg/L	64	<0.2	<0.2
Mg^{2+}	mg/L	17	<0.1	<0.1
Fe^{3+}	mg/L	0.03	< 0.005	< 0.005
Mn^{2+}	mg/L	0.084	< 0.0004	< 0.0004
NH_4^+	mg/L	4	<0.05	0.05
Al^{3+}	mg/L	0.006	0.003	0.002
Ba^{2+}	mg/L	0.0035	0.001	< 0.001
Sr^{2+}	mg/L	0.28	< 0.001	< 0.001

Bacterial Growth Curves IX Feed Aliquots – RO Feed Quality 1

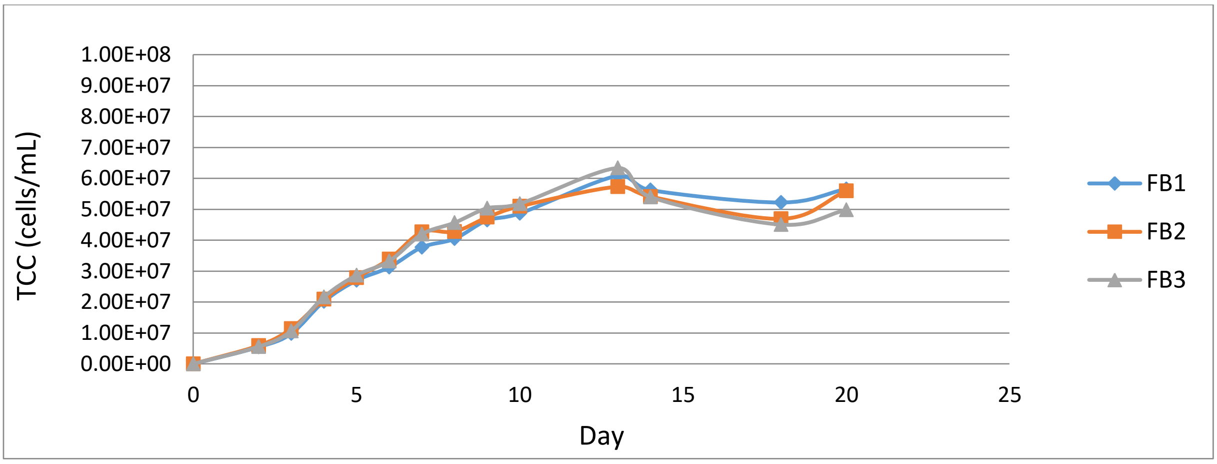

Figure H.1: Bacterial growth curves of FB triplicates

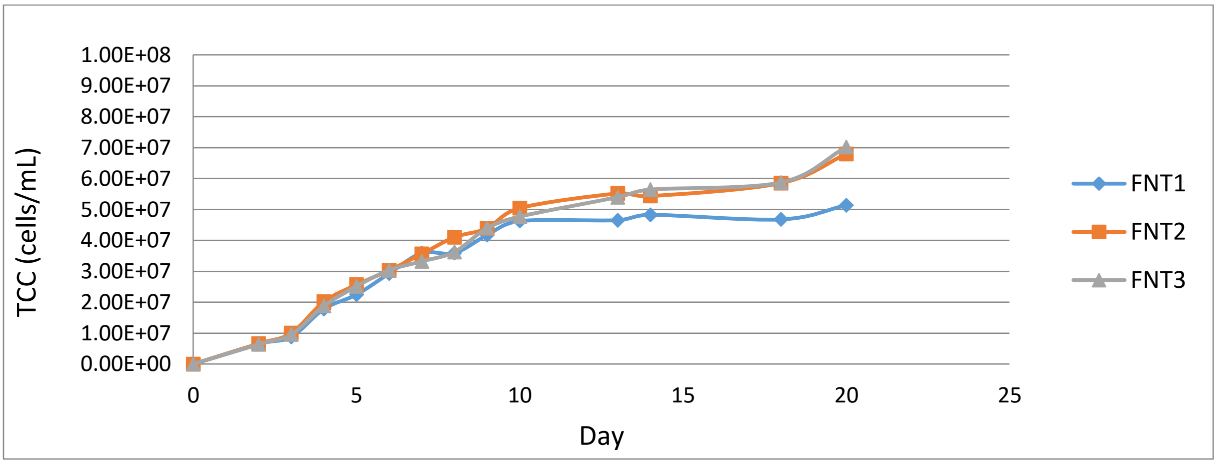

Figure H.2: Bacterial growth curves of FNT triplicates

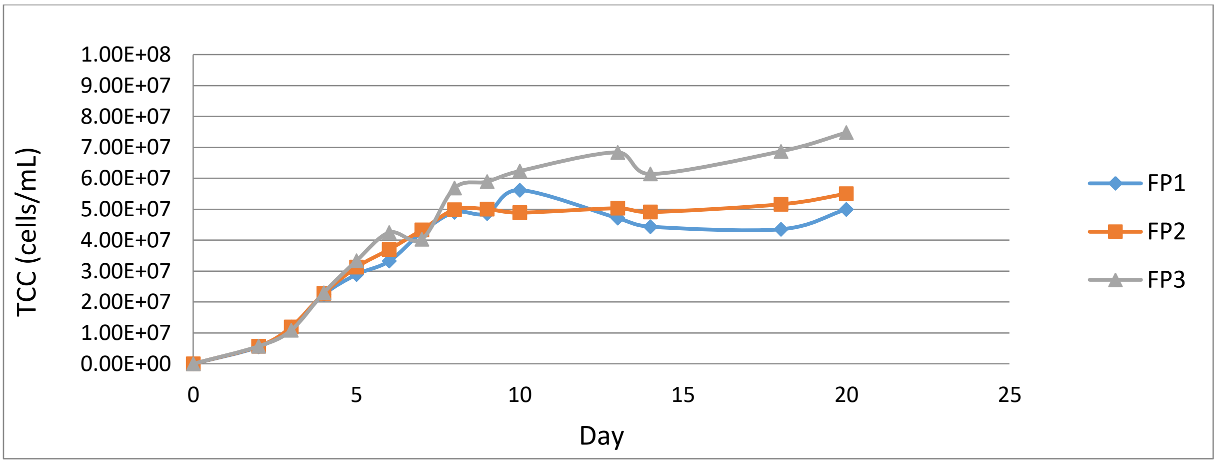

Figure H.3: Bacterial growth curves of FP triplicates

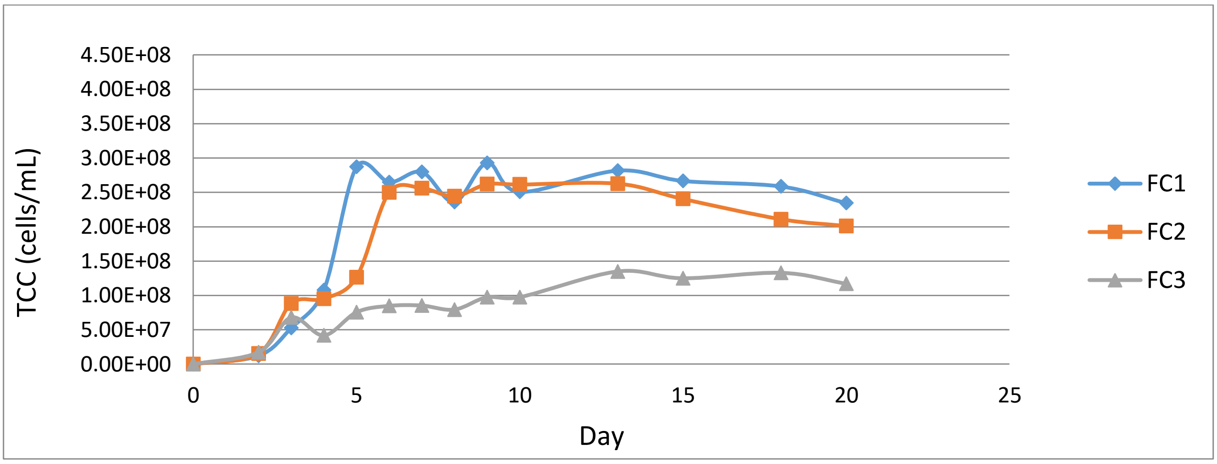

Figure H.4 Bacterial growth curves of FC triplicates

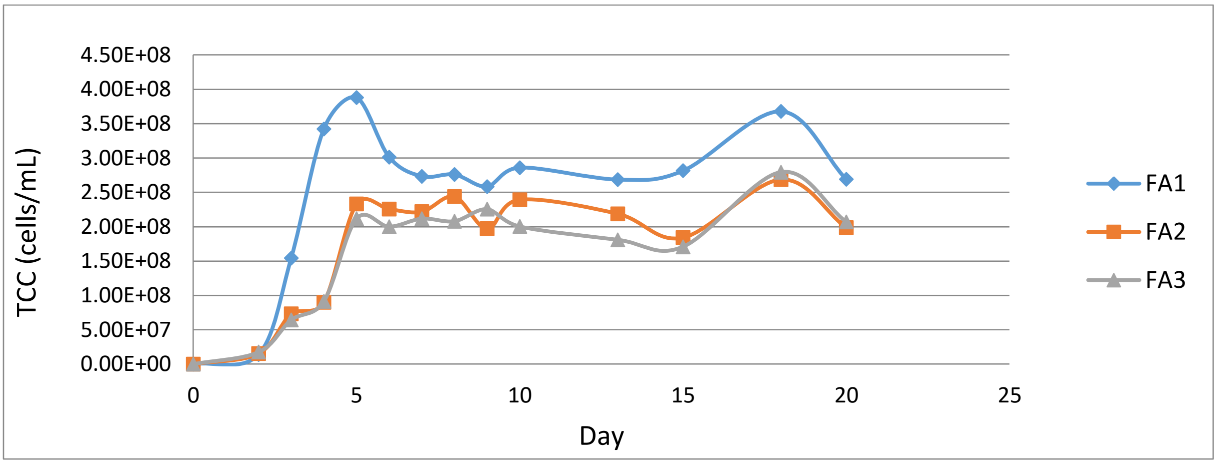

Figure H.5: Bacterial growth curves of FA triplicates

Bacterial Growth Curves Product 1 Aliquots – RO Feed Quality 2

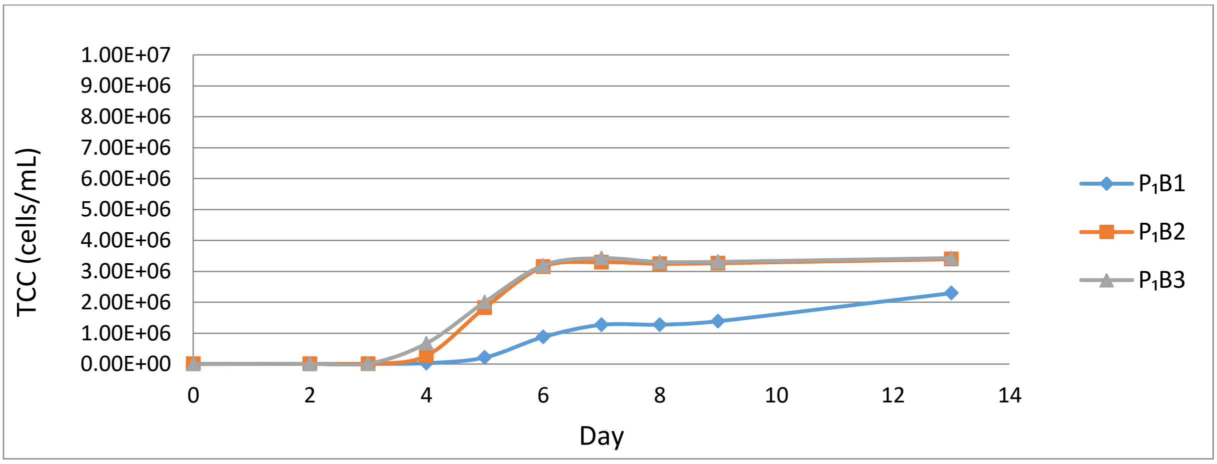

Figure H.6: Bacterial growth curves of P_1B triplicates

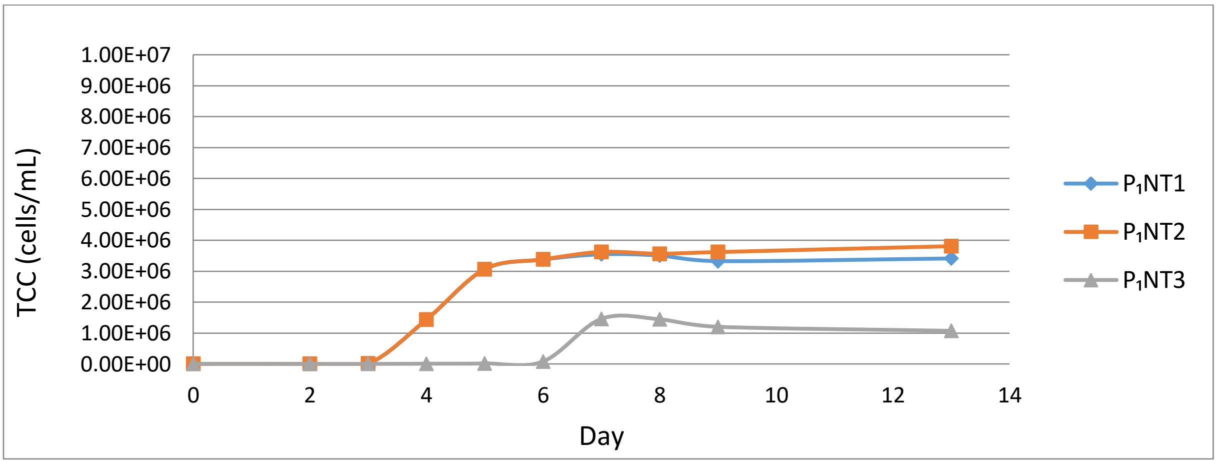

Figure H.7: Bacterial growth curves of P_1NT triplicates

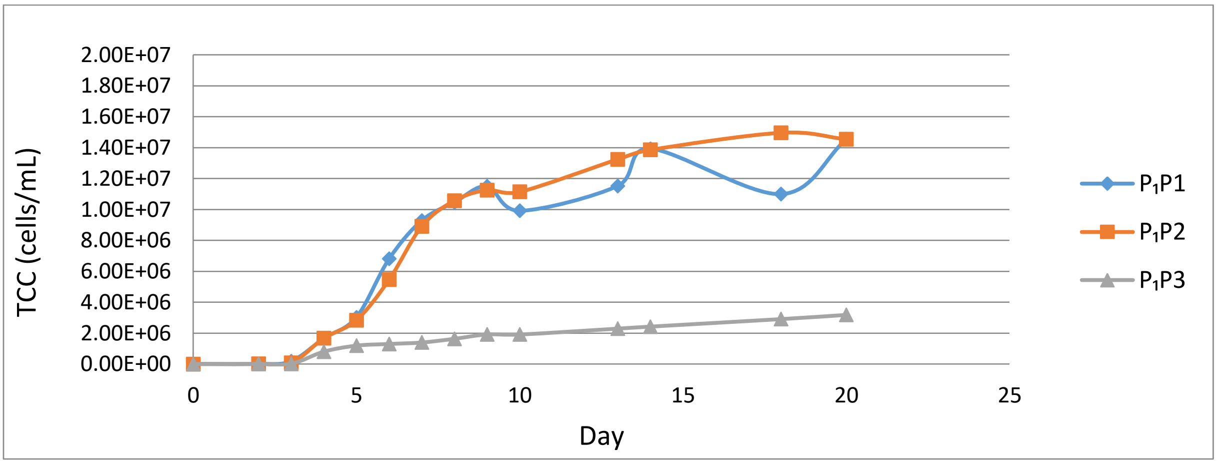

Figure H.8: Bacterial growth curves of P_1P triplicates

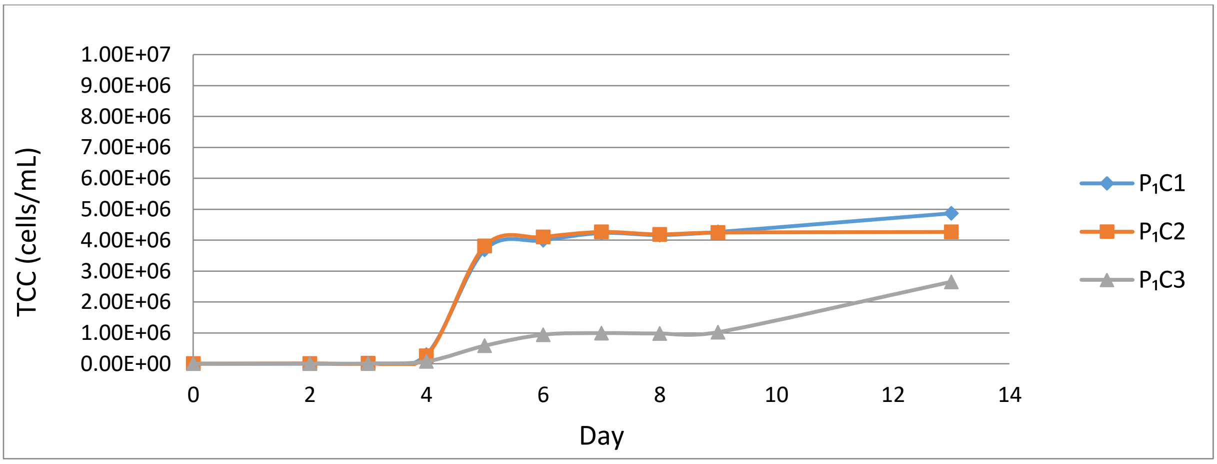

Figure H.9: Bacterial growth curves of P_1C triplicates

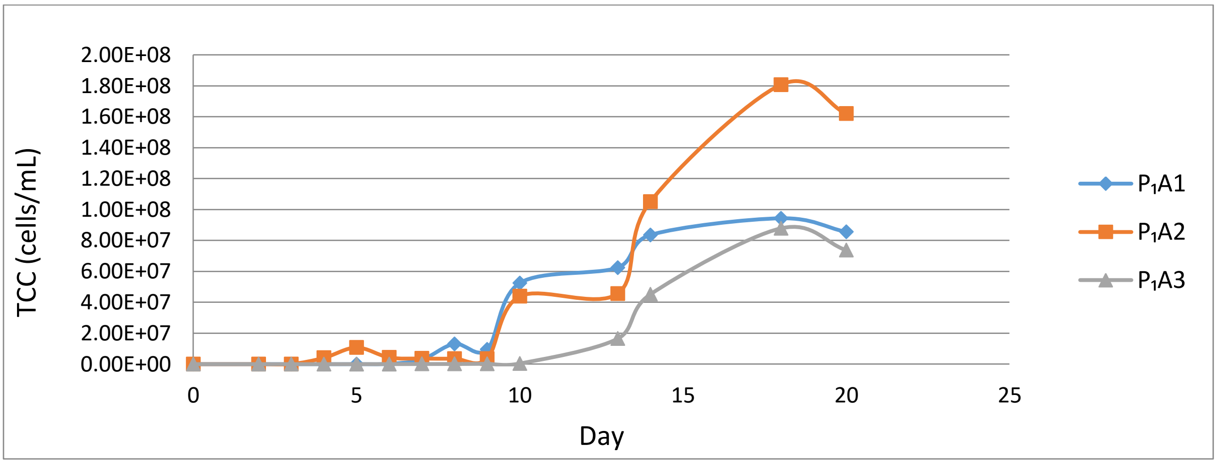

Figure H.10: Bacterial growth curves of P_1A triplicates

Bacterial Growth Curves Product 2 Aliquots – RO Feed Quality 3

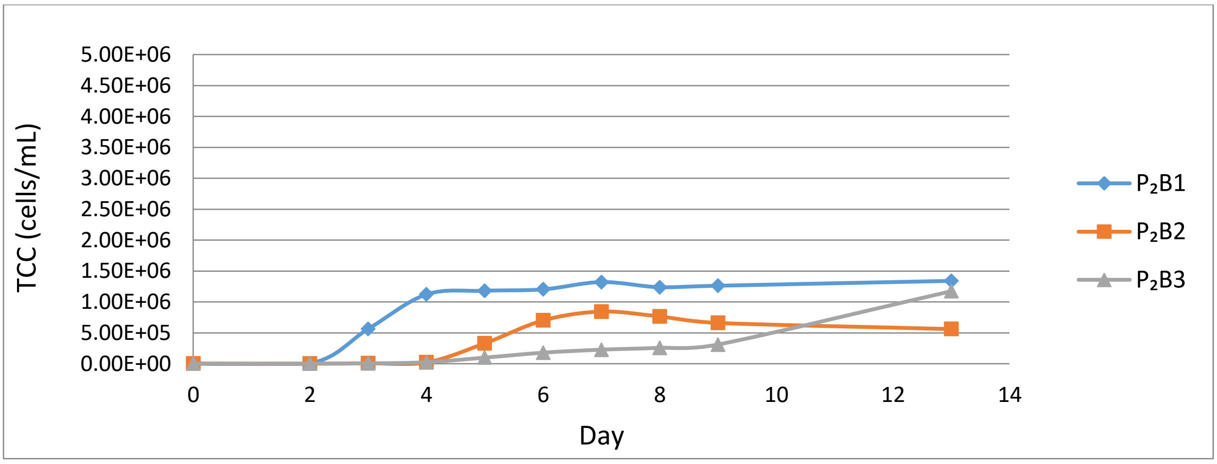

Figure H.11: Bacterial growth curves of P_2B triplicates

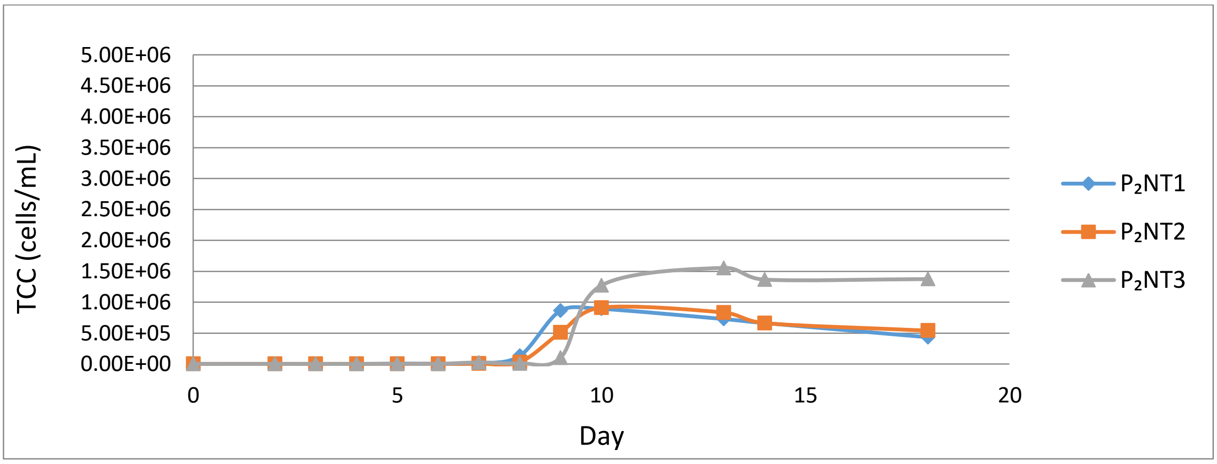

Figure H.12: Bacterial growth curves of P_2NT triplicates

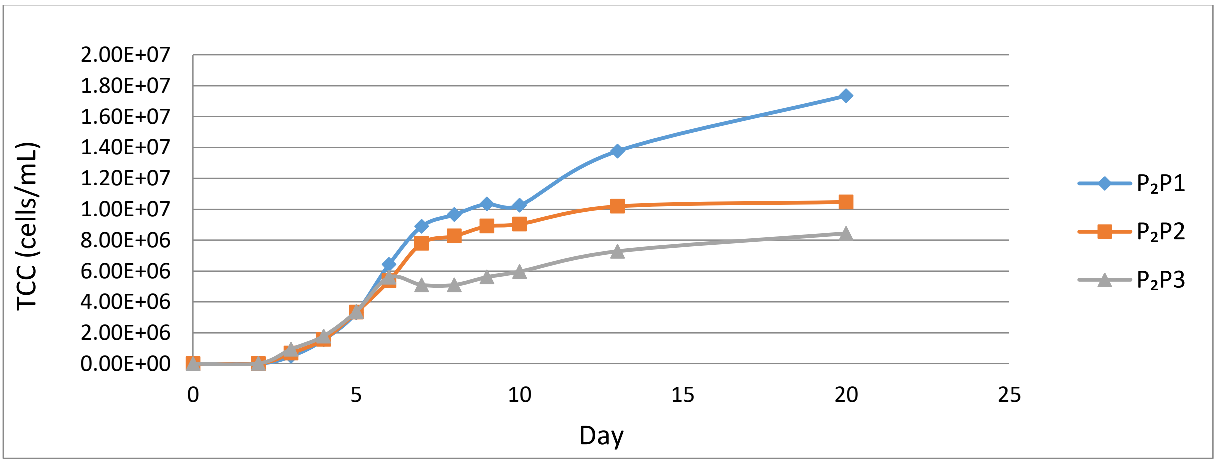

Figure H.13: Bacterial growth curves of P_2P triplicates

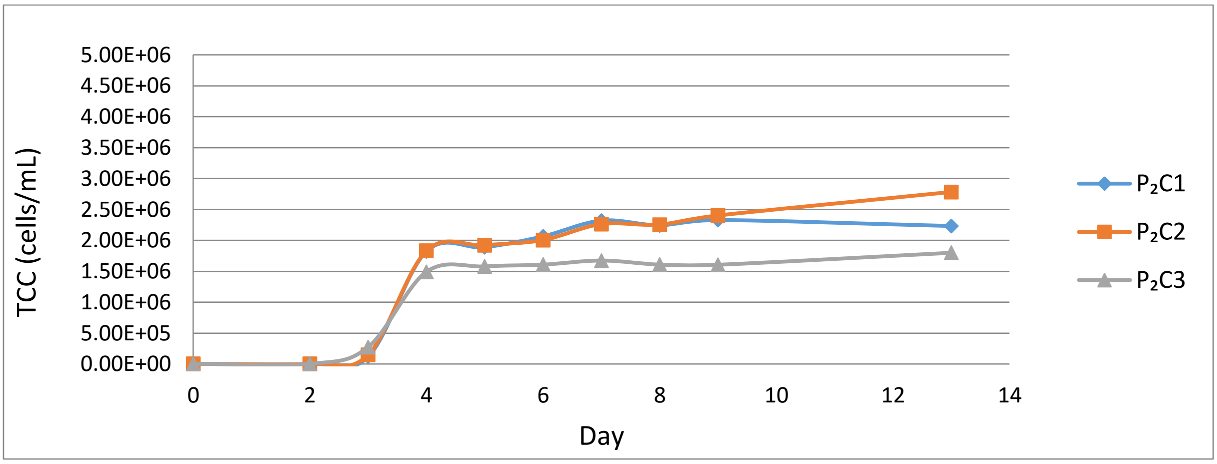

Figure H.14: Bacterial growth curves of P_2C triplicates

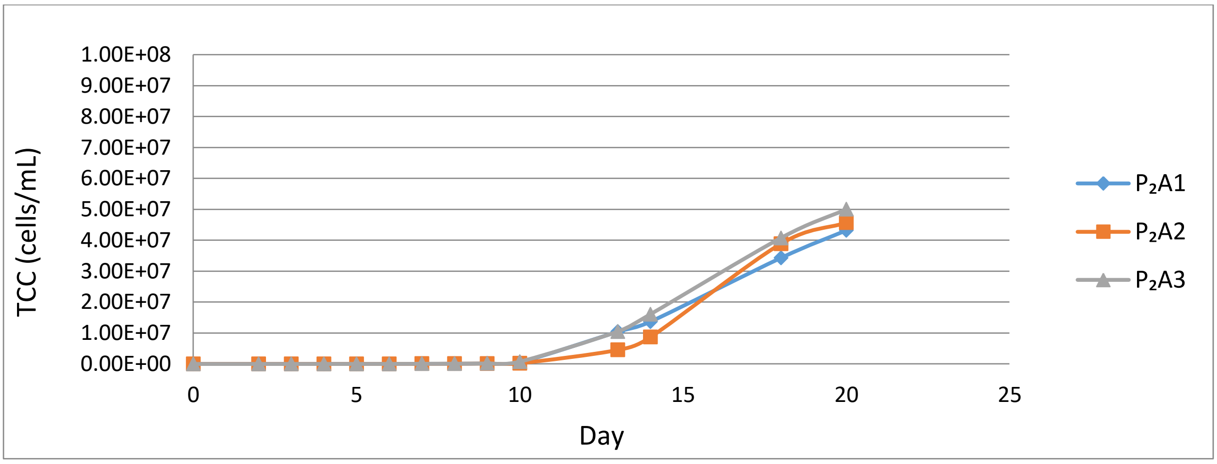

Figure H.15: Bacterial growth curves of P_2A triplicates

WAVE Design Software Results:

Table H.4: RO feed, RO concentrate and RO permeate water quality for IX Feed - RO feed quality 1

Relevant tests 1.5 and 2.5		RO feed	RO concentrate	RO permeate
pH	-	7.61	8	6
HCO_3^-	mg/L	202.7	1285	4.98
CO_3^{2-}	mg/L	0.73	21.67	0
Cl^-	mg/L	205.1	1353	2.13
SO_4^{2-}	mg/L	86	573.8	0.32
NO_3^-	mg/L	49.75	321.9	1.66
HPO_4^{2-}-P	mg P/L	1.9	12.67	0
SiO_2	mg Si/L	4.59	30.05	0.08
F^-	mg/L	0.2	1.31	0.00
Na^+	mg/L	143.75	919.1	2.75
K^+	mg/L	25.87	168.2	0.71
Ca^{2+}	mg/L	65.96	4369	0.4
Mg^{2+}	mg/L	17.66	116.9	0.11
Fe^{3+}	mg/L	0.03	0.20	0
Mn^{2+}	mg/L	0.084	0.56	0
NH_4^+	mg/L	4	26.54	0.14
Al^{3+}	mg/L	0.006	0.04	0
Ba^{2+}	mg/L	0.0035	0.02	0
Sr^{2+}	mg/L	0.28	2.04	0

Table H.5: RO feed, RO concentrate and RO permeate water quality for Product 1 - RO feed quality 2

Relevant tests 1.5		RO feed	RO concentrate	RO permeate
pH	-	9.6	9.4	9.1
HCO_3^-	mg/L	91.74	579.6	2.9
CO_3^{2-}	mg/L	31.46	222.8	0.16
Cl^-	mg/L	332.4	2191	3.85
SO_4^{2-}	mg/L	2.5	16.55	0.02
NO_3^-	mg/L	9.5	61.57	0.3
HPO_4^{2-}-P	mg P/L	0.01	0.07	0
SiO_2	mg Si/L	4.12	26.96	0.07
F^-	mg/L	0.2	1.31	0
Na^+	mg/L	280.9	1847	4.03
K^+	mg/L	0.11	0.74	0
Ca^{2+}	mg/L	0.11	0.75	0
Mg^{2+}	mg/L	0.06	0.38	0
Fe^{3+}	mg/L	0.0025	0.02	0
Mn^{2+}	mg/L	0.0002	0.001	0
NH_4^+	mg/L	0.03	0.18	0
Al^{3+}	mg/L	0.003	0.02	0
Ba^{2+}	mg/L	0.001	0.01	0
Sr^{2+}	mg/L	0.0005	0.003	0

Table H.6: RO feed, RO concentrate and RO permeate water quality for Product 2 - RO feed quality 3

Relevant tests 2.5		RO feed	RO concentrate	RO permeate
pH	-	8.3	8.3	6.9
HCO_3^-	mg/L	131.9	838.2	3.29
CO_3^{2-}	mg/L	2.22	25.47	0
Cl^-	mg/L	324.2	2137	3.73
SO_4^{2-}	mg/L	2.5	16.55	0.02
NO_3^-	mg/L	10.9	70.65	0.34
HPO_4^{2-}-P	mg P/L	0.01	0.07	0
SiO_2	mg Si/L	4.18	27.44	0.07
F^-	mg/L	0.2	1.31	0
Na^+	mg/L	266.8	1754	3.78
K^+	mg/L	0.23	1.5	0.01
Ca^{2+}	mg/L	0.11	0.76	0
Mg^{2+}	mg/L	0.06	0.38	0
Fe^{3+}	mg/L	0.0025	0.02	0
Mn^{2+}	mg/L	0.0002	0.001	0
NH_4^+	mg/L	0.05	0.37	0
Al^{3+}	mg/L	0.002	0.01	0
Ba^{2+}	mg/L	0.0005	0.003	0
Sr^{2+}	mg/L	0.0005	0.003	0

PHREEQC Version 3 Software Results:

Table H.7: All saturation index results of the RO feed and RO concentrate for the three RO feed qualities

RO feed quality	1		2		3	
Name	IX Feed		Product 1		Product 2	
Saturation index (SI)	Feed	Concentrate	Feed	Concentrate	Feed	Concentrate
Albite ($NaAlSi_3O_8$)	-2.02	2.00	-2.70	1.25	-2.34	1.55
Alunite ($KAl_3(SO_4)_2(OH)_6$)	-5.25	-3.50	-23.43	-19.19	-15.83	-11.97
Anhydrite ($CaSO_4$)	-2.12	-1.02	-6.40	-5.30	-6.32	-5.13
Anorthite ($CaAl_2Si_2O_8$)	-4.16	-0.38	-8.02	-4.34	-7.93	-4.36
Aragonite ($CaCO_3$)	-0.04	1.65	-1.24	-0.06	-2.25	-0.89
Barite ($BaSO_4$)	-1.30	-0.29	-3.26	-2.94	-3.53	-2.41
Ca-Montmorillonite ($Ca_{0.165}Al_{2.33}Si_{3.67}O_{10}(OH)_2$)	0.52	4.65	-5.48	-0.64	-2.60	2.05
Calcite ($CaCO_3$)	0.11	1.80	-1.09	0.09	-2.10	-0.74
Celestite ($SrSO_4$)	-2.42	-1.27	-6.62	-5.52	-6.59	-5.45
Chalcedony (SiO_2)	-0.18	0.65	-0.41	0.39	-0.23	0.60
Chlorite (14A) ($Mg_5Al_2Si_3O_{10}(OH)_8$)	-4.75	5.37	-2.38	4.27	-12.35	-5.62
Chrysotile ($Mg_3Si_2O_5(OH)_4$)	-4.94	0.85	-0.81	2.41	-8.11	-4.68
Dolomite ($CaMg(CO_3)_2$)	-0.07	3.31	-2.13	0.20	-4.17	-1.48
Fluorite (CaF_2)	-2.45	-0.42	-5.23	-3.20	-5.16	-3.04
Gibbsite ($Al(OH)_3$)	0.49	0.87	-1.80	-1.03	-0.68	-0.03
Goethite (FeOOH)	7.30	8.17	5.71	6.58	6.26	7.16
Gypsum ($CaSO_4 \cdot 2H_2O$)	-1.76	-0.66	-6.04	-4.94	-5.96	-4.77
Halite (NaCl)	-6.12	-4.59	-5.60	-4.08	-5.63	-4.10
Hausmannite (Mn_3O_4)	-12.04	-8.16	-6.49	-6.26	-14.65	-14.20
Hematite (Fe_2O_3)	16.59	18.32	13.40	15.14	14.50	16.30
Hydroxyapatite ($Ca_5(PO_4)_3OH$)	4.24	10.15	-7.86	-3.43	-12.75	-7.83
Illite ($K_{0.6}Mg_{0.25}Al_{2.3}Si_{3.5}O_{10}(OH)_2$)	0.35	5.15	-5.57	-0.38	-3.56	1.42
Jarosite-K ($KFe_3(SO_4)_2(OH)_6$)	-4.40	-1.19	-20.50	-15.97	-14.62	-10.01
K-feldspar ($KAlSi_3O_8$)	-0.35	3.65	-3.71	0.25	-3.01	0.88
K-mica ($KAl_3Si_3O_{10}(OH)_2$)	6.21	10.97	-1.73	3.78	1.22	6.40
Kaolinite ($Al_2Si_2O_5(OH)_4$)	2.32	4.72	-2.73	0.42	-0.12	2.84
Manganite (MnOOH)	-4.72	-3.30	-2.21	-2.13	-5.36	-5.21
Pyrochroite ($Mn(OH)_2$)	-6.18	-5.16	-5.67	-5.59	-7.52	-35.71
Pyrolusite ($MnO_2 \cdot H2O$)	-9.98	-8.15	-5.46	5.39	-9.91	-9.77
Quartz (SiO_2)	0.27	1.09	0.03	0.84	0.22	1.04
Rhodochrosite ($MnCO_3$)	-0.39	0.95	-2.27	-1.54	-2.60	-1.70
Sepiolite ($Mg_2Si_3O_{7.5}OH \cdot 3H_2O$)	-3.61	1.62	-1.25	2.23	-8.57	-2.15
Strontianite ($SrCO_3$)	-1.78	-0.05	-2.91	-1.72	-3.96	-2.65
Sylvite (KCl)	-6.40	-4.88	-8.55	-7.01	-8.24	-6.72
Talc ($Mg_3Si_4O_{10}(OH)_2$)	-1.66	5.77	2.00	6.83	-4.93	0.15
Witherite ($BaCO_3$)	-4.62	-3.02	-3.50	-3.10	-4.86	-3.56